MATTER-WAVE BRIGHT SOLITONS
IN
BOSE-EINSTEIN CONDENSATE

ABDELAZIZ BENSEGHIR

FACULTY OF SCIENCE
UNIVERSITY OF MALAYA
KUALA LUMPUR

2015

MATTER-WAVE BRIGHT SOLITONS
IN
BOSE-EINSTEIN CONDENSATE

ABDELAZIZ BENSEGHIR

THESIS SUBMITTED IN FULFILLMENT OF THE
REQUIREMENTS FOR THE DEGREE OF
DOCTOR OF PHILOSOPHY

FACULTY OF SCIENCE
UNIVERSITY OF MALAYA
KUALA LUMPUR

2015

UNIVERSITI MALAYA

ORIGINAL LITERARY WORK DECLARATION

Name of Candidate: Abdelaziz Benseghir   (I.C/Passport No: 146253431)

Registration/Matric No: SHC100087

Name of Degree: Doctor of philosophy

Title of Project Paper/Research Report/Dissertation/Thesis ("this Work"):

Matter-wave bright solitons in Bose-Einstein condensate

Field of Study: Atomic physics

I do solemnly and sincerely declare that:

(1)   I am the sole author/writer of this Work;
(2)   This Work is original;
(3)   Any use of any work in which copyright exists was done by way of fair dealing and for permitted purposes and any excerpt or extract from, or reference to or reproduction of any copyright work has been disclosed expressly and sufficiently and the title of the Work and its authorship have been acknowledged in this Work;
(4)   I do not have any actual knowledge nor do I ought reasonably to know that the making of this work constitutes an infringement of any copyright work;
(5)   I hereby assign all and every rights in the copyright to this Work to the University of Malaya ("UM"), who henceforth shall be owner of the copyright in this Work and that any reproduction or use in any form or by any means whatsoever is prohibited without the written consent of UM having been first had and obtained;
(6)   I am fully aware that if in the course of making this Work I have infringed any copyright whether intentionally or otherwise, I may be subject to legal action or any other action as may be determined by UM.

Candidate's Signature   Date: 08/06/2015

Subscribed and solemnly declared before,

Witness's Signature Date

Name

Designation:

Abstract

We investigate the properties of modulational instability in the Salerno equation in quasi-one dimension in Bose-Einstein condensate (BEC). We analyzed the regions of modulational instability of nonlinear plane waves and determine the conditions of its existence in BEC.

The existence and stability of strongly localized modes in discrete media is investigated with the framework of the Salerno model by using a linear analysis method. The regions of stability and instability are determined. Also the existence of localized modes for different values of parameters is shown numerically by homoclinic orbits intersection method.

The response of Bose–Einstein condensates is studied with strong dipole–dipole atomic interactions to periodically varying perturbation. The dynamics is governed by the Gross–Pitaevskii equation with an additional nonlinear term, corresponding to nonlocal dipolar interactions. A mathematical model, based on the variational approximation, has been developed and applied to study parametric excitation of the condensates due to coefficient of nonlocal nonlinearity varying periodically. The model predicts the waveform of solitons in dipolar condensates and describes their small amplitude dynamics quite accurately. Theoretical predictions are verified by numerical simulations of the nonlocal Gross–Pitaevskii equation and a good agreement between them is found. The results can lead to better understanding of the properties of ultra-cold quantum gases, such as ^{52}Cr, ^{164}Dy and ^{168}Er, where the long-range dipolar atomic interactions dominate the usual contact interactions.

Dynamics of a matter wave soliton bouncing on the reflecting surface (atomic mirror) under the effect of gravity has been studied by analytical and numerical means. The

analytical description is based on the variational approach. Resonant oscillations of the soliton's center of mass and width, induced by appropriate modulation of the atomic scattering length and the slope of the linear potential are analyzed. In numerical experiments, we observe the Fermi type acceleration of the soliton when the vertical position of the reflecting surface is periodically varied in time. Analytical predictions are compared with the results of numerical simulations of the Gross-Pitaevskii equation and a qualitative agreement between them is found.

Abstrak

Kami menyiasat sifat-sifat ketidakstabilan modulasi di dalam persamaan Salerno dalam quasi satu dimensi intuk kondensat Bose-Einstein (BEC). Kami menganalisis kawasan ketidakstabilan modulasi gelombang planar tidak linear dan menentukan syarat kewujudannya dalam BEC.

Kewujudan dan kestabilan mod kuat setempat dikaji di dalam media diskret di dalam model Salerno dengan menggunakan kaedah analisis linear. Kawasan kestabilan dan ketidakstabilan ditentukan. Juga kewujudan mod setempat untuk nilai parameter yang berbeza ditunjukkan dengan kaedah persimpangan orbit homoklinik.

Tindak balas daripada kondensat Bose-Einstein dikaji dengan interaksi atom kuat dwikutub-dwikutub untuk usikan secara berkala yang berbeza-beza. Dinamik dikawal oleh persamaan Gross-Pitaevskii dengan tidak linear tambahan, menghasillan dengan satu interaksi dipol tidak bersetempat. Model matematik, berdasarkan variasi anggaran, telah dihasilkan dan digunakan untuk pengujaan parametrik kondensat kerana pekali berkala yang berbeza-beza daripada ketaklelurusan tidak bersetempat. Model ini meramalkan bentuk gelombang bagi soliton dalam kondensat dipol dan menerangkan amplitud dinamik kecil dengan agak tepat. Ramalan teori disahkan oleh simulasi persamaan tidak bersetempat Gross-Pitaevskii dan persamaan yang baik di antara mereka didapati. Keputusan boleh membawa kepada pemahaman yang lebih baik mengenai sifat-sifat gas kuantum ultra-sejuk, seperti ^{52}Cr, ^{164}Dy dan ^{168}Er, di mana jarak jauh interaksi atom dwikutub menguasai interaksi biasa.

Dinamik lantunan gelombang soliton di permukaan (cermin atom) di bawah kesan graviti telah dikaji melalui analisis simulasi. Penerangan analisis adalah berdasarkan kepada teknik variasi. Ayunan salunan pusat jisim soliton, disebabkan oleh modulasi

panjang penyerakan atom dan kecerunan keupayaan linear telah dianalisis. Dalam ujikaji berangka kita memerhatikan pecutan soliton apabila kedudukan permukaan dan berubah secara berkala. Ramalan Analisis dibandingkan dengan hasil simulasi berangka persamaan Gross-Pitaevskii dan persamaan kualitatif di antara mereka didapati.

I would like to dedicate my this work to

*Spirit of my father **Omar** (Rahmat Allah upon him), my mother **Fatma**, my beloved wife*

Nassima,** my lovely children **Mariam, Munib** and **Mohamed

*my brothers: **Salah, Abdarrhman, Hocine** and **Nasserddine***

*my sisters: **Horia, Samira, Simouna** and **Zahia***

Acknowledgement

Table of contents

Table of figures

List of abbreviation

Abbreviation in the text

BEC   Bose-Einstein condensation

GPE   Gross-Pitaevskii equation

DDI   dipole-dipole interaction

SILMs   Strongly Intrinsic Localized Modes

DNLS   Discrete Non-Linear Schrödinger

FFT   fast Fourier transform

Fundamental Physical constants

denotation	Symbol	value
Plank constant	h	$6.62606876 \ 10^{-34} \, Js$
	$\hbar = \dfrac{h}{2\pi}$	$1.05457159 \ 10^{-34} \, Js$
Boltzmann constant	k_B	$1.3806503 \ 10^{-23} \, JK^{-1}$
Mass of electron	m_e	$9.109382 \ 10^{-31} \, kg$
Bohr magneton	$\mu_B = \dfrac{e\hbar}{2m_e}$	$9.27400968 \ 10^{-24} \, JT^{-1}$

List of used Symbols

Symbol	Denotation
Ψ	Condensate wave function
ψ	Scaled condensate wave function
H	Hamiltonian
U_0	Two-body interaction strength
$V_{tr}(r)$	Trapping potential
M, m	Atomic mass
μ	Chemical potential
N	Number of condensed atoms
a_s	s-wave scattering length
λ_{dB}	de Broglie wave length
n	The density of condensate
$\omega_\perp$, $\omega_\parallel$	The radial, longitudinal frequency
g_{1D}, γ and μ	Nonlinearity coefficients
$\Re(...)$	Real part of …
$\Im(...)$	Imaginary part of …

1 Introduction to
Bose-Einstein condensate

The background area of research of this study shall be presented. The main subject of this study is *Bose-Einstein condensate*. In this chapter, the definition of Bose-Einstein condensate is given. The history of Bose-Einstein condensation is briefly reviewed based on classic textbooks and scientific literatures. In this study, the mathematical models employed to describe the phenomenon in different approaches and different aspects, are developed. Finally, we take a glimpse into variational approximation, modulation instability, intrinsic localized modes, dipolar interaction and finally, the bouncing of matter wave solitons reflecting on mirror.

1.1 Outline of thesis

The thesis contains five chapters, and it is structured as the follows. In chapter one, the definition of Bose-Einstein condensate is given and brief history of its development is presented, which was a big challenge to orient the experimental physicist. In addition, Gross-Pitaevskii equation is reviewed in time-dependent scheme and then deduced into time-independent equation. Furthermore, a short introduction and review on the variational approximation approach, the modulation instability, and intrinsic localized modes and dipolar local (short arrange) and nonlocal interaction (long-arrange) are given. Finally, the bouncing of a matter wave solitons reflecting on mirror is reviewed.

In second chapter, the modulation instability in one-dimension in discrete system is investigated, which was described by Salerno equation. The model can applied to Bose-Einstein condensate in deep optical lattice. The analytical expression for the modulation instability gain spectra is obtained. The regions and conditions of instability of plan wave solutions in the parameter space of the governing Salerno model are determined by using linear perturbation theory. The existence solutions and stability criteria for the different type strongly localized modes in discrete Salerno model have been derived. In addition, by applying the homoclinic orbits intersection method, the localized solutions of Salerno model were obtained numerically

In third chapter, the dipolar interaction is studied. The concepts of nonlocal interactions between particles are briefly introduced. The convenient model for this problem is suggested and the trial function is chosen. The variational approximation method is applied then the problem is simulated numerically. The analytical results and numerical results were compared.

In fourth chapter, the bouncing of particles of Bose-Einstein condensate on mirror is studied, the mirrors were created by strongly magnetic field using similar method.

In fifth and last chapter, we conclude and highlight the main results of this study.

1.2 Bose-Einstein condensation

Recently, there has been increased interest in the study of theoretical, experimental and numerical simulations of Bose-Einstein condensates in different aspects; see for example (Abdullaev, Gammal, Malomed, & Tomio, 2013; Alamoudi, Al Khawaja, & Baizakov, 2014; M. H. Anderson, Ensher, Matthews, Wieman, & Cornell, 1995; Bradley, Sackett, Tollett, & Hulet, 1995; Davis et al., 1995; Grossmann & Holthaus,

1995; Ketterle & Van Druten, 1996; Lin, Jimenez-Garcia, & Spielman, 2011; Plumhof, Stöferle, Mai, Scherf, & Mahrt, 2013).

Let us first introduce the definition of Bose-Einstein condensation. A *Bose-Einstein condensation is the phenomenon of a macroscopic population of the ground state of the many body quantum system at finite temperature. Bose-Einstein condensate is considered a coherent matter wave*.

In this section, a short introduction about Bose-Einstein condensate is presented. First, the history of Bose-Einstein condensate is presented and then, the basic idea of Gross-Pitaevskii equation is described. At the end of this section, the recent literature related to the subject of this study is surveyed.

1.2.1 Brief history of Bose-Einstein condensation

At the beginning of first quarter of last century in 1924, Satyendra Nath Bose proposed new statistical approach to describe quantum statistical distribution of light quanta (photons) (Bose, 1924) at low temperature. Bose's paper was rejected for publication. He then sent it to Albert Einstein to review and evaluate his article. Albert Einstein translated the paper to German and published the work in a journal in Germany. Albert Einstein extended Bose's approach to massive particles (Einstein, 1924). Einstein's approach was different from the Bose approach. The number of massive particles is conserved in Einstein's approach, however, the number of photons is non-conserved in Bose's approach. Einstein predicted theoretically that, it is possible to condense massive particles under certain conditions such as temperature (below critical temperature). At the critical temperature, a new phase starts to occur and a part of particles will condense into the new quantum state which has the lowest state energy, and which is called

ground state energy with non-interaction between particles. This means that the condensate particles occupy the single quantum state and then it creates a new quantum state of matter, which is called "The Bose-Einstein condensate".

Since then, attempts have been made to achieve this phase of matter experimentally. The first experiment connecting to The Bose-Einstein condensation was superfluidity. The work was proposed by F. London (London, 1938), who worked on liquid helium. L. Keldysh applied the idea of Bose-Einstein condensates on the condensation of excitons in semiconductor in 1968 (Keldysh & Kozlov, 1968).

There had not been any real experiment producing Bose-Einstein condensates until 1995. Bose-Einstein condensates have been observed in the weakly interaction Bose gas for vapor of rubidium $\left(^{87}\text{Rb} \right)$ (M. H. Anderson et al., 1995), in sodium $\left(^{23}Na \right)$ (Davis et al., 1995) and in Lithium $\left(^{4}Li \right)$ (Bradley, Sackett, & Hulet, 1997). The particles are trapped by a magnetic potential, the atoms cooled to micro-Kelvin by using evaporative cooling. For this work, Cornell, Wieman and Ketterle won the Nobel prize in 2001 (Cornell & Wieman, 2002).

It is easy to achieve Bose-Einstein condensates in alkali gases due to the level structure of atoms. Lasers can be applied for cooling atoms. Since these atoms have magnetic moments, they can be trapped using a magnetic potential. Up to this date (2014), Bose-Einstein condensate was realized by around 13 elements Rb (Rubidium), Na (Sodium), Li (Lithium), K (Potassium), Cs (Cesium), H (Hydrogen), He (Helium), Yb (Ytterbium), Cr (Chromium), Ca (Calcium), Sr (Strontium), Dy (Dysprosium), Er (Erbium). The typical experimental parameters are given, the density of Bose-Einstein condensate is around $10^3 - 10^4 \, \text{atom/cm}^3$, The dilute gases density is ,

$n \approx 10^{13} - 10^{14}$ atom/cm^3 with we know the air density very dilute gases is around $n \approx 10^{19}$ atom/cm^3.

The properties of cold quantum gases are mainly determined by interaction forces between particles. For dilute gases of alkali atoms, which constitute the major part of the Bose-Einstein condensate family, the interaction potential in the ultra-cold regime can be modeled, to a very good precision, by a delta function

$$U_{cont}(r) = \frac{4\pi\hbar^2 a_s}{m} . \delta(r). \tag{1.1}$$

This corresponds to an isotropic contact interaction between particles of mass m, whose strength is proportional to the *s*-wave atomic scattering length a_s. Such a single parameter pseudo-potential has been quite successfully used in the interpretation of experimental data obtained in the mean field regime (Dalfovo, Giorgini, Pitaevskii, & Stringari, 1999; Kevrekidis, Frantzeskakis, & Carretero-González, 2007).

As it is known, a Bose-Einstein condensate starts to form when the distance between particles is comparable to the de Broglie wave length in thermal equilibrium, which has form

$$\lambda_{dB} = \sqrt{\frac{\hbar}{2\pi m k_B T}}, \tag{1.2}$$

where T is the temperature of the particles, k_B is Boltzmann's constant and m is the mass of the particles which share to construct condensate.

The definition of an ultra-cold gas is the system which satisfies the condition (Baranov, 2001)

$$\lambda_{dB} \geq n^{-1/3}, \qquad\qquad\qquad (1.3)$$

where n is the density of the gas. In this case, the atomic wave function starts to overlap and the single wave function can describe the system.
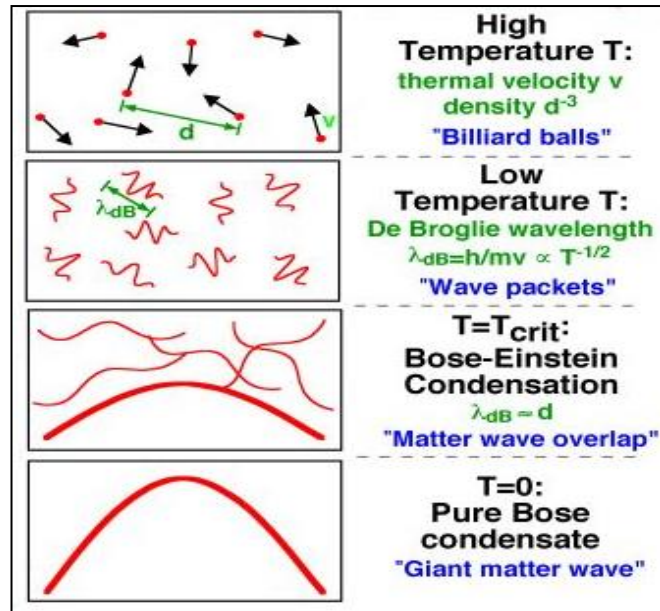
Figure 1.1: Showing the occurrence of Bose-Einstein condensate (BEC) is depended by decreasing the temperature zero. ref (Durfee & Ketterle, 1998)*.*

Bose-Einstein condensate is produced by a dynamical evaporation method to create Bose Einstein condensates.

As we know, a matter has five kinds of phases in the nature, gas, liquid, solid, plasma and Bose-Einstein condensation. So, the phase of the matter was changes from one phase to other by changing some parameters such as temperature, pressure, density of particles, potential trap and so on. A Bose-Einstein condensation is a phase transition in a macroscopic number of particles which have the same quantum states under special conditions, which will be discussed later. Bose-Einstein condensation is considered as a

very interesting and exciting area of research in physical systems. There are many recently hot topics which are related to Bose-Einstein Condensation such as spin-orbit coupled Bose-Einstein Condensation, dipolar interaction in single or coupled Bose-Einstein condensation, bouncing matter wave bright solitons of Bose-Einstein condensation on mirror, which is affected by the potential of gravity, and so on.

The aim of this thesis is studying the proprieties of Bose-Einstein condensate. In this study, we suggest some models, to describe Bose-Einstein condensate and its properties. Let us first gives a short survey of existing models before describing the model studied in this thesis.

1.2.2 Description of Gross-Pitaevskii equation

The Gross-Pitaevskii equation (GPE) is one of the main models that can properly describe the behavior of condensate particles below to critical temperature. Gross. and Pitaevskii (Gross, 1961; Pitavskii,1961; Pitaevskii, Stringari, & Leggett, 2004) have developed the main field theory for describing the interaction in Bose-Einstein condensation by using the mean field approach. Gross-Pitaevskii equation is considered as Schrödinger equation valid below the critical temperature, where all particles (bosons) exist in the same quantum states. It is derived and applied to the calculation of ground-state energy of the system. The Hamiltonian can be formulated as follows:

$$ H = \int dr \hat{\Psi}^{\dagger}(r) \left[-\frac{\hbar^2}{2m} \nabla^2 + V(r) \right] \hat{\Psi}(r) + \frac{1}{2} \int dr dr' \hat{\Psi}^{\dagger}(r) \hat{\Psi}^{\dagger}(r') V(r-r') \hat{\Psi}(r') \hat{\Psi}(r). \qquad (1.3) $$

where $\Psi^{\dagger}(r)$ is the creation of operator, $\hat{\Psi}(r)$ is the annihilation of operator at position r in second quantization and $V(r-r')$ is the two body interaction potential.

The field operator $\hat{\Psi}(r,t)$ decomposed into two parts,

$$\hat{\Psi}(r,t) = \Psi(r,t) + \Psi'(r,t) \qquad (1.4)$$

where $\Psi(r,t) = \langle \hat{\Psi}(r,t) \rangle$ represents the macroscopic wave function of the condensate. $\hat{\Psi}'(r,t)$ represents the non-condensate part at temperatures below T_c. Which is neglected in the present study. Thus, we assume that

$$\hat{\Psi}'(r,t) = 0 \qquad (1.5)$$

For deriving the equation of Gross-Pitaevskii, The Heisenberg equation should be used

$$i\hbar \frac{d \Psi(r,t)}{dt} = [\Psi, H] \qquad (1.6)$$

Gross-Pitaevskii has famous form, which is given (Pethick & Smith, 2002) as

$$i\hbar \frac{\partial \Psi(r)}{\partial t} = \left(\frac{\hbar^2}{2m} \nabla^2 + V_{ext}(r) + g_{3d} |\Psi(r)|^2 \right) \Psi(r). \qquad (1.7)$$

where $g_{3d} = \dfrac{4\pi\hbar^2 a_s}{m}$ is the nonlinear coefficient and that discribes effective interaction between particles in three dimensional. a_s is s-wave scattering length and it is negative (positive) for attractive (repulsive) interactions. m is mass of an atom. $\Psi(r)$ is the wave function, which describes the macroscopic condensates. It is important to know that the description of the interaction as a mean field as it done in the GPE is valid for a dilute gas, where $na_s^3 \ll 1$ as mentioned early.

The ground state energy is given

$$E = \int \left(\frac{\hbar^2}{2m} |\nabla \psi|^2 + V(r)|\psi|^2 + \frac{1}{2} g |\psi|^4 \right) dr, \qquad (1.8)$$

For time independent phenomena, we have

$$\Psi(r,t) = \psi(r)\exp\left(-i\frac{\mu t}{\hbar}\right) \tag{1.9}$$

where $\psi(r)$ is real function and normalized to the total number of particles as

$$\int_{-\infty}^{+\infty} |\psi(r,t)|^2 \, dr = N. \tag{1.10}$$

Then the time independent Gross-Pitaevskii equation (GPE) is obtained

$$\mu\psi(r) = \left(\frac{\hbar^2}{2m}\nabla^2 + V_{ext}(r) + g|\psi(r)|^2\right)\psi(r) \tag{1.11}$$

Obtaining the ground State Energy from stationary solution of the GPE, using the formalism the mean field theory

$$\psi(r) = \sqrt{n} = constant. \tag{1.12}$$

At a temperature very close to the zero temperature $T = 0$, the chemical potential is given by

$$\mu = \frac{dE}{dN}. \tag{1.13}$$

For a special case in absence of external potential $V = 0, \quad E_{kinitic} = 0$

$$\mu = E_{Kinitic} + V_{ext} + g|\psi|^2 = gn \tag{1.14}$$

where $n = |\psi|^2$ is the density of Bose gas.

Then, the ground state energy is

$$\frac{E}{N} = \frac{2\pi a_s \hbar^2 n}{m}$$

(1.15)

1.3 Description of variational approximation

In this section, we will present the short introduction and description of variational approximation method. We will use this method in chapter three and four for our analysis. The variational approximation method (Malomed, 2002) is one of the important tools to help us describe the dynamical of parameters of soliton solution of the non-integrable model, where the model of equation is a complicated partial differential equation (PDE) , which has non-integral analytical solutions. It was first developed for studying pulse propagation in the optical fibers (D. Anderson, 1983) and later applied to many other areas of nonlinear physics (Malomed, 2002).

So, the main idea of variational method is to find the Lagrangian density, which yields the main equations using the Euler-Lagrangian equation.

$$\frac{d}{dt}\frac{\partial \mathcal{L}\left(q,q_x,q_t,x,t\right)}{\partial q_t} + \frac{d}{dx}\frac{\partial \mathcal{L}\left(q,q_x,q_t,x,t\right)}{\partial q_x} - \frac{\partial \mathcal{L}\left(q,q_x,q_t,x,t\right)}{\partial q} = 0$$

(1.16)

Where q, q_x and q_t are general coordinates, x and t are space and time coordinates respectively.

Starting from this equation to find the averaged Lagrangian L

$$L = \int\limits_{-\infty}^{+\infty} \mathcal{L}dx.$$

(1.17)

Using the Euler-Lagrange equations again but with parameters variation of soliton (trial solution), we obtain the system of ordinary differential equations. Solving the ordinary differential equations gives the dynamical solutions of parameters, which means that, the parameters of trial function solution are obtained. Furthermore, useful relations between soliton parameters will be obtained. Additionally, we will treat the main model (PDE) numerically. Then in this step, we will compare the results between analytical results obtained from variational approximation method and numerical results from the PDE. It is worthy to mention here that the initial conditions affect the results. So, it is very important to choose suitable parameters at the initial time t_0.

In selecting the trial function for a soliton shape, there are many potential forms such as

- The Gaussian Ansatz is applied in (Benseghir, Abdullah, Baizakov, & Abdullaev, 2014)

$$\psi(x,t) = A(t)e^{-\frac{(x-\xi(t))^2}{2a(t)^2}+ib(t)(x-\xi(t))^2+ik(t)(x-\xi(t))+i\varphi(t)}. \qquad (1.18)$$

This trial function will be applied in the third chapter, good to specify conditions for the applicability of this ansatz.

- The Hyperbolic Secant Ansatz is applied in (Benseghir, Abdullah, Umarov, & Baizakov, 2013)

$$\psi(x,t) = A(t)\operatorname{sech}\frac{(x-\xi(t))}{a(t)}e^{ib(t)(x-\xi(t))^2+ik(t)(x-\xi(t))+i\varphi(t)}. \qquad (1.19)$$

This trial function, we will be applied in the fourth chapter.

where A is amplitude, a is width, ξ is center of mass position, b is the chirp, k is the velocity and φ is the phase of soliton. These parameters are called the time dependent variational parameters.

The Gaussian trial function is convenient for strong enough trapping potential and nonlinearity is defocussing. The hyperbolic scant trial function is more suitable for week confining potential and self-focusing nonlinearity.

Justification for the use of variational approximation, when the soliton solution is available, can have some advantages provided by the variational approximation in the analysis of existence and stability of soliton.

1.4 **Modulation Instability in Bose-Einstein condensation**

Modulational instability is one of the physical phenomenon which is known as the fundamental aspect of theory of nonlinear waves. This phenomenon consists of the instability of nonlinear plane waves against weak long-scale modulations with wave numbers (frequency) lower than some critical values. It has been predicted by Benjamin and Feir (Benjamin & Feir, 1967) for waves in deep water and by Bespalov and Talanov (Bespalov & Talanov, 1966) for electro-magnetic waves in nonlinear media with cubic nonlinearity. Later, it was observed in nonlinear optics (Karpman, 1967; Ostrovskii, 1967; Taniuti & Washimi, 1968), plasma physics (Gómez-Gardeñes, Malomed, Floría, & Bishop, 2006; Hasegawa, 1970), and condensate matter (Bose-Einstein Condensate, long Josephson junction,...) (Nicolin, Carretero-González, & Kevrekidis, 2007; Strecker, Partridge, Truscott, & Hulet, 2002). The phenomenon of modulational instability will be investigated in the next chapter.

1.5 Intrinsic Localized modes in Salerno equation

In the last decades much attention has been directed toward the investigation of localized solutions based on nonlinear models in different areas of physics and engineering. In particular, the dynamical nonlinear localization phenomena (Flach & Gorbach, 2008; Kevrekidis, 2009; Lederer et al., 2008) have been observed in spatially discrete system by both theoretical, experimental and numerical simulation studies. Spatial localized oscillations are called localized modes, which can exist in impure harmonic crystal. For lattices free from impurities, the localized modes can exist due to the nonlinearity of on-site and inter-site interactions. In this section, we review strongly localized nonlinear modes in anti-continuum in the well-known Salerno discrete model (Salerno, 1992). This model has been applied to describe Bose-Einstein condensation in nonlocal optical lattices (Gómez-Gardeñes et al., 2006) and in biophysics of DNA (Tabi, Mohamadou, & Kofane, 2010).

1.6 Long-range dipolar interaction in Bose-Einstein condensates

Bose-Einstein condensation of chromium with anisotropic and long-range dipolar atomic interactions has opened a new direction in the physics of ultra-cold quantum gases (Griesmaier, Werner, Hensler, Stuhler, & Pfau, 2005; Lahaye, Menotti, Santos, Lewenstein, & Pfau, 2009). Subsequently, two other species with strong dipolar interactions, namely dysprosium (Lu, Burdick, Youn, & Lev, 2011) and erbium (Aikawa et al., 2012), were confirmed to be Bose condensed. The principal difference of chromium condensates from the alkali atom condensates is that, ^{52}Cr has a large permanent magnetic dipole moment $\mu = 6\mu_B$, where $\mu_B = \dfrac{e\hbar}{2m_e}$ is the Bohr magneton.

Since the dipole-dipole force is proportional to the square of the magnetic moment, the

dipolar interactions in chromium condensate is a factor of 36 times stronger than in alkali atom condensates, like ^{87}Rb. Similar arguments pertain also for other dipolar quantum gases, ^{164}Dy and ^{168}Er. There is another group of alkaline-earth elements ^{40}Ca and ^{84}Sr, Bose-condensation which do not carry the magnetic moment, were reported in Ref. (Kraft, Vogt, Appel, Riehle, & Sterr, 2009) and Ref. (Stellmer, Tey, Huang, Grimm, & Schreck, 2009) respectively,. The peculiarity of this group is that, the condensate can be held and manipulated in optical traps. In addition, magnetic Feshbach resonances frequently applied to tune the scattering properties of other atomic systems. The optical Feshbach resonance technique (Ciuryło, Tiesinga, & Julienne, 2005; Naidon & Julienne, 2006), instead of magnetic, serves the purpose in BEC of alkaline-earth elements. This group holds promise for wide applications in metrology, quantum computation, quantum simulators of many-body phenomena and ultracold plasmas.

Long-range and anisotropic character of atomic interactions drastically modify the properties of dipolar condensates compared to other BECs that have been found (Griesmaier, 2007). Tunability of contact interactions by a Feshbach resonance (Chin, Grimm, Julienne, & Tiesinga, 2010; Köhler, Góral, & Julienne, 2006) allows to enter the regime of dominant dipolar interactions by lowering the contact interactions. In fact continuous transition between both regimes, with dominant contact or long range interactions is possible by this technique.

Interactions between atoms in Bose-Einstein condensate is the factor leading to nonlinearity of the governing equation. Although these interactions are very weak in dilute gases, all essential properties of Bose-Einstein condensates are determined by the strength, range and symmetry of interatomic forces. For short range contact interactions and sufficiently low temperature the dynamics of Bose-Einstein condensates is well described by the Gross-Pitaevskii equation with local cubic nonlinearity (Pethick &

Smith, 2002; Pitaevskii et al., 2004). In contrast to other elements in the Bose-Einstein condensates family, the atomic interactions of dipolar gases are long-range and anisotropic. This circumstance substantially changes the properties and mathematical treatment of dipolar Bose-Einstein condensates. Due to the long-range correlations, not only the local density but also the whole density distribution in the condensate determines the interaction potential of an atom in the cloud. This interaction leads to the nonlocal Gross-Pitaevskii equation for description of the dynamics of dipolar condensates.

The nonlocal characteristics of atomic interactions prevents the collapse of a two-dimensional (2D) Bose-Einstein condensate loaded in a pancake-shaped trap and gives rise to stable isotropic (Pedri & Santos, 2005) and anisotropic 2D solitons (Tikhonenkov, Malomed, & Vardi, 2008), whose properties are well described by the variational approximation. Some essential properties of 1D bright solitons in dipolar Bose-Einstein condensates with competing local and nonlocal atomic interactions, including the existence regimes, stability and collision dynamics, were reported in ref (Cuevas, Malomed, Kevrekidis, & Frantzeskakis, 2009). Recently a model for describing the dipolar condensate has been introduced, in which the dipole-dipole interaction is periodically modulated in space (Abdullaev et al., 2013). It was shown that the variational approximation (VA) provides accurate predictions for the shape of solitons and their stability by means of the Vakhitov-Kolokolov criterion. The importance of low energy shape oscillations of matter-wave packets in studying the microscopic properties of dipolar quantum gases was pointed out in Ref. (Yi & You, 2002). A non-integral form of the Gross-Pitaevskii equation for polarized molecules was proposed in (Andreev, Magomedbekov, & Sicking, 2013) and applied to the investigate of the collective excitation spectrum of dipolar Bose-Einstein condensate.

The existence regime of bright solitons in the electrically polarized Bose-Einstein condensates was identified using the proposed model.

1.7 **The bouncing of matter-wave bright soliton in Bose-Einstein condensates**

A particle bouncing on the reflecting surface under the effect of gravity represents one of the analytically solvable models in quantum mechanics (Flügge, 1971; Sakurai, 1994). Gibbs introduced the name "quantum bounce" (Gibbs, 1975) for the object, and it was extensively studied in many articles of pedagogical orientation (Desko & Bord, 1983; Gea-Banacloche, 1999, 2000; Goodings & Szeredi, 1991; Langhoff, 1971; Whineray, 1992) and original research papers (for a recent review see (Belloni & Robinett, 2014)). The practical interest in this model has emerged from recent experiments aimed at probing the coherence properties of Bose-Einstein condensates falling under gravity and bouncing off a mirror formed by a far-detuned sheet of light (Bongs et al., 1999; Perrin, Colombe, Mercier, Lorent, & Henkel, 2006; Savalli et al., 2002), quantum reflection of matter waves (Cornish et al., 2009; Lee & Brand, 2006; T. Pasquini et al., 2006; T. A. Pasquini et al., 2004), and measuring the Casimir-Polder force acting upon the atoms near solid surfaces (Harber, Obrecht, McGuirk, & Cornell, 2005; Obrecht et al., 2007; Sorrentino et al., 2009).

Another important result linked to the quantum bouncer problem has been the experimental observation of quantum bound states of neutrons in the Earth's gravitational field (Abele & Leeb, 2012; Ichikawa, Komamiya, & Kamiya, 2014; Nesvizhevsky et al., 2002). In these pioneering experiments the quantum states of matter formed by a gravitational field were observed for the first time. Also, the model is of particular interest from the viewpoints of the physics and applications of quantum states of nanoparticles in the vicinity of surfaces (Canaguier-Durand et al., 2011). An optical analogue of the quantum bouncer, a photon bouncing ball, was experimentally

demonstrated using a circularly curved optical waveguide (Della Valle et al., 2009). Significance of the model for the study of the dynamics of particles in quantum-classical interface was pointed out in (Belloni, Doncheski, & Robinett, 2005; M. Doncheski & Robinett, 2001; M. A. Doncheski & Robinett, 1999).

This work extends the quantum bouncer model to the nonlinear domain by considering the dynamics of a matter wave soliton that are governed by the Gross-Pitaevskii equation. The linear potential entering the Gross-Pitaevskii equation represents the Earth's gravitational field acting on the soliton along the vertical direction, while the horizontal atomic mirror (Kasevich, Weiss, & Chu, 1990) created by a laser beam or magnetic field stands for the reflecting surface. The matter wave soliton performs bounded motion in such a gravitational cavity. The effect of nonlinearity, originating from the atomic interactions in Bose-Einstein condensate (BEC), shows up as an ability of the bouncing wave packet to remain localized during the evolution, behaving like a rigid ball, rather than a deformable wave packet. The possibility of tuning the atomic interactions in the condensate by external magnetic (Köhler et al., 2006) and optical (Ciuryło et al., 2005) fields opens perspectives in exploring the bouncer problem in both the quantum and classical limits.

The main objective under this subject is to develop analytical descriptions for describing the dynamics of soliton above the atomic mirror under the effect of gravity. As an illustration of the developed model, we considered the resonant oscillations of the soliton's center of mass position under periodically varying strength of nonlinearity and the slope of the quasi-1D trap with respect to the horizontal reflecting surface. The strength of nonlinearity can be tuned using the Feshbach resonance technique (Köhler et al., 2006), or alternatively, by changing the strength of the radial confinement. The Fermi type acceleration of the soliton is demonstrated by numerical simulation when the

vertical position of the mirror is periodically varied in time. It should be noted that Fermi acceleration of matter wave packets was previously considered in (Saif, Naseer, & Ayub, 2014; Saif & Rehman, 2007) for the case of non-interacting BEC, in the setting where matter wave solitons do not exist. This work a non-dispersive acceleration of the wave packet was reported to take place under certain conditions, when the modulation strength and frequency provide the dynamical localization of the matter wave.

The advantage of the present setting is that, the bouncing matter wave packet preserves its integrity due to the focusing nonlinearity of BEC, which counteracts the dispersive spreading. Another interesting approach to acceleration of a single quantum particle, also feasible in the context of matter waves, was reported in (Granot & Malomed, 2011). The mechanism consists in binding the wave packet by a delta function potential well and evolving in accelerated motion along with the potential. In the linear case and ideal mirror potential our model reduces to the equation which has analytic solution in terms of Airy functions. The dynamics of Airy beams currently represents one of the actively explored topics motivated by important applications in optical communications and nonlinear optics (Broky, Siviloglou, Dogariu, & Christodoulides, 2008; Chamorro-Posada, Sánchez-Curto, Aceves, & McDonald, 2014; Chremmos & Efremidis, 2012; Siviloglou, Broky, Dogariu, & Christodoulides, 2007)

In the final of this chapter, I should mention to the objectives of this study.

- We investigate the properties of Modulational Instability in the Salerno equation in quasi-one dimension in Bose-Einstein condensate (BEC).

- We analyzed the regions of modulational instability of Nonlinear plane waves and determine the conditions of its existence in BEC

- We investigate the Strongly localized modes in nonlinear models in different areas of physics and engineering.

- We compare the analytical results of SLM in spatial discrete system with numerical simulation

- We study the response of a Bose-Einstein condensate with strong dipole-dipole atomic interaction to periodically varying perturbation.

- To develop analytical description of soliton's dynamic above the atomic mirror under the effect of the gravity, we consider the resonant oscillations of the soliton's center of mass position under periodically varying strength of nonlinearity and slop of quasi 1D

- Use the numerical tools to investigate Bose-Einstein condensate s through solving the GPE (Nonlinear PDE)

2 Modulation instability and strongly Localized Modes in discrete 1D Systems

In this chapter, the modulation of instability of plane waves and intrinsic localized modes are investigated in discrete system by using the Salerno model.

2.1 Modulational Instability in Salerno Model

In this section, the modulation instability in Salerno model will be studied, the regions and conditions of existence of modulational instability are determined in Bose-Einstein condensates in a periodic potential trap, in this case we choose the potential trap as optical lattices, which are created by laser beams.

2.1.1 The model equation

It is very important to investigate the modulational instability in different models. We restrict ourselves to the Salerno model for Bose-Einstein condensate in optical lattice in quasi-1D. This model is a combination of the discrete non-linear Schrodinger (DNLS) equation (Eilbeck & Johansson, 2003) with cubic nonlinearity and Ablowitz-Ladik (AL) equation (Ablowitz, Prinari, & Trubatch, 2004) s follows (Gómez-Gardeñes et al., 2006).

$$i\dot{\phi} + \left(1 + \mu|\phi_n|^2\right)\left(\phi_{n+1} + \phi_{n-1}\right) + 2\upsilon|\phi_n|^2 \phi_n = 0 \qquad (2.1)$$

where ϕ_n is the complex field amplitude at n^{th} site of the lattice, μ is the nonlinearity of (AL) equation, and υ is the nonlinearity of the discrete nonlinear Schrödinger (DNLS) equation.

2.1.2 Modulational Instability of nonlinear plane wave

The nonlinear discrete equation (2.1) has a plane wave solution

$$\phi_n = \phi_0 \exp\left[i\left(qn + \omega t\right)\right], \tag{2.2}$$

where ϕ_0 is the amplitude q is wave number and ω is the frequency of plane wave. When substituted in equation (2.1), we obtain

$$\left[-\omega + 2\cos(q)\left(1 + \mu\phi_0^2\right) + 2\upsilon\phi_0^2\right]\phi_n = 0 \tag{2.3}$$

Equation (2.3) has two solutions, one is the trivial solution for $\phi_n = 0$, this solution is not important and it does not give us any information on our system, the other solution is

$$-\omega + 2\cos(q)\left(1 + \mu\phi_0^2\right) + 2\upsilon\phi_0^2 = 0.$$

Then, this solution gives us the relationship between the frequency and wave number, which is called " *dispersion relation*".

$$\omega = 2\cos(q)\left(1 + \mu\phi_0^2\right) + 2\upsilon\phi_0^2 \tag{2.4}$$

For an unstaggered solution, when $q = 0$, the dispersion becomes

$$\omega = 2 + 2\left(\mu + \upsilon\right)\phi_0^2 ,$$

for the staggered solution, when $q = \pi$ the dispersion becomes

$$\omega = -2 - 2\left(\mu - \upsilon\right)\phi_0^2 ,$$

we find the same result as in (Hasegawa, 1970).

For investigating the stability of the plane wave solution in equation (2.2) against small perturbation $\delta\phi_n(t)$, we use the perturbation theory and linear approximation theory by adding a small perturbation to the amplitude of the plane wave solution such that

$$\phi_n = \left(\phi_0 + \delta\phi_n(t)\right)\exp\left[i\left(qn + \omega t\right)\right] \tag{2.5}$$

and examine the evolution of the perturbation $\delta\phi_n(t)$ using the linear stability analysis.

Substituting equation.(2.5) into equation.(2.1) and linearizing for $\delta\phi_n$, it becomes

$$i\delta\dot{\phi}_n - 2\cos(q)\delta\phi_n + 2\cos(q)\mu\phi_0^2\,\delta\bar{\phi}_n + \left(1 + \mu\phi_0^2\right)\left(\exp[iq]\delta\phi_{n+1} + \exp[-iq]\delta\phi_{n-1}\right)$$

$$+2\upsilon\phi_0^2\left(\delta\phi_n + \delta\bar{\phi}_n\right) = 0 \tag{2.6}$$

where $q = 0$ or $q = \pi$ then $\sin(q) = 0$, so the equation (2.6) becomes

$$i\,\delta\dot{\phi}_n - 2\cos(q)\delta\phi_n + 2\cos(q)\mu\phi_0^2\,\delta\bar{\phi}_n + \cos(q)\left(1 + \mu\phi_0^2\right)\left(\delta\phi_{n+1} + \delta\phi_{n-1}\right)$$

$$+2\upsilon\phi_0^2\left(\delta\phi_n + \delta\bar{\phi}_n\right) = 0$$

After simplifying the above equation, we obtain

$$i\delta\dot{\phi}_n + \cos(q)\left(1 + \mu\phi_0^2\right)\left(\delta\phi_{n+1} + \delta\phi_{n-1}\right) + 2\cos(q)\left[\mu\phi_0^2\,\delta\bar{\phi}_n - \delta\phi_n\right]$$

$$+2\upsilon\phi_0^2\left(\delta\phi_n + \delta\bar{\phi}_n\right) = 0$$

$$\tag{2.7}$$

to consider the modulational in the form below $\delta\phi_n = u_n + i v_n$ then its complex conjugate is $\delta\bar{\phi}_n = u_n - i v_n$, substituting the terms above into equation (2.6), we find

$$i\left(\dot{u}_n + i\dot{v}_n\right) + \cos\left(q\right)\left(1 + \mu\phi_0^2\right)\left(u_{n+1} + u_{n-1} + i\left(v_{n+1} + v_{n-1}\right)\right) +$$

$$2\cos\left(q\right)\left[\mu\phi_0^2\left(u_n - iv_n\right) - u_n - iv_n\right] + 2\upsilon\phi_0^2\left(2u_n\right) = 0 \qquad (2.8)$$

it is important to separate the last equation into real part and imaginary part as shown below

$$\begin{cases} \dot{u}_n + \cos\left(q\right)\left(1 + \mu\phi_0^2\right)\left(v_{n+1} + v_{n-1} - 2v_n\right) = 0 \\ \\ -\dot{v}_n + \cos\left(q\right)\left(1 + \mu\phi_0^2\right)\left(u_{n+1} + u_{n-1} - 2u_n\right) + 4v\phi_0^2 u_n = 0 \end{cases} \qquad (2.9)$$

It is then considered the modulation in the new form below

$$\begin{bmatrix} u \\ v \end{bmatrix} = \begin{bmatrix} \alpha \\ \beta \end{bmatrix} exp\left[i\left(Qn + \Omega t\right)\right] \qquad (2.10)$$

Where Q and Ω are the wave number and frequency of the perturbation respectively.

α, β are the amplitude of the small perturbation .

Substituting equation (2.10) into equation (2.9), we then obtain a system of equations as follow:

$$\begin{cases} i\Omega\alpha - 4\cos\left(q\right)\sin^2\left(\dfrac{Q}{2}\right)\left(1 + \mu\phi_0^2\right)\beta = 0 \\ \\ \left[4v\phi_0^2 - 4\cos\left(q\right)\left(\sin^2\left(\dfrac{Q}{2}\right)\left(1 + \mu\phi_0^2\right) - \mu\phi_0^2\right)\right]\alpha - i\Omega\beta = 0 \end{cases}$$

This system of equations is rewritten in matrix form

$$
\begin{bmatrix}
i\Omega & -4\cos(q)\sin^2\left(\dfrac{Q}{2}\right)\left(1+\mu\phi_0^2\right) \\[2em]
v\phi_0^2 - 4\cos(q)\left[\sin^2\left(\dfrac{Q}{2}\right)\left(1+\mu\phi_0^2\right)-\mu\phi_0^2\right] & -i\Omega
\end{bmatrix}
\begin{bmatrix} \alpha \\[2em] \beta \end{bmatrix} = 0
$$

If $\det(A) \neq 0$, the system has trivial solution where

$$
A = \begin{bmatrix}
i\Omega & -4\cos(q)\sin^2\left(\dfrac{Q}{2}\right)\left(1+\mu\phi_0^2\right) \\[2em]
v\phi_0^2 - 4\cos(q)\left[\sin^2\left(\dfrac{Q}{2}\right)\left(1+\mu\phi_0^2\right)-\mu\phi_0^2\right] & -i\Omega
\end{bmatrix}
$$

Computing the determinant of matrix, requiring $\det(A)=0$, it is found that

$$
\Omega^2 + 16\cos(q)\sin^2\left(\frac{Q}{2}\right)\left(1+\mu\phi_0^2\right)\left[v\phi_0^2 - \cos(q)\sin^2\left(\frac{Q}{2}\right)\left(1+\mu\phi_0^2\right)+\mu\phi_0^2\right] = 0
$$

Then, the frequency of perturbation modulation is given by

$$
-\Omega^2 = 16\cos(q)\sin^2\left(\frac{Q}{2}\right)\left(1+\mu\phi_0^2\right)\left[v\phi_0^2 - \cos(q)\left(\sin^2\left(\frac{Q}{2}\right)\left(1+\mu\phi_0^2\right)-\mu\phi_0^2\right)\right]
$$

Then, we derive the gain which has form

$$
g = \Im m|\Omega| = \left|4\sin\left(\frac{Q}{2}\right)\cos(q)\left(1+\mu\phi_0^2\right)\right|\sqrt{\frac{v\,\phi_0^2}{\cos(q)\left(1+\mu\,\phi_0^2\right)}+\frac{\mu\,\phi_0^2}{\left(1+\mu\,\phi_0^2\right)}-\sin^2\left(\frac{Q}{2}\right)}.
\tag{2.11}
$$

From the gain equation (2.11), we determine the regions of modulational instability. If the expression under square root is negative then the frequency of perturbation is real, and the modulation is stable. Hence the perturbation leads to small oscillations. If the expression under square root is positive then the gain g is positive, the modulation is unstable, it means that the modulation is grows exponentially over time.

24

From the gain equation (2.11), we can see that the unstaggered solution $q = 0$ is

unstable whenever $\upsilon > \dfrac{1}{\phi_0^2}$, and the staggered solution $q = \pi$ is unstable whenever

$\upsilon < -\dfrac{1}{\phi_0^2}$. In the general case where q takes any value, we can distinguish two regions of

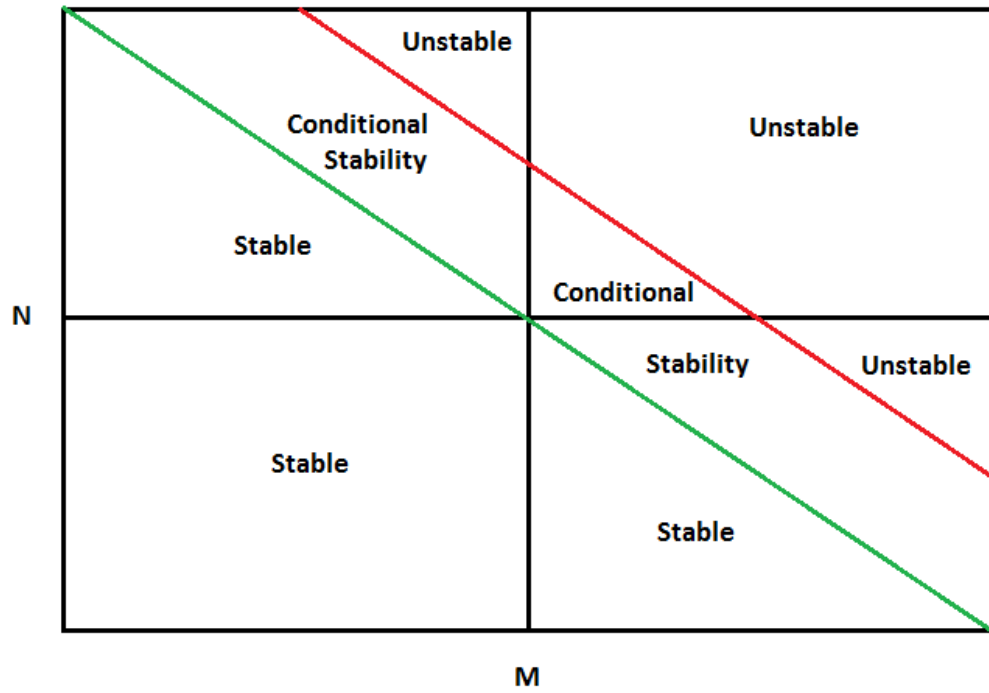modulational instability as shown in figure (Fig 2.1).

Figure 2.1: Modulational Instability regions

$$N = \frac{\upsilon \phi_0}{\cos(q)(1 + \mu \phi_0^2)}, \text{ and } M = \frac{\mu \phi_0^2}{\cos(q)(1 + \mu \phi_0^2)}$$

One region is fully unstable and other is conditionally stable, it means that it depends on the wave number of carrier waves (q) and wave number of perturbation (Q) as shown in the figure 2.1.

2.2 Strongly Localized Modes in Discrete Salerno Model

In this section, strongly localized nonlinear modes will be investigated in anti-continuum in discrete Salerno model. This model has been applied to describe Bose-Einstein condensate in nonlocal optical lattices.

2.2.1 The Model Equation

The Salerno Model is given as follows (Salerno, 1992; Umarov, Benseghir, & Messikh, 2011)

$$i\frac{\partial \Psi_n}{\partial t} + c\left(1 + \mu|\Psi_n|^2\right)\left(\Psi_{n+1} + \Psi_{n-1}\right) + v|\Psi_n|^2 \Psi_n = 0 \tag{2.12}$$

where t is the evolution parameter, n is the site index, Ψ_n represents the excitation at the nth site, c is the linear coupling coefficient, μ and υ are the effective non-linear coefficient, if $\mu = 0$, equation (2.12) reduces to discrete nonlinear Schrödinger equation, which is non-integrable, if $v = 0$ the equation (2.12) is the Ablowitz-Ladik equation, which is integrable (Umarov et al., 2011), all quantities are dimensionless.

In order to identify strongly localized intrinsic modes (SLIMs), we follow the method of ref. (Darmanyan, Kobyakov, & Lederer, 1998). We will consider two major types of solutions, the first one is the even mode or centered between sites modes, the second is odd or on site centered modes as shown in the figure 2.2.
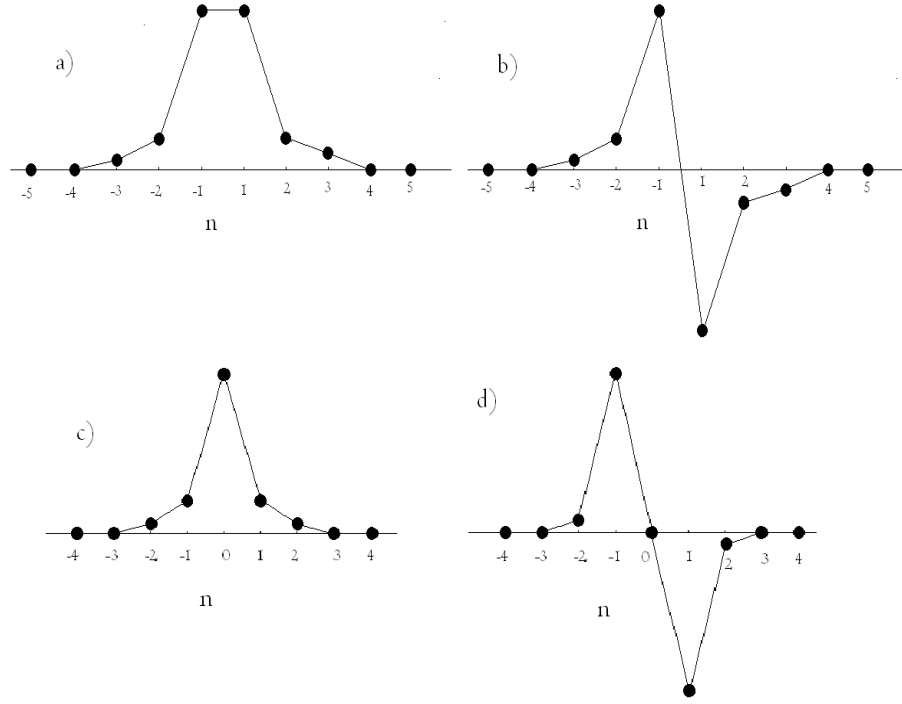
Figure 2.3: Strongly localized modes a) symmetric (in-phase oscillation) even mode (centred inter-sites) b)antisymmetric (out-phase oscillations) even mode c) symmetric odd mode (centred on a site) d) antisymmteric odd mode

Inserting

$$\Psi_n(t) = \psi_n \exp(i\omega t)$$

into equation (2.12), where ψ_n represents the respective amplitudes of a bright localized modes, we obtain the system of equations for the even mode solutions

$$\psi_n = A\left(\ldots, 0, \quad \alpha_3, \quad \alpha_2, \quad 1, \quad s, \quad s\,\alpha_2, \quad s\,\alpha_3, \quad 0\ldots\right),$$

where $|n| = 1,2,3,\ldots$ and $s = \pm 1$. For symmetry reasons the subscript $n = 0$ has been dropped. We can see that

$$\psi_{-n} = s\,\psi_n$$

the parameters defines the symmetry of the mode. For strong localization

$$|\alpha_3| << |\alpha_2| << 1$$

it follows that $\alpha_n \approx 0$ for $n > 3$.

$$\omega \cong \omega_{even} = \nu A^2 + sLc + \frac{Lc^2}{\nu A^2} \qquad (2.13)$$

$$\alpha_2 = c\nu A^2 - sL\left(\frac{c^2}{\nu A^2}\right) \qquad (2.14)$$

$$\alpha_3 = \alpha_2^2 = \left(\frac{c^2}{\nu A^2}\right)^2 \qquad (2.15)$$

where $L = 1 + \mu A^2$.

For the odd mode, the ansatz is

$$\psi_n = B\left(..., 0, \quad \beta_2, \quad \beta_1, \quad \beta_0, \quad s\beta_1, \quad s\beta_2, \quad 0...\right).$$

For the symmetric odd mode $s = 1, \quad \beta_0 = 1$

$$\omega \cong \omega_{oddsm} = \nu B^2 + 2K \frac{c^2}{\nu B^2} \qquad (2.16)$$

$$\beta_1 = \beta = \frac{c}{\nu B^2} \qquad (2.17)$$

$$\beta_2 = \beta^2 = \left(\frac{c^2}{\nu B^2}\right)^2 \qquad (2.18)$$

Where $K = 1 + \mu B^2$. For the antisymmetric mode $s = -1, \quad \beta_0 = 0, \quad \beta_1 = 1$.

$$\omega \cong \omega_{oddantsm} = \nu B^2 + 2K \frac{c^2}{\nu B^2} \tag{2.19}$$

$$\beta_2 = \beta = \frac{c}{\nu B^2} \tag{2.20}$$

The illustrations of different modes are given in figure (2.2).

To study the stability of Strongly Intrinsic Localized modes (SILMs), we impose complex perturbation $\delta(t)$ to each non-zero excitation amplitude (Darmanyan et al., 1998).

For even mode, we insert the perturbed profile

$$\psi_n = A\left(...,0, \alpha + \delta_2, 1 + \delta_1, s + \delta_1, s\alpha + \delta_2, 0,...\right)$$

into equation (2.12). Considerable simplification can be achieved by decomposition of the perturbations into symmetric and anti-symmetric component as

$$\delta_j^{\pm} = \delta_{+j} + \delta_{-j},$$

where (j=1,2) (Flach & Gorbach, 2008), which leads to decoupling the system. Separating the real and imaginary part of the perturbation, scaling time $\tau = \omega_e t$, we get two independent systems for the vector

$$\tilde{\delta}_j = \left(\tilde{\delta}_{1r}, \tilde{\delta}_{1i}, \tilde{\delta}_{2r}, \tilde{\delta}_{2i}\right)$$

$$\frac{d\tilde{\delta}^{\pm}}{d\tau} = \begin{pmatrix} 0 & (s-p)L\alpha & 0 & -(1+\mu A^2)\alpha \\ 2\left(1+s\frac{\mu}{v}\right)+2\left(\frac{\mu}{v}\right)+L\left(\frac{p-3s}{2}-\frac{\mu}{v}\right)\alpha & 0 & L\alpha & 0 \\ 0 & -\alpha & 0 & 1 \\ \alpha & 0 & -1 & 0 \end{pmatrix} \tilde{\delta}^{\pm} \qquad (2.21)$$

where $p = \pm 1$ depends with symmetric $(\tilde{\delta}_j^+)$ and antisymmetric $(\tilde{\delta}_j^-)$ perturbation.

Introducing $\tilde{\delta}_j \propto \exp(g\tau)$ (Kevrekidis, 2009), then the eigenvalue g of equation (2.21) is given by

$$g^4 + \left[2L\left((s-p)L\frac{\mu}{v}+(p-s)\frac{\mu}{v}-2L(ps-1)+1\right)\alpha^2 + 2L\left(p-s+(ps-1)\frac{\mu}{v}\right)\alpha+1\right]g^2$$

$$+L^2\alpha^4 + 2L\left(L(p-2s)+(1-L)\frac{\mu}{v}\right)\alpha^3 + 2L\left(2L(1-ps)+(s-p)L\frac{\mu}{v}+p\frac{\mu}{v}+1\right)\alpha^2 \qquad (2.22)$$

$$+2L\left((p-s)-(1-ps)\frac{\mu}{v}\right)\alpha = 0$$

where $s = \pm 1$ and $p = \pm 1$.

Solving equation (2.22) with unknown g. The system is stable when $\Re(g) = 0$ and otherwise unstable. Let us discuss the stability of system for different values of coefficients of Salerno equation equation (2.12). To be able to obtain the analytical results we ignore the higher powers of α . When $s = p$,

$$g = \sqrt{-1+8L\mu vs\alpha^2} ,$$

if $s = -1$, then the system exhibits the stability, if $s = 1$, the system is unstable if

$\alpha = \alpha_{cr} > \sqrt{8L\mu vs\alpha^2}$. When $s = -p$,

$$g \approx \sqrt{L(s + \mu v)\alpha} \ .$$

If $s = 1$, then we have the instability if $\alpha > 0$, $\mu < -\frac{1}{A^2}$ and $0 < v < |\mu|$, or α, μ and v are positive, if v is negative then $v > |\mu|$. In case α and v are negative and μ positive then $|v| < \mu$ or $0 > \mu > -\frac{1}{A^2}$ and $v > 0$ then $v < |\mu|$.

The system is stable in the following cases, when α and v are positive and $\mu < -\frac{1}{A^2}$, then $v < |\mu|$ or $\mu > 0$ then $0 > v > -\mu$ or $\alpha > 0$, $0 > \mu > -\frac{1}{A^2}$, and $\mu > o > 0$. For α negative, μ and v are positive, or α and v are negative $|v| > \mu > 0$. If $\alpha < 0, \mu < -\frac{1}{A^2}$ then $0 < v < |\mu|$.

For odd modes, we will follow the same procedure to study the stability of odd strongly localized modes with ignoring the second order β_2 for the odd symmetric, we identify the term of gain as

$$g = \sqrt{-1 + 2K\beta^2} \ .$$

The system is unstable if $\beta > \beta_{cr}$, where $\beta_{cr} = \frac{1}{2 + 2\mu B^2}$, it may be stable if $\beta < \beta_{cr}$ and μ is negative and $\mu > \frac{1}{B^2}$.

2.2.2 Two-Dimensional map

In this part, we aim to look for a solution in the form

$$\Psi_n = u_n e^{-i\lambda t}, \quad c = 1 \tag{2.23}$$

Inserting the previous equation into equation (2.12), it is found

$$\lambda u_n + \left(1 + \mu u_n^2\right)\left(u_{n+1} + u_{n-1}\right) + 2\nu u_n^3 = 0 \tag{2.24}$$

With the transformation $V_n = u_{n-1}$, the equation (2.24) becomes a two-dimensional map

$$u_{n+1} = -V_n - \left(\frac{\lambda + 2\nu u_n^2}{1 + \mu u_n^2}\right) u_n \tag{2.25}$$

Now we can apply the method developed in (Carretero-González, Talley, Chong, & Malomed, 2006), to get the localized solutions of equation (2.25). But before showing how to use this map, to obtain the solution of equation (2.25), we give a brief introduction on homoclinic orbits. It is known that a fixed point in two-dimensional map is a saddle point if the two eigenvalues of the Jacobian of the map, λ_1 and λ_2, satisfy the following inequalities

$$|\lambda_1| < 1, \quad |\lambda_2| > 1 \tag{2.26}$$

A saddle fixed point has a stable manifold and an unstable manifold. The stable manifold corresponds to the eigenvalue λ_1, while the unstable manifold corresponds to the other eigenvalue λ_2. A point of intersection between the stable and unstable manifolds is called a homoclinic point. The orbit that contains this point is called a homoclinic orbit. It is clear that any point in a homoclinic orbit will converge to the

saddle fixed point by forward and backward iterations. Finding an homoclinc point is important for us to investugate the type of soliton we can get.

Returning back to our map, equation (2.25), we can see that it has a singularity at $u_n = \pm \dfrac{1}{\sqrt{-\mu}}$ for negative values of μ. The fixed points for this map are found by solving the following set of equations

$$\begin{cases} u_{n+1} = u_{n,} \\ V_{n+1} = V_n \end{cases} \qquad (2.27)$$

Which leads to the following equation

$$u \left[2(\mu + \nu)u^2 + 2 + \lambda \right] = 0. \qquad (2.28)$$

From equation (2.28), one can see that the value $u = 0$ is always a fixed point. In addition to this, one can show that it is a saddle point only if $|\lambda| > 2$.

For the case when $\mu + \nu = 0$ and $\lambda = -2$, any value of u is indeed a fixed point but not a saddle point. For the case when $\mu + \nu \neq 0$ there are at most three fixed points corresponding to the values

$$\begin{cases} u_0 = 0, \\ \\ u_+ = +\sqrt{\dfrac{-1 - \lambda/2}{\mu + \nu}} \\ \\ u_- = -\sqrt{\dfrac{-1 - \lambda/2}{\mu + \nu}} \end{cases} \qquad (2.29)$$

We will focus on solutions where $u_n = 0$ when $n \to \infty$. This corresponds to the saddle fixed point $u_0 = 0$ with $|\lambda| > 2$.

It is worth mentioning that if the parameter $v \neq 0$, one can set $v > 0$ by using the transformation $\Psi_n = (-1)^n \Psi_n$, and then set it to one by scaling

$$
\begin{cases}
\Psi_n \to \dfrac{\Psi_n}{\sqrt{n}} \\[3mm]
\mu \to \mu v
\end{cases}
,
\tag{2.30}
$$

In figure (2.3), we plot the homoclinic orbits. The point denoted by a square symbol which is approximately at $(0.99, 0.77)$ is a homoclinic point. This points leads to the type of soliton depicted in figure (2.4)
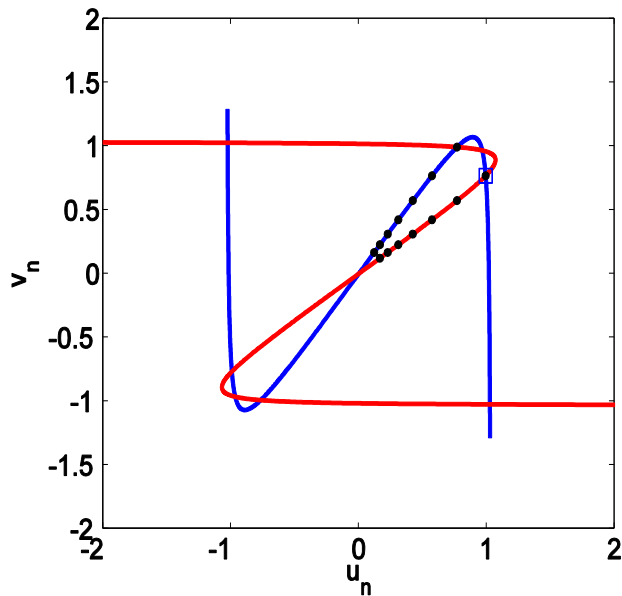
Figure 2.4: Homoclinic orbits intersections. The stable manifold (blue color) and the unstable manifold (red color). We choose the intersection point at the square symbol. The dots are resulted from forward and backward iterations of the map. The parameters are: $\mu = -0.93$, $v = 1$, and $\lambda = -2.10$.

The parameters used are $v = 1$ and $\lambda = -2.091$. As we know, we have to use $|\lambda| > 2$ in order to have saddle point at zero. The solutions are the intersection between the stable and unstable manifolds. The more the manifolds intersect the more solitons exist.

From the figures we can conclude that. For $\mu \geq 0$ the model is not rich, we have loop. The stable manifold coincides with the unstable manifold. Increasing μ results in decreasing the central pick magnitude (see Fig.2.4).
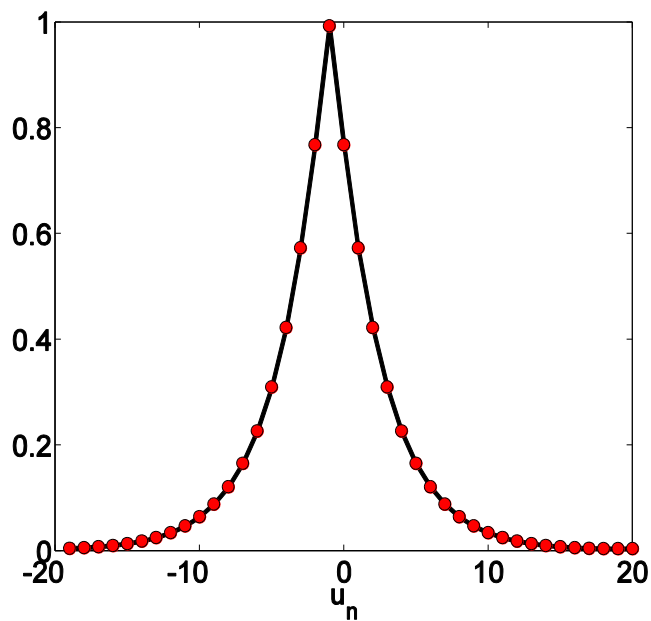
Figure 2.5: The type of soliton resulted from picking an intersection point from the homoclinic orbits. The parameters are the same as in Fig.2.3

For $\mu < 0$, increasing $|\mu|$ will destroy the loop and the stable manifold will be different than the unstable manifold. The two manifolds intersect and the model becomes rich, i.e., there are many different soliton solutions. when μ approaches -1, the homoclinic

orbits become more complicated and the intersection are hard to see. May be this an index that there are more soliton types. Increasing $|\mu|$ the homoclinic orbits intersections are clear (see Fig.2.4).

3 Parametric Excitation of solitons in dipolar interaction of Bose-Einstein condensate

The aim of this chapter to study the dynamics of a dipolar BEC governed by the nonlocal GPE by means of variational approximation (D. Anderson, 1983) and perform numerical simulations. Recently, similar approach has been applied to interaction of a soliton with a weak potential barrier in the middle of the parabolic trap (Abdullaev & Brazhnyi, 2012). This work distinguishes itself from other relevant publications in that, we obtain explicit ordinary differential equation for parameters of the soliton, instead of integro-differential equations, involving special functions. Also, we provide thorough comparison between the results of variational approximation and numerical simulations of the Gross-Pitaevskii equation.

In this chapter, the potential of dipolar interactions between atoms and the nonlocal Gross-Pitaevskii equation are briefly described. Therefore, the variational approximation for the nonlocal Gross-Pitaevskii equation has been developed and applied to low energy shape oscillations of the condensate.

3.1 The interaction potential and governing equation

Atomic density in dilute quantum gases is in the range $\approx 10^{13} - 10^{15} \, \text{cm}^{-3}$, which is four to six orders of magnitude smaller than the molecular density in air at room temperature and normal atmospheric pressure $\approx 10^{19} \, \text{cm}^{-3}$. Despite the extremely low atomic density of BECs, their properties are strongly influenced by interatomic interactions. In ultra-cold quantum gases without significant magnetic or electric dipole moments, usually only short-range, isotropic contact interactions are important.

When atoms have significant dipole moment a new kind of interaction via long-range and anisotropic dipolar forces arises, in addition to the contact interactions. The corresponding potential of dipole-dipole interactions is (Lahaye et al., 2009)

$$U_{dd}(r,\theta) = \frac{C_{dd}}{4\pi} \cdot \frac{1 - 3\cos(2\theta)}{r^3} \tag{3.1}$$

where the coupling constant $C_{dd} = \mu_0 \mu^2$ for atoms having permanent magnetic dipole moment μ (μ_0 is the permeability of vacuum), and $C_{dd} = \frac{d^2}{\varepsilon_0}$ for atoms having permanent electric dipole moment d (ε_0 is the permittivity of vacuum), θ is the angle between the direction joining the two dipoles, and the orientation of the dipoles (here we assumed that all dipoles are aligned along the same direction). It should be pointed out that electric dipole moment can also be induced by exposing the gas to DC electric fields (Marinescu & You, 1998).

It is evident from equation (3.1) that dipolar interactions are anisotropic. For instance, two dipoles placed head-to-tail $(\theta = 0)$ attract each other, while placed side-by-side $\left(\theta = \frac{\pi}{2}\right)$ repel. Tuning the strength of dipolar interaction is also possible by fast rotation of the orientation of dipoles in the polarizing field (Giovanazzi, Görlitz, & Pfau, 2002). The time averaged potential has the form (Lahaye et al., 2009)

$$\langle U_{dd}(r,\theta,\phi) \rangle = \frac{\mu_0 \mu^2}{4\pi} \frac{1 - 3\cos(2\theta)}{r^3} \left[\frac{3\cos^2(\phi) - 1}{2} \right] \tag{3.2}$$

When the tilt angle changes in the interval $\phi \in \left[0, \ \frac{\pi}{2} \right]$ the term in the rectangular brackets changes from 1 to -1/2.

In real experimental conditions, there is always a competition between the dipolar and contact interactions. A dimensionless coefficient, characterizing the relative strength of these two kinds of atomic forces has been introduced (Lahaye et al., 2009)

$$\varepsilon_{dd} = \frac{\mu_0 \mu^2 m}{12\pi\hbar^2 a_s}, \tag{3.3}$$

where the numerical factors are chosen in such a way that, the homogeneous condensate is stable against 3D collapse, when $\varepsilon_{dd} < 1$. In particular, for ^{52}Cr atoms with the $s-wave$ scattering length $a_s = 16a_B$ and magnetic dipole moment $\mu = 6\mu_B$, where a_B and μ_B are the Bohr radius and the Bohr magneton respectively, one has $\varepsilon_{dd} = 0.16$. This can be compared to the ordinary case of ^{87}Rb atoms with $a_s = 0.7a_B$ and $\mu = 1.0\mu_B$, when the calculation gives $\varepsilon_{dd} = 0.007$. Therefore, the effect of dipolar interactions in ^{52}Cr condensate is much stronger than in ^{87}Rb condensate. The GPE for the wave function of a dipolar condensate has the form (Góral, Rzążewski, & Pfau, 2000; Santos, Shlyapnikov, Zoller, & Lewenstein, 2000; Yi & You, 2000)

$$i\hbar\frac{\partial\Psi}{\partial t} = -\frac{\hbar^2}{2m}\Delta\Psi + \left[V_{ext}(r) + \frac{4\pi\hbar^2 a_s}{m}|\Psi|^2 + \int U_{dd}(r-r',t)|\Psi(r',t)|^2 dr'\right]\Psi, \tag{3.4}$$

where $V_{ext}(r)$ is the external trapping potential for the condensate.

In this chapter, it is considered the dynamics of a dipolar condensate in quasi-1D geometry. Experimentally this setting can be realized by loading the condensate in a cigar shaped trap with a tight radial confinement and a weak axial confinements. The dipoles are assumed to be aligned along the axial x-direction, therefore the dipolar interaction is attractive. When the radial confinement is strong enough, one can assume that the radial dynamics is frozen and factorize the wave function can be expressed as

$$\Psi(x,\rho,t) = \psi(x,t)\phi(\rho),$$

where

$$\phi(\rho) = \frac{1}{\sqrt{\pi}l}\exp\left(-\frac{\rho^2}{2l^2}\right)$$

is the ground state of a 2D harmonic oscillator with

$$l = \sqrt{\frac{\hbar}{m\omega_\perp}}$$

being the radial harmonic oscillator length, $\omega_\perp$ is the radial trap frequency. Inserting the above the factorized wave function into equation (3.4) and performing integration with respect to variable ρ, the following reduced 1D GPE can be obtained

$$i\hbar\frac{\partial\psi}{\partial t} = -\frac{\hbar^2}{2m}\frac{\partial^2\psi}{\partial x^2} + \left[V_{ext}(x) + g_{1D}|\psi|^2 + \int_{-\infty}^{+\infty}U_{dd}(|x-\xi|)|\psi(\xi,t)|^2\,d\xi\right]\psi, \qquad (3.5)$$

where $g_{1D} = 2\hbar\omega a_s$ is the reduced 1D nonlinear coupling constant,

$$V_{ext}(x) = \frac{1}{2}m\omega^2 x^2$$

is axially confining potential (parabolic trap with frequency ω). The reduced 1D potential of dipolar interactions was derived in (Sinha & Santos, 2007)

$$U_{dd}(x) = -\frac{2\alpha d^2}{l^3}\left[2|x| - \sqrt{\pi}\left(1+2x^2\right)\exp\left(x^2\right)\mathrm{erfc}\left(|x|\right)\right], \qquad (3.6)$$

where d is the dipole moment, l is the harmonic oscillator length of strong radial confinement, α is a variable that may change between $\alpha = 1(\theta = 0)$ and

$\alpha = -\frac{1}{2}\left(\theta = \frac{\pi}{2}\right)$. Note that although the original 3D potential of dipole-dipole

interactions is singular at $r = 0$, the reduced 1D potential is regularized and finite at

$x = 0$. The equation (3.5) can be further reduced to dimensionless form by introducing

variables:

$$\begin{cases} x \to \dfrac{x}{l} \\[2em] t \to \omega t \\[2em] \psi \to \sqrt{2a_s}\,\psi \\[2em] d \to \dfrac{1}{\sqrt{l^3 \hbar \omega}}\,d \end{cases}$$

We can rewrite the equation

$$i\hbar \frac{\partial \psi}{\partial t} = -\frac{1}{2}\frac{\partial^2 \psi}{\partial x^2} + \left[V_{ext}(x) - q|\psi|^2 - 2\alpha d^2 \int_{-\infty}^{+\infty} R(|x-\xi|)|\psi(\xi,t)|^2 \, d\xi \right]\psi, \qquad (3.7)$$

where $R(x) \sim U_{dd}(x)$ is the dimensionless nonlocal kernel function, and $q \sim -\mathrm{sgn}(a_s)$ is

the dimensionless strength of contact interactions.

In absence of an external potential, the nonlocal integral term of equation (3.7) is the

well known 1D nonlinear Schrödinger equation, which supports a spectrum of exact

soliton solutions. In experiments, one approaches this limit by confining the condensate

in an elongated cigar shaped trap with tight radial confinements. Although the presence

of a weak axial trap $V_{ext}(x)$ breaks the integrability of the governing equation, many

properties of localized states remain close to those of the classical solitons, as

demonstrated in the recent experiment (Marchant et al., 2013). The nonlocal term in

equation (3.7) also breaks the integrability, but it does not exclude the existence of stable localized states in the system in particular regions of the parameter space (Cuevas et al., 2009). Since we are mainly interested in self-trapped localized states of BEC, for our purposes the external trap potential can be set to zero $V_{ext}(x) = 0$, and this will be assumed below. It should be pointed out, that the external potential can be easily incorporated into the scheme of VA (D. Anderson, 1983).

Thus, when the dipolar atomic interactions are taken into account, the equation governing the dynamics of the condensate is the nonlocal GPE (3.7). Both the contact interactions in equation (3.7) represented by the cubic nonlinearity, and dipolar interactions represented by the integral term, are tunable by the Feshbach resonance technique. In the following we shall be interested in periodic variation of the dipolar interactions at fixed strength of contact interactions.

3.2 **The variational approximation in non-local interaction**

We consider the following equation describing the dynamics of the condensate in presence of both dipolar and contact interactions

$$i\frac{\partial \psi}{\partial t} + \frac{1}{2}\frac{\partial^2 \psi}{\partial x^2} + q\,|\psi|^2\,\psi + g(t)\psi \int_{-\infty}^{+\infty} R(|x-\xi|)|\psi(\xi,t)|^2\,d\xi = 0, \qquad (3.8)$$

where $g(t) = 2\,\alpha(t)\,d^2$ is the strength of dipolar interactions, which can be varied through time dependent $\alpha(t)$. The wave function $\psi(x,t)$ is normalized to

$$N = \int_{-\infty}^{+\infty} |\psi(x)|^2\,dx$$
,

which is a conserved quantity of equation (3.8), proportional to the number of atoms in the condensate.

The kernel function (3.6) is complicated for the variational analysis. For a qualitative understanding of the effect of non-locality on the dynamics of dipolar BEC we consider analytically tractable Gaussian ansatz for the response function

$$R(x) = \frac{1}{\sqrt{2\pi}w}\exp\left(-\frac{x^2}{2w^2}\right)$$
(3.9)

which is normalized to one

$$\int_{-\infty}^{+\infty} R(x)dx = 1,$$

and Gaussian ansatz

$$\psi(x,t) = A(t)\exp\left[-\frac{x^2}{2a(t)^2} + ib(t)x^2 + i\phi(t)\right]$$
(3.10)

with norm

$$N = \int |\psi(x)|^2\,dx = A^2 a\sqrt{\pi}.$$

Equation (3.8) can be derived from the Lagrangian density

$$\mathcal{L} = \frac{i}{2}(\psi\psi_t^* - \psi^*\psi_t) + \frac{1}{2}|\psi_x|^2 - \frac{1}{2}q|\psi|^4 - \frac{1}{2}g(t)|\psi(x,t)|^2\int_{-\infty}^{\infty} R(x-\xi)|\psi(\xi,t)|^2\,d\xi, \quad (3.11)$$

where the subscript denotes derivative with respect to corresponding variable,

i.e $\psi_t = \frac{\partial\psi}{\partial t}$ and $\psi_x = \frac{\partial\psi}{\partial x}$.

Now using the trial function (3.10) one obtains

$$\mathcal{L}_1 = \frac{i}{2}(\psi\psi_t^* - \psi^*\psi_t)$$

$$= A^2 e^{-x^2/a^2}(b_t x^2 + \phi_t)$$

(3.12)

$$\mathcal{L}_2 = \frac{1}{2}|\psi_x|^2$$

$$= \frac{1}{2}A^2\left(\frac{1}{a^4} + 4b^2\right)x^2 e^{-x^2/a^2},$$

(3.13)

$$L_3 = -\frac{1}{2}q|\psi|^4$$

$$= -\frac{1}{2}qA^4 e^{-2x^2/a^2},$$

(3.14)

$$\mathcal{L}_4 = -\frac{1}{2}g(t)|\psi|^2\int\limits_{-\infty}^{\infty} R(x-\xi)|\psi(\xi,t)|^2\, d\xi$$

$$= -\frac{g(t)A^4}{2\sqrt{2\pi}w}\int\limits_{-\infty}^{\infty}\exp\left[-\frac{(x-\xi)^2}{2w^2}\right]\exp\left[-\frac{x^2+\xi^2}{a^2}\right]d\xi.$$

(3.15)

To evaluate the last integral in $\mathcal{L}_4$ we make the change of variables (Abdullaev & Brazhnyi, 2012)

$$\begin{cases} z = \frac{1}{2}(x-\xi), \\ \\ y = \frac{1}{2}(x+\xi), \end{cases}$$

therefore

$$\begin{cases} x = y + z \\ \\ \xi = y - z \end{cases}$$

i.e. we have functional dependence between old and new variables

$$\begin{cases} x = x(y, z) \\ \\ \xi = \xi(y, z) \end{cases}.$$

Then for the Jacobian of the transformation we have

$$J = \left| x_y \xi_z - x_z \xi_y \right| = 2.$$

Consequently $dx\, d\xi = 2dy\, dz$. The averaged Lagrangian terms become

$$L_i = \int \mathcal{L}_i dx, \quad i = \overline{1, 4}$$

are computed straightforwardly

$$L_1 = A^2 a \sqrt{\pi} \left(\frac{1}{2} a^2 b_t + \phi_t \right), \tag{3.16}$$

$$L_2 = A^2 a \sqrt{\pi} \left(\frac{1}{4a^2} + a^2 b^2 \right), \tag{3.17}$$

$$L_3 = -\frac{q A^4 \sqrt{\pi} a}{2\sqrt{2}}, \tag{3.18}$$

$$L_4 = -\frac{g(t)A^4}{\sqrt{2\pi}w} \int\limits_{-\infty}^{+\infty}\int\limits_{-\infty}^{+\infty} \exp\left[-\frac{2z^2}{w^2}\right]\exp\left[-\frac{2(y^2+z^2)}{a^2}\right]dydz$$

(3.19)

$$= -\frac{g(t)A^4 a^2 \sqrt{\pi}}{2\sqrt{2}\sqrt{a^2+w^2}}.$$

Then the final expression for the averaged Lagrangian is

$$\text{L} = \sum_{i=1}^{4} L_i = \text{L}_1 + \text{L}_2 + \text{L}_3 + \text{L}_4$$

$$\frac{L}{N} = \frac{1}{4a^2} + a^2b^2 + \frac{1}{2}a^2b_t + \phi_t - \frac{qN}{2\sqrt{2\pi}a} - \frac{g(t)N}{2\sqrt{2\pi}(a^2+w^2)^{1/2}}. \qquad (3.20)$$

The Euler-Lagrange equations is given

$$\frac{d}{dt}\left(\frac{\partial L}{\partial v_t}\right) - \frac{\partial L}{\partial v} = 0,$$

for variational parameters $v \to \phi, b, a$ yield the following system

$$\begin{cases} N_t = 0, \\[2mm] a_t = 2ab, \\[2mm] b_t = \dfrac{1}{2a^4} - 2b^2 - \dfrac{qN}{2\sqrt{2\pi}a^3} - \dfrac{g(t)N}{2\sqrt{2\pi}(a^2+w^2)^{3/2}}. \end{cases} \qquad (3.21)$$

The first equation in (3.21) is decoupled from others and declares the conservation of the wave packet's norm. The equation for the width of the soliton can be derived from the last two equations in (3.21)

$$a_{tt} = \frac{1}{a^3} - \frac{qN}{\sqrt{2\pi}a^2} - \frac{g(t)N}{\sqrt{2\pi}}\frac{a}{(a^2+w^2)^{3/2}}. \qquad (3.22)$$

This equation is similar to equation of motion for a unit mass particle in the anharmonic potential

$$a_{tt} = -\frac{\partial U}{\partial a}$$

with

$$U(a) = \frac{1}{2a^2} - \frac{qN}{\sqrt{2\pi}a} - \frac{gN}{\sqrt{2\pi}(a^2 + w^2)^{1/2}}. \qquad (3.23)$$

The stationary state corresponding to the minimum of the potential well

$$\frac{\partial U}{\partial a} = 0$$

gives the width of the soliton and its amplitude via the norm as

$$A = \sqrt{\frac{N}{a\sqrt{\pi}}}.$$

Therefore, the shape of the soliton, given by equation (3.10) can be determined by the variational approximation.

Solving equation (3.22), which gives the stationary solution of the original GPE (3.8) that describes its dynamics near the fixed point, corresponds to the main result of the present work. At large departures from the stationary state, the waveform (3.10) can deviate from the Gaussian shape, and the predictions of the VA become less accurate.

The stationary width of the soliton a_0 is calculated from the following condition:

$$\frac{a_0^4}{(a_0^2 + w^3)^{3/2}} + \frac{q}{g}a_0 - \frac{\sqrt{2\pi}}{gN} = 0. \qquad (3.24)$$

Figure 3.1 illustrates the shape of the potential $U(a)$ for a pure dipolar condensate $(q=0)$, and when the contact interactions are also present $(q=\pm 1)$. The stationary state solutions of the GPE for these cases are obtained by the method of relaxation in imaginary time, as described in (Chiofalo, Succi, & Tosi, 2000). As can be seen from this figure, the soliton in a pure dipolar condensate $(q=0)$ is perfectly described by the Gaussian function. The result of numerical solution of the GPE is indistinguishable from the prediction of VA.
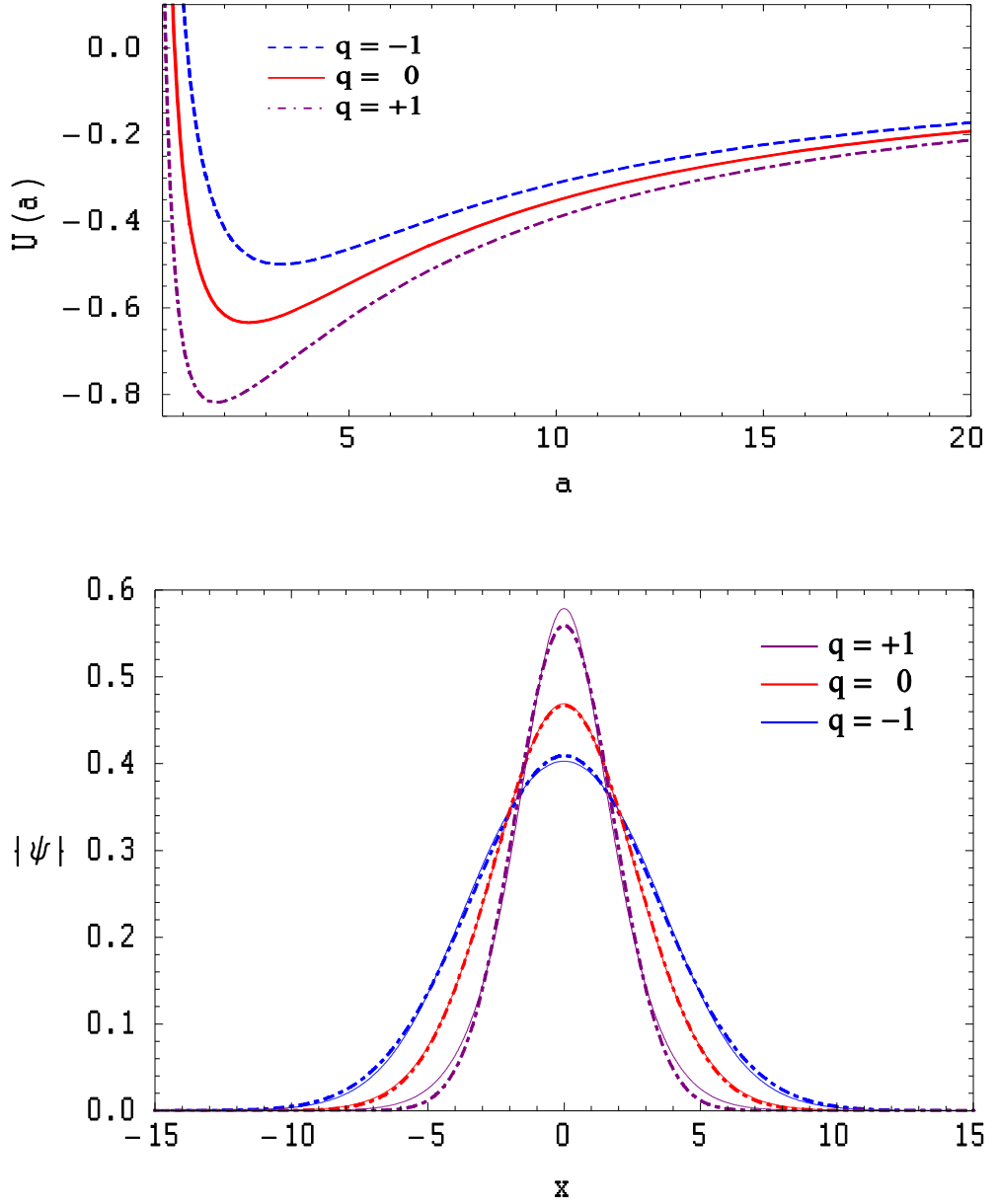
Figure 3.1: Top panel: The shape of the anharmonic potential given by equation (3.23) for pure dipole-dipole interactions ($q = 0$, red solid line), and in presence of repulsive ($q = -1$, blue dashed line) and attractive ($q = +1$, purple dot-dashed line) contact interactions. The stationary width of the soliton corresponding to these cases are $a_0 = 2.59$, $a_0 = 3.37$, and $a_0 = 1.80$ respectively. Bottom panel: Stationary localized solutions of the GPE(3.8) with Gaussian response function (3.9) for pure dipolar interactions (red line) and in presence of repulsive (blue line) and attractive (purple line) contact interactions. Dashed lines correspond to predictions of the VA. Parameter values: $N = 1$, $w = 5.0$, $g = 10$.

In presence of contact interactions $(q = \pm 1)$ noticeable deviation from the Gaussian shape is seen near the peak and periphery of the wave packet.

The frequency of small amplitude oscillations around the fixed point a_0 is

$$\omega_0 = \left[\frac{3}{a_0^4} - \frac{2qN}{\sqrt{2\pi}a_0^3} - \frac{gN}{\sqrt{2\pi}(a_0^2 + w^2)^{3/2}} \left(\frac{3a_0^2}{a_0^2 + w^2} - 1 \right) \right]^{1/2}. \qquad (3.25)$$

The repulsive contact interactions $(q < 0)$ give rise to decreasing of the frequency of oscillations compared to the case of pure dipolar interactions $(q = 0)$, while the effect of attractive interactions $(q > 0)$ is opposite, leading to increasing of the oscillations frequency. In figure (3.2) we depict the frequency of shape oscillations of the soliton as a function of the strength of contact interactions, according to equation (3.25). The same figure shows the stationary width of the soliton for a given strength of contact interactions, obtained from equation (3.24). Comparison between the prediction of VA and the result of numerical solution of the governing GPE (3.8), expressed by symbols, reveals fairly good agreement.

Low energy collective oscillations of atoms can provide essential information about the interatomic forces in BEC (Jin, Ensher, Matthews, Wieman, & Cornell, 1996). In this regard, the analytic expression (3.25) for the frequency of shape oscillations of a matter-wave packet can be useful in relevant experiments with dipolar BEC.
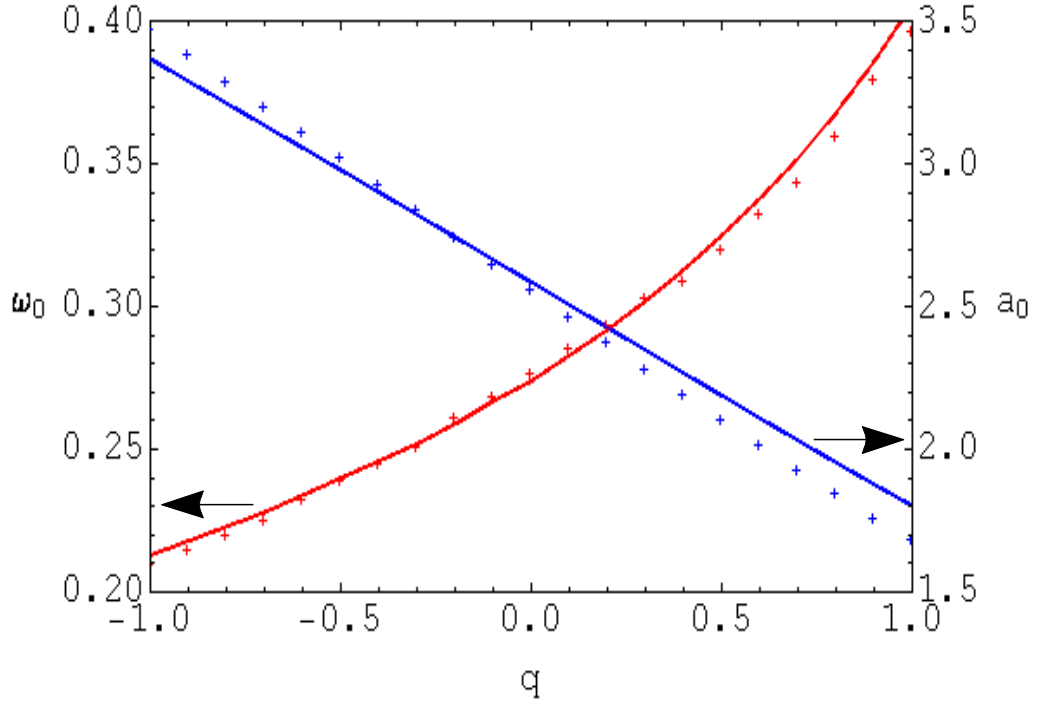
Figure 3.2: The frequency of low energy shape oscillations (ω_0) of a matter-wave packet in dipolar BEC as a function of the strength of contact interactions q, according to equation (3.25). (red solid line), and the stationary width of the soliton a_0 obtained from equation. (3.24) (blue line). The symbols indicate the results of numerical solution of the GPE(3.8). Parameter values: $N = 1, w = 5, g = 10$.

Figure 3.3 illustrates the oscillations of the soliton's width under periodic variation of the strength of nonlocal interactions. As for the physical implementation of this setting, changing the strength of dipole-dipole interactions can be performed by means of a rotating polarizing magnetic field (Giovanazzi et al., 2002). Such a field gives rise to precession of dipoles (arranged in "head-to-tail" configuration $\theta = 0$, in a quasi-one dimensional trap) around the axial direction, on a cone of aperture 2ϕ. When the angular frequency of rotation Ω is small than the Larmor frequency, but much greater than the trapping frequencies, only the time average over the period $2\pi/\Omega$ determines

the effective strength of dipole-dipole interactions, given by equation (3.2). Thus, by introducing periodic variation of the tilt angle ϕ one can induce the periodic change of the strength of dipolar interactions.

As can be seen in the left panel of figure (3.3), the amplitude of oscillations $\left(a_{max} - a_{min}\right)$ increases linearly at the initial stage, which is characteristic to the resonance phenomenon. Scanning over the interval of frequencies $\omega = 0 - 1$ reveals the parametric resonance at $2\omega_0$ in addition to the main peak at ω_0. To retrieve the width of the wave packet from the solution of the GPE we use the following relation

$$a(t) = \left(2 \cdot \frac{\int_{-\infty}^{\infty} x^2 \, |\psi(x,t)|^2 \, dx}{\int_{-\infty}^{\infty} |\psi(x,t)|^2 \, dx} \right)^{1/2}. \qquad (3.26)$$

In figure (3.4), we show the evolution of the matter-wave packet under periodically changing coefficient of nonlocal interactions. Excitation of regular oscillations with the frequency of parametric driving is clearly observed. A gradual increase of the amplitude of oscillations is due to the resonance phenomenon.
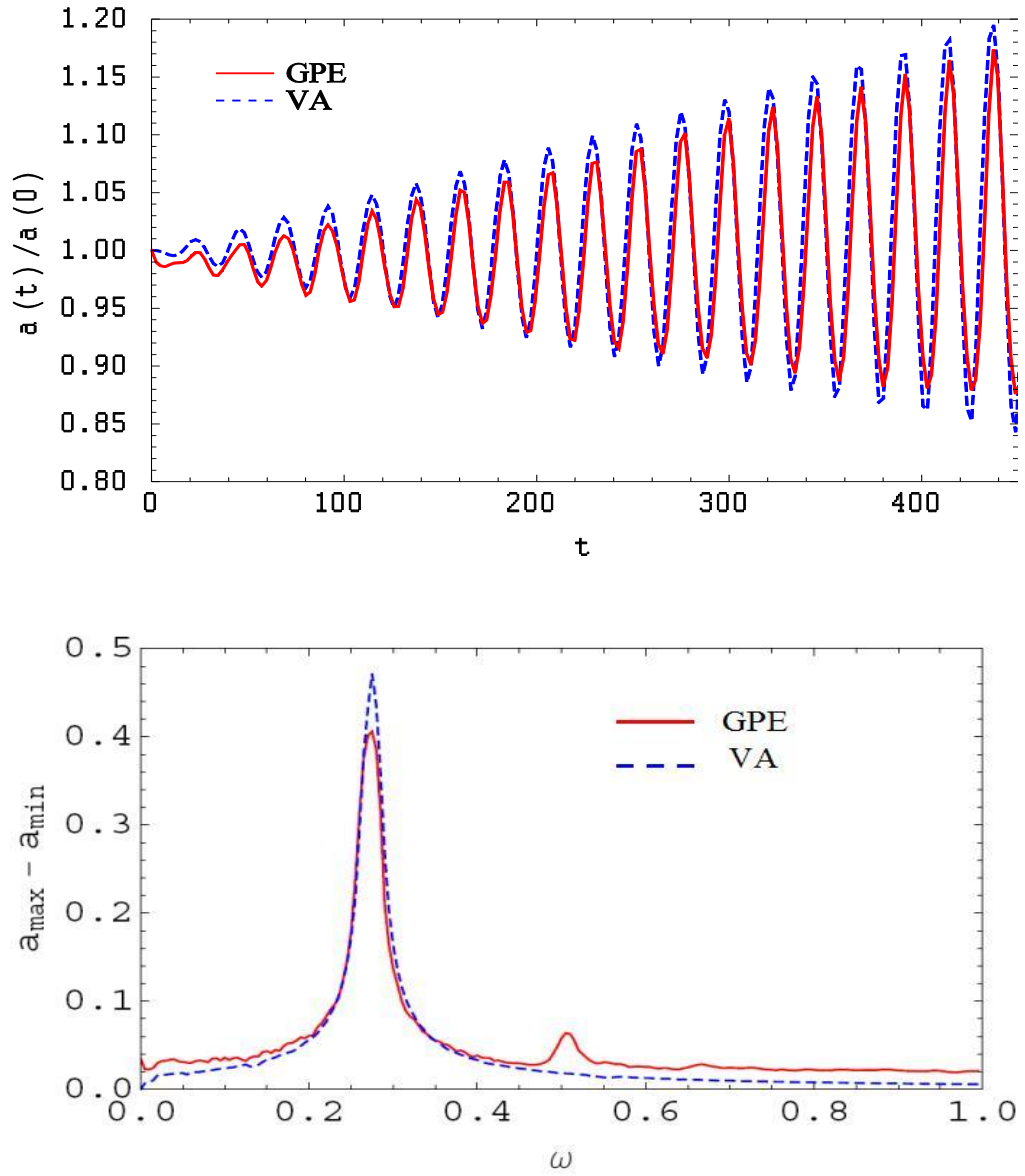
Figure 3.3: Above panel: Periodic variation of the coefficient of nonlocal nonlinearity $g(t) = 2d^2\alpha(t)$ at resonant frequency $\alpha(t) = 1 + 0.01\sin(\omega_0 t)$, with $d = \sqrt{5}$, $\omega_0 = 0.274$ gives rise to oscillations of the soliton's width The amplitude of oscillations increases linearly at the initial stage, as characteristic to resonant response. Down panel: Scan over some interval of frequencies $\omega \in [0,1]$ reveals also the parametric resonance at $\omega \approx 0.54$, which is the twice of the main resonance frequency ω_0. In both panels the red solid line corresponds to numerical solution of the. GPE (3.8), while blue dashed line to variational approximation (3.22). All parameters are the same as in figure (3.1) for pure dipolar interactions
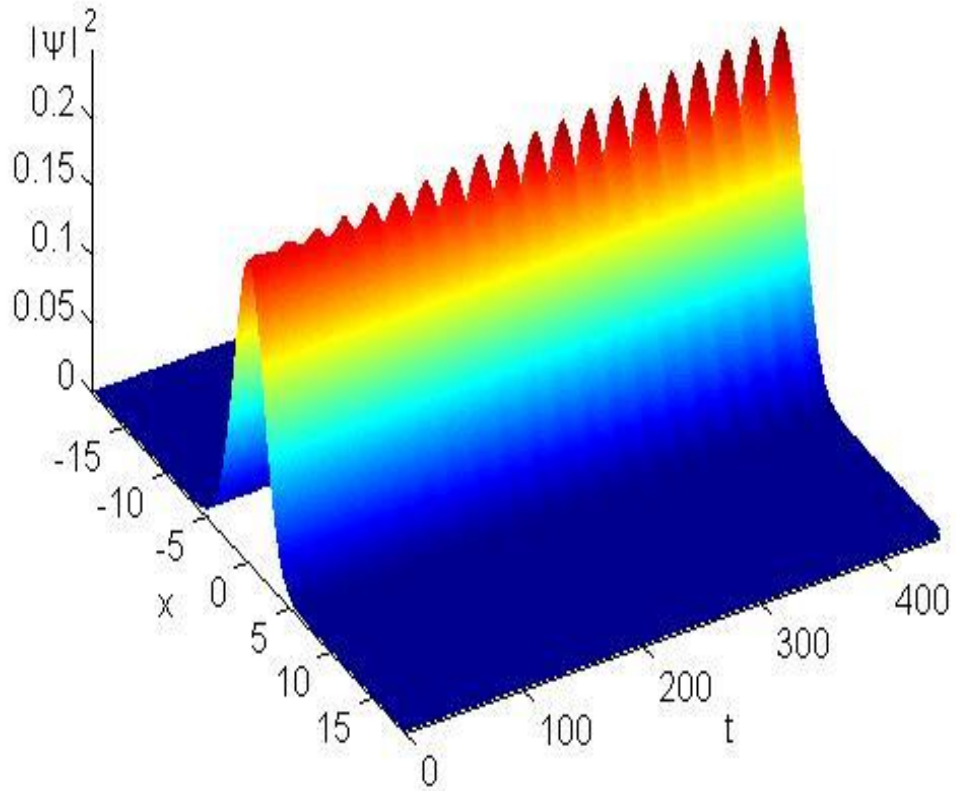
Figure 3.4: Evolution of the matter-wave packet under periodic variation of the strength of dipolar interactions. Excitation ofshape oscillations under parametric perturbation is evident. The initial condition for the GPE (3.8) is taken as stationary solution predicted by the variational approximation $\psi(x,0) = A_0 \exp\left(-\dfrac{x^2}{2a_0^2}\right)$, with $A_0 = 0.467$ and $a_0 = 2.586$. The coefficient of nonlocal nonlinearity is periodically changed at resonant frequency $\omega_0 = 0.274$ as $g(t) = 10 \cdot \left(1 + 0.01 \cdot \sin\left(\omega_0 t\right)\right)$

For numerical simulations of the GPE (3.8), we employ the split-step method (Agrawal, 2007) with 1024 Fourier modes in the integration domain $x \in [-6\pi,\, 6\pi]$. The time step was set to $\Delta t = 0.001$. To speed up the evaluation of the integral in the nonlocal term, the convolution theorem has been used (Press, Flannery, Teukolsky, & Vetterling, 1990). It is well known, that soliton under perturbation emits linear waves, which can re-enter the integration domain due to reflection from the domain boundaries. For emulation of the infinite integration domain length and preventing the interference of the soliton with the emitted linear waves, we use the absorbing boundary technique (Berg, If, Christiansen, & Skovgaard, 1987).

4 Matter-Wave Soliton Bouncing
On a Reflecting Surface

In this chapter, the mathematical model will be introduced to illustrate the distinctive features of the nonlinear model as compared to its linear counterpart. The variational approach for analytical treatment of the nonlinear model has been developed. The predicted results are compared with numerical simulations of the original Gross-Pitaevskii equation. The resonant oscillations of the wave packet above the mirror is explored, and the Fermi type of acceleration of matter wave solitons when the vertical position of the reflecting surface is periodically varied in time is investigated.

4.1 **The model**

The Bose-Einstein condensate is a giant matter wave packet which is strongly affected by gravity. In particular, a matter wave packet released from the trap falls towards Earth like a bunch of coherent atoms. The effect of gravity is essential for the operation of atom lasers (Bolpasi et al., 2014; Mewes et al., 1997).

In the present model the gravitational field is acting on atoms in the vertical direction and a horizontal atom mirror which reflects them back, form a cavity for the matter wave packet. In the following we consider the motion of a matter wave soliton within such a gravitational cavity. The model is based on the following one dimensional GPE

$$i\hbar \frac{\partial \psi}{\partial t} = -\frac{\hbar^2}{2m}\frac{\partial^2 \psi}{\partial x^2} + mgx\psi + U(x)\psi + 2\hbar\omega_\perp a_s |\psi|^2 \psi, \qquad (4.1)$$

where $\psi(x,t)$ is the wave function of the condensate trapped in a tight quasi-1D trap, x is the spatial coordinate of the wave packet above the horizontal atomic mirror, represented by the reflecting potential $U(x)$, g is the strength of the gravitational potential, ω is the trap frequency in the tightly confining radial direction, m, a_s are the atomic mass and s-wave scattering length, respectively.

The gravitational units of space and time, defined as

$$
\begin{cases}
l_g = \left(\dfrac{\hbar^2}{m^2 g} \right)^{1/3}, \\[4mm]
\mathrm{t}_g = \left(\dfrac{\hbar}{mg^2} \right)^{1/3},
\end{cases}
\tag{4.2}
$$

allows to rewrite the equation (4.1) in the dimensionless form

$$
i\psi_t + \frac{1}{2}\psi_{xx} + \gamma |\psi|^2 \psi - \alpha x\psi + V(x)\psi = 0,
\tag{4.3}
$$

where the new variables are defined as

$$
\begin{cases}
x \rightarrow \mathrm{x}/l_g, \\[3mm]
t \rightarrow \mathrm{t}/\mathrm{t}_g, \\[3mm]
\mathrm{V}(x) = -U(x)/(mgl_g), \\[3mm]
\psi \rightarrow \sqrt{2\omega_\perp |a_s| t_g}\,\psi.
\end{cases}
$$

Here we consider that for BEC with attractive atomic interactions, $a_s < 0$. The norm of the dimensionless wave function is defined by

$$N = \int_{-\infty}^{\infty} |\psi(x)|^2 \, dx,$$

and it is proportional to the number of atoms in the condensate. In equation (4.3) the linear potential term $(\sim x)$ accounts for the effect of gravity, while the atomic mirror is represented by $V(x)$. We introduced an additional parameter

$$\alpha = \sin(\beta)$$

to account for the possibility of altering the effect of gravity by changing the angle β formed by the axis of the quasi-1D waveguide and the horizontal reflecting surface. For vertical position $(\beta = \pi / 2)$ of the waveguide $\alpha = 1$, at smaller angles $0 < \beta < \dfrac{\pi}{2}$, then $0 < \alpha < 1$. Such a setting is of interest in view of recent research on the behavior of BEC in microgravity (van Zoest et al., 2010) and the quantum reflection of matter waves (Cornish et al., 2009; Lee & Brand, 2006; T. Pasquini et al., 2006; T. A. Pasquini et al., 2004), where the cold atoms should approach the attractive potential at very low speed. Similarly, the additional parameter γ can be used for nonlinearity management $\gamma(t) = a_s(t) / a_s^0$, then in the normalization for ψ in equation (4.3) the background value of a_s^0 should be assumed. The following two cases will be relevant to our further analysis

    a)   an ideal mirror

$$V(x) = \begin{cases} 0, & \text{if } x \geq 0 \\ +\infty, & \text{if } x < 0 \end{cases},$$

b) a weakly transparent reflecting surface

$$V(x) = V_0 \, \delta(x), \tag{4.4}$$

where $\delta(x)$ is the Dirac delta function which has been multiplied by the strength V_0.

A detailed study of the wave packet dynamics described by equation (4.3) in the linear model ($\gamma = 0$) for ideal mirror was reported in Ref. (Gea-Banacloche, 1999). Before proceeding to analytical description of the nonlinear model ($\gamma = 1$) it is instructive to compare these two limits by numerical simulations of the governing equation (4.3). Such a preliminary study will help to elucidate the effect of nonlinearity on the dynamics of a wave packet bouncing above the atomic mirror.

In figure (4.1), we illustrate the features of the linear and nonlinear models for the dynamics of the wave packet dropped from the height $x_0 = 10$ above the mirror positioned at $x = 0$. The main difference appears to be enhanced spreading of the wave packet and strong interference with reflected waves in the linear model, as compared to the nonlinear case, where these phenomena do not show up.
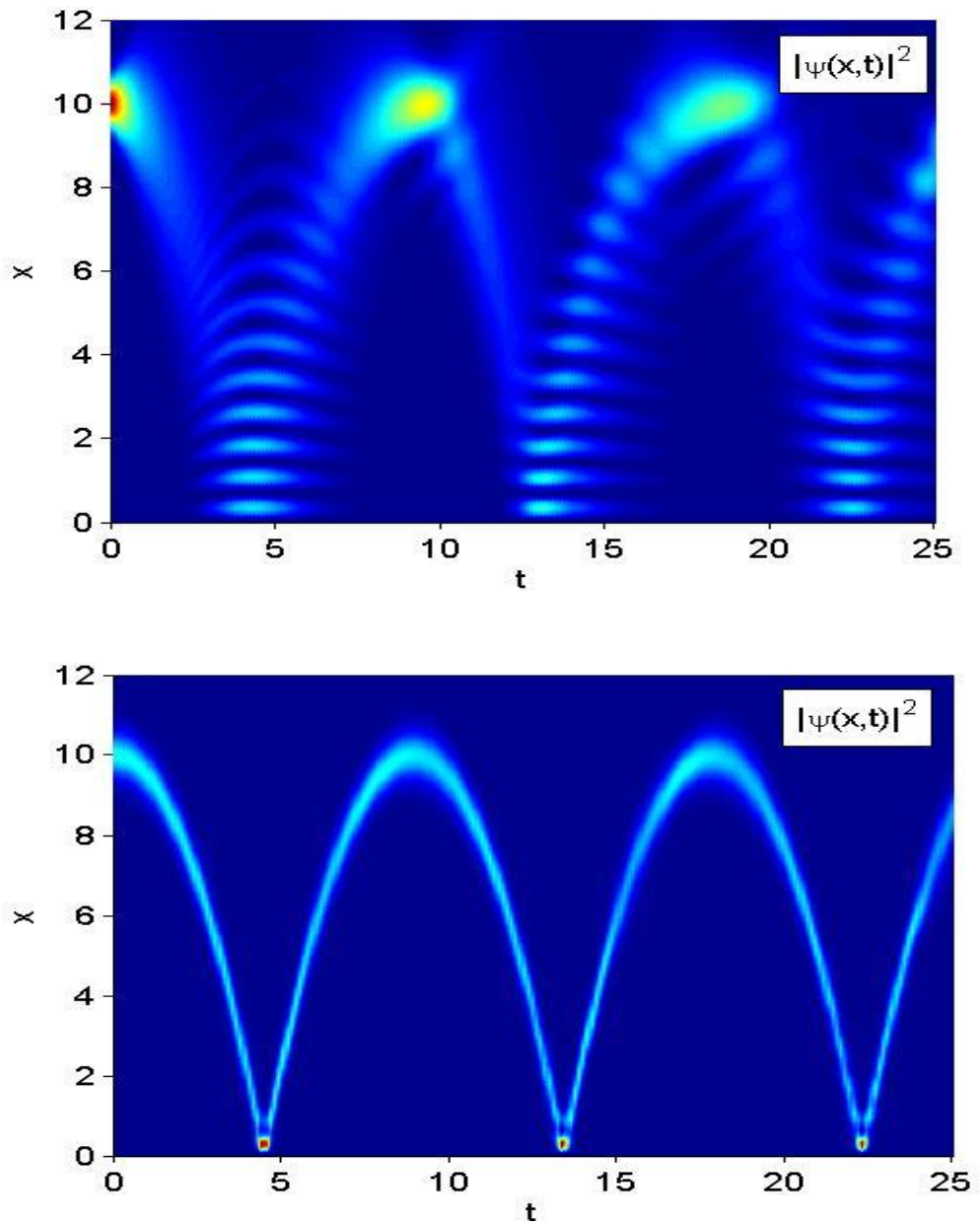
Figure 4.1: Above panel: The first three bouncing of the wave packet from the ideal mirror for the linear model $(\gamma = 0)$ is shown through the density plot $|\psi(x,t)|^2$. Down panel: The same for the nonlinear model $(\gamma = 1)$. In both cases a wave packet $\psi(x,0) = A\exp(-(x-x_0)^2/a^2)$ with $A = 2, a = 0.8$ and $x_0 = 10$ has been employed as initial condition for the governing equation (4.3), with the coefficient of linear potential $\alpha = 1$

The distinctions between the two models is clearly observed in figure (4.2), where we compare the corresponding wave profiles at different times during one period of bouncing T_b, which is estimated from classical equation $\frac{d^2 x}{dt^2} = -g$. In dimensionless units introduced for equation (4.3), we need to set $g = 1$. Then a classical particle dropped from the height x_0 reaches the ground at

$$t_b = \sqrt{2x_0} \,,$$
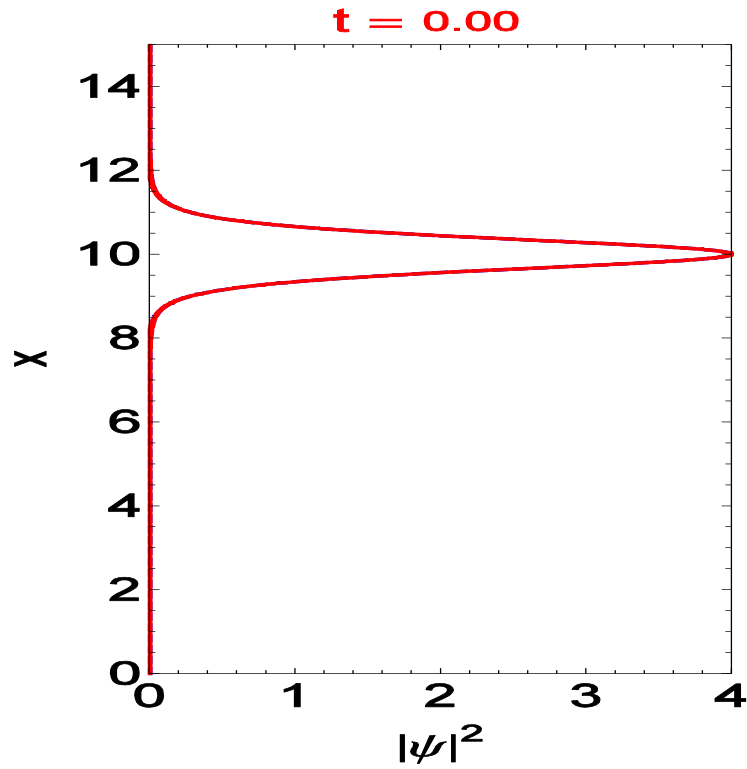
Figure 4.2: (Part I) Snapshots of the wave packet dropped from the height $x_0 = 10$ at $t = 0$ (shown on different time for each figure) during one bouncing period $T_b = 8.94$. In the linear model the wave packet quickly expands and shows strong interference with waves reflected by the mirror placed at $x = 0$ (blue dashed line). At final time T_b the wave packet does not fully recover its initial form. In the nonlinear case the wave packet better keeps its integrity during the evolution and almost fully recovers its initial form at T_b (red solid line). All parameters are the same as in the previous figure. (Continuous)

Figure 4.2: (Part II) Snapshots of the wave packet dropped from the height $x_0 = 10$ at $t = 2.24$. All parameters are the same as in the previous figure. (Continuous)

Figure 4.2: (Part III) Snapshots of the wave packet dropped from the height $x_0 = 10$ at $t = 2.47$. All parameters are the same as in the previous figure. (Continuous)
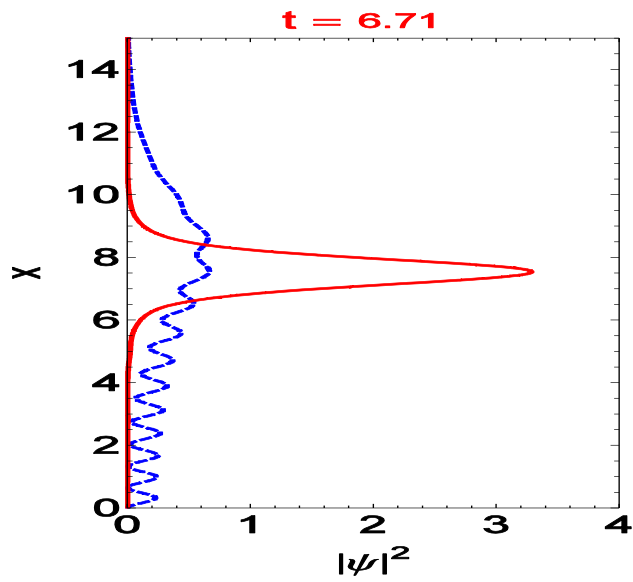
Figure 4.2: (Part IV) Snapshots of the wave packet dropped from the height $x_0 = 10$ at $t = 6.71$. All parameters are the same as in the previous figure. (Continuous)
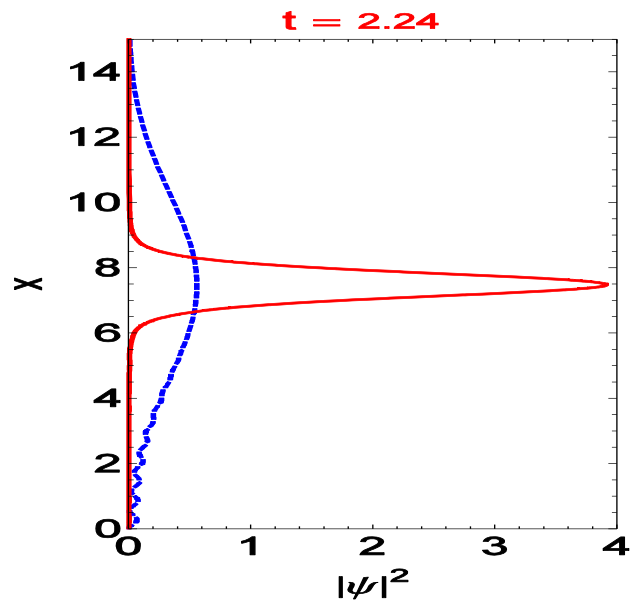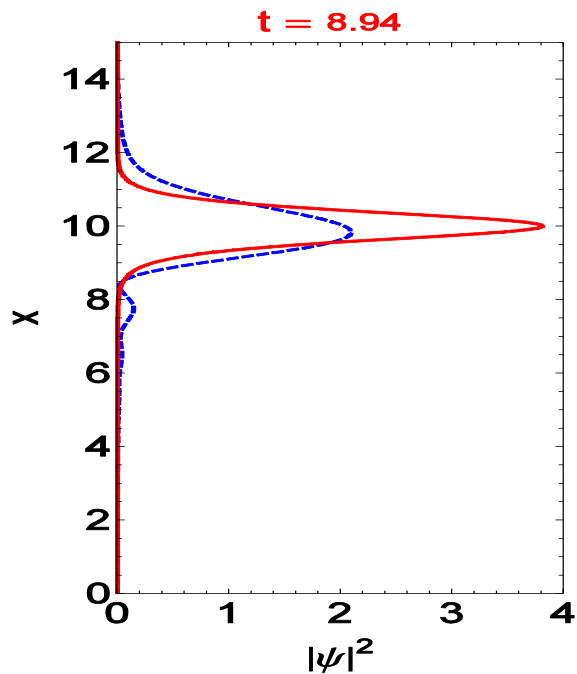

Figure 4.2: (Part II) Snapshots of the wave packet dropped from the height $x_0 = 10$ at $t = 8.94$. All parameters are the same as in the previous figure. (continuous)
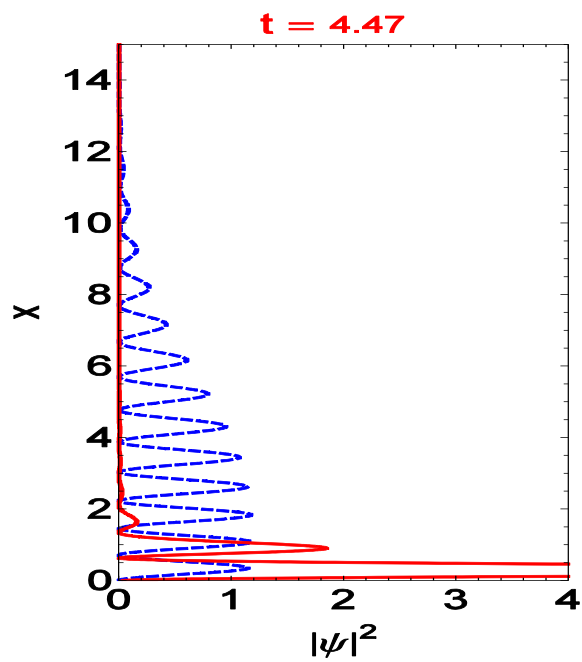
therefore the classical bouncing period is

$$T_b = 2t_b = 2\sqrt{2x_0}$$.

It should be noted that in figure (4.2), we show the situation, when the wave packet is dropped from a quite large height and the effect of gravity is maximal ($\alpha = 1$). This gives rise to notable deformation of the nonlinear wave packet too, in proximity of the mirror (see the middle panel). After the instant interaction with the mirror at $t = \dfrac{T_b}{2}$, soliton quickly recovers its form. Asymmetric deformation of the wave packet and emergence of side peaks (interference fringes) during the evolution are the main factors compromising the precision of analytical description developed in the next section.

To estimate the parameters of the model we consider the ^{58}Rb condensate, for which $a_s = -20nm$, $l_g \approx 1.3\mu m$, $t_g = 0.36ms$. At the strength of radial confinement $\omega_\perp = 10^3 rad/s$ we have $\gamma = 1$. For $N = 4$ the soliton contains ≈ 720 atoms. Similar estimates for ^7Li condensate with $a_s = -1.6nm$ gives $l_g \approx 7\mu m$, $t_g = 0.84ms$, $\omega_\perp = 10^4 rad/s$, the soliton contains ≈ 1400 atoms.

4.2 Variational approximation method

For arbitrary forms of the reflecting potential $V(x)$, the governing equation (4.3) cannot be analytically investigated. One of the efficient approaches to the problem in such cases is the variational approximation (VA).

In the following we develop the VA for the governing equation using the second choice (b) for the potential equation (4.4). It is well known from quantum mechanics textbooks that the wave packet falling on the delta potential barrier is always partially transmitted. However, by increasing the strength of the barrier (V_0) the transmission coefficient can be reduced to negligible level. This allows us to consider the norm of the wave packet above the mirror as a conserved quantity and to develop the VA using an appropriate ansatz for the pulse shape.

Equation (4.3) can be generated from the following Lagrangian density

$$\mathcal{L} = \frac{i}{2}(\psi\psi_t^* - \psi^*\psi_t) + \frac{1}{2}|\psi_x|^2 + \alpha x|\psi|^2 - V(x)|\psi|^2 - \frac{\gamma}{2}|\psi|^4. \qquad (4.5)$$

An important step in the development of VA is the proper choice of the trial function. We shall consider the following hyperbolic secant ansatz

$$\psi(x,t) = A\operatorname{sech}\left(\frac{x-\zeta}{a}\right)e^{ib(x-\zeta)^2 + i\xi(x-\zeta) + i\varphi}, \qquad (4.6)$$

where $A(t)$, $a(t)$, $\zeta(t)$, $\xi(t)$, $b(t)$, $\varphi(t)$ are variational parameters representing the amplitude, width, center of mass position, velocity, chirp parameter and phase of the wave packet, respectively. This choice is motivated by the fact that when the wave packet is sufficiently far from the reflecting potential $V(x)$ (and therefore its effect can be neglected), equation (4.3) has the exact accelerated soliton solution of the hyperbolic secant form (Chen & Liu, 1976).

Substituting the ansatz equation (4.6) into equation (4.5)

$$\mathcal{L}_1 = \frac{i}{2}(\psi\psi_t^* - \psi^*\psi_t)$$

$$= A^2\left(b_t(x-\zeta)^2 - (2b\zeta_t - v_t)(x-\zeta) - v\zeta_t + \varphi_t\right)\mathrm{sech}\left[\frac{(x-\zeta)}{a}\right]^2$$

$$\mathcal{L}_2 = \frac{1}{2}|\psi_x|^2 = \frac{1}{2}\psi_x\psi_x^*$$

$$= \frac{1}{2}A^2\left(\frac{1}{a^2}\tanh\left(\frac{x-\zeta}{a}\right)^2 + \left(4b^2(x-\zeta)^2 + 4b\xi(x-\zeta) + \xi^2\right)\right)\mathrm{sech}\left[\frac{(x-\zeta)}{a}\right]^2$$

$$\mathcal{L}_3 = (\alpha x - V(x,t))|\psi|^2$$

$$= A^2(\alpha x - v_0\delta(x))\,\mathrm{sech}\left[\frac{(x-\zeta)}{a}\right]^2$$

$$\mathcal{L}_4 = -\frac{1}{2}|\psi|^4$$

$$= \frac{\gamma}{2}A^4\mathrm{sech}^4\left[\frac{(x-\zeta)}{a}\right]$$

integrating over the space variable, we get the averaged Lagrangian

$$L = \sum_{i=1}^{4}L_i = \sum_{i=1}^{4}\left(\int_{-\infty}^{\infty}\mathcal{L}_i dx\right)$$

$$L_1 = \int_{-\infty}^{\infty}\mathcal{L}_1 dx$$

$$= A^2 a\sqrt{\pi}\left(\frac{1}{2}a^2 b_t - \xi\zeta_t + \varphi_t\right)$$

$$= N\left(\frac{1}{12}\pi^2 a^2 b_t - \xi\zeta_t + \varphi_t\right)$$

$$L_2 = \int_{-\infty}^{\infty} \mathcal{L}_2 \, dx$$

$$= A^2 a \sqrt{\pi} \left(\frac{1}{6a^2} + \frac{1}{6} \pi^2 a^2 b^2 + \frac{1}{2} \xi^2 \right)$$

$$= N \left(\frac{1}{6a^2} + \frac{1}{6} \pi^2 a^2 b^2 + \frac{1}{2} \xi^2 \right)$$

$$L_3 = \int_{-\infty}^{\infty} \mathcal{L}_3 \, dx$$

$$= A^2 a \sqrt{\pi} \left(\alpha \zeta - \frac{v_0}{2a} \operatorname{sech}^2 \left[\frac{\zeta}{a} \right] \right)$$

$$= N \left(\alpha \zeta - \frac{v_0}{2a} \operatorname{sech}^2 \left[\frac{\zeta}{a} \right] \right)$$

$$L_4 = \int_{-\infty}^{\infty} \mathcal{L}_4 \, dx$$

$$= -\frac{\gamma}{6a} N^2$$

Then, the total averaged Lagrangian is obtained

$$L = N \left[\frac{\pi^2}{12} a^2 b_t + \frac{\pi^2}{6} a^2 b^2 - \frac{1}{2} \zeta_t^2 - \alpha \zeta + \varphi_t + \frac{1}{6a^2} + \frac{V_0}{2a} \operatorname{sech}^2 \left(\frac{\zeta}{a} \right) - \frac{\gamma N}{6a} \right], \qquad (4.7)$$

where we have taken into account that the velocity is equal to the time derivative of the center of mass position $\xi = \zeta_t$ and $A^2 = N/(2a)$, with the norm of the wave packet

$$N = \int_{-\infty}^{\infty} |\psi(x)|^2 \, dx = 2A^2 a$$

being the conserved quantity. Now the usual procedure of the VA, applied to equation (4.7) leads to the following set of equations for the width and center of mass position of the wave packet

$$a_{tt} = \frac{4}{\pi^2 a^3} + \frac{6V_0}{\pi^2 a^2}\text{sech}^2\left(\frac{\varsigma}{a}\right)\left[1 - \frac{2\varsigma}{a}\tanh\left(\frac{\varsigma}{a}\right)\right] - \frac{2\gamma N}{\pi^2 a^2},$$ (4.8)

$$\varsigma_{tt} = -\alpha + \frac{V_0}{a^2}\text{sech}^2\left(\frac{\varsigma}{a}\right)\tanh\left(\frac{\varsigma}{a}\right).$$ (4.9)

The coupled system of equations (4.8) and (4.9) represents the main result of this section. Its fixed points provides the stationary width of the soliton (a_0) and its distance from the mirror (ς_0), where the actions of the gravity and repulsive potential $V(\varsigma)$ cancel each other. As a result of this balance, the soliton placed at a fixed point remains at rest (levitates) above the mirror. Small amplitude dynamics of the soliton's width and center of mass position near the stationary state can be described as motion of a unit mass particle in the anharmonic potentials $U_1(a)$ and $U_2(\varsigma)$, respectively,

$$a_{tt} = -\frac{\partial U_1}{\partial a},$$

(4.10)

$$U_1(a) = \frac{2}{\pi^2 a^2} - \frac{2\gamma N}{\pi^2 a} - \frac{6V_0}{\pi^2 a}\text{sech}^2\left(\frac{\varsigma_0}{a}\right),$$

$$\varsigma_{tt} = -\frac{\partial U_2}{\partial \varsigma},$$

(4.11)

$$U_2(\varsigma) = \alpha\varsigma + \frac{V_0}{2a_0}\text{sech}^2\left(\frac{\varsigma}{a_0}\right).$$

In figure (4.3) the shapes of the potentials in equations (4.10) and (4.11) and examples of soliton bouncing dynamics over the reflecting surface, modeled by a delta function, are illustrated. As expected, when the soliton is positioned at a fixed point (ς_0, a_0), it stays motionless (lower pair of curves in the middle panel). Small amplitude oscillations in PDE data is due to the fact that the VA gives approximate values for the fixed point. When the soliton is dropped towards the mirror from a height $x_0 = 3$, it performs

bouncing motion. Slow decay of the amplitude of oscillations and increase of its bouncing frequency are due to partial escape of the wave packet via tunnel effect (upper pair of curves in the middle panel).

The frequency of small amplitude oscillations of the soliton's motion can be estimated from VA by linearizing the Eqs. (4.8)-(4.9) near the fixed point (ζ_0, a_0).

$$\omega_0 = \left(V_0 / a_0^3\right)^{1/2} \operatorname{sech}^2(\zeta_0 / a_0)\left[2\sinh^2(\zeta_0 / a_0) - 1\right]^{1/2}. \tag{4.12}$$

The corresponding period for $V_0 = 1$, $\zeta_0 = 1.213$ and $a_0 = 0.468$ is $T_0 = 2\pi / \omega_0 > 9.7$. This is in quite good agreement with numerical simulations of the GPE equation (4.3) for equilibrium state, as shown in the middle panel of Fig. (4.3). An expression similar to equation (4.12) can be derived for the frequency of the soliton's width.

$$\Omega_0 = \left(\frac{2}{\pi a_0^2}\right)\left[3 - \gamma N a_0 + \frac{3V_0}{a_0}\operatorname{sech}^2\left(\frac{\zeta_0}{a_0}\right)\left(a_0^2 + 2\zeta_0^2 - 4a_0\zeta_0\tanh\left(\frac{\zeta_0}{a_0}\right) - 3\zeta_0^2\operatorname{sech}^2\left(\frac{\zeta_0}{a_0}\right)\right)\right]^{1/2}. \tag{4.13}$$
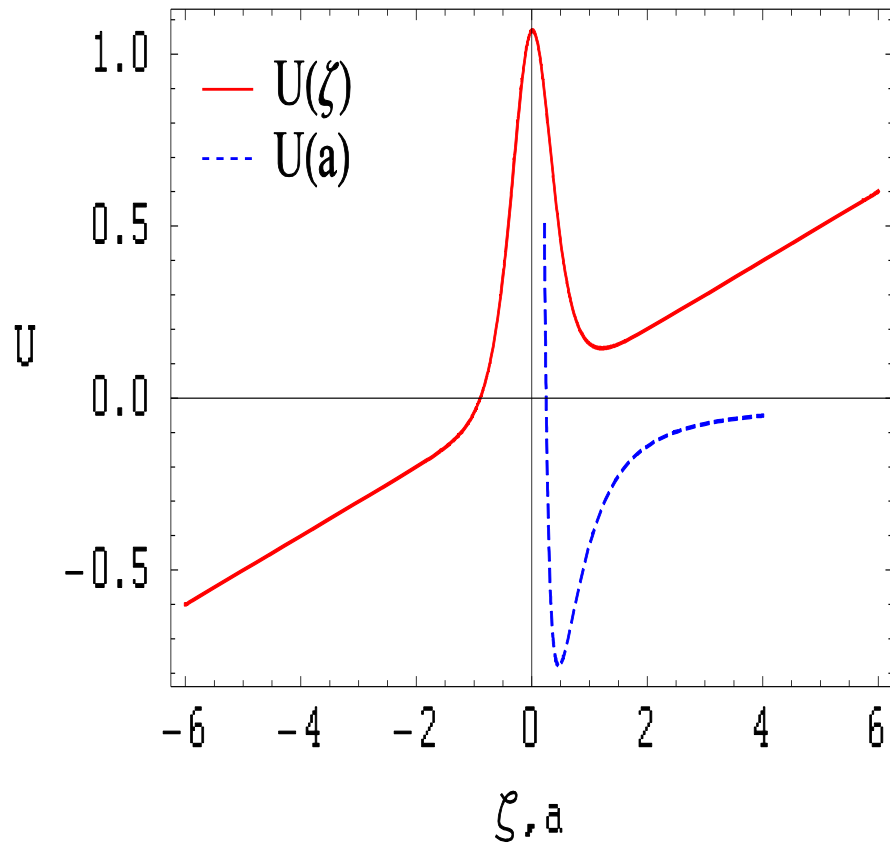
Figure 4.3: (Part I) Comparison of the center of mass position as a function of time, obtained from solving the VA equation (4,8) and numerical simulation of the governing equation (4.3) for the reflecting surface of the delta function type $V(x) = V_0\delta(x)$. The lower pair of curves corresponds to the fixed point initial conditions, while the upper pair of curves corresponds to dropping the wave packet from height $x_0 = 3$ above the mirror.
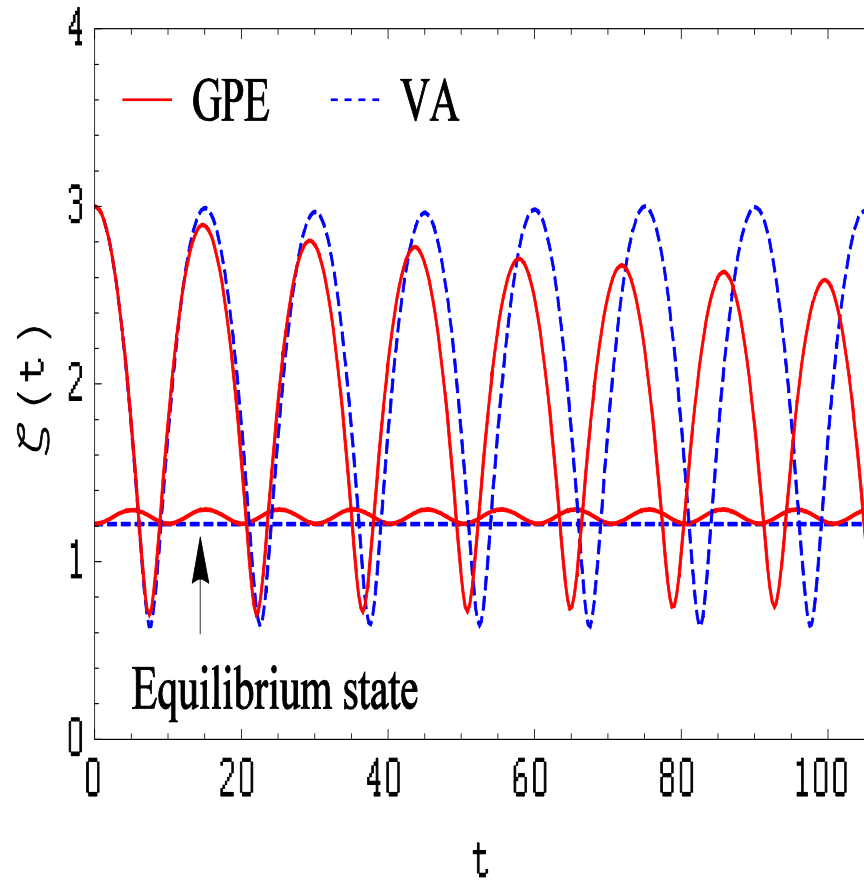
Figure 4.3: (Part II) Anharmonic potentials for the center of mass $U(\zeta)$ and width $U(a)$ of the soliton, according to equations (4.10)-(4.11). For the set of parameters $N=4$, $\gamma=1$, $\alpha=0.1$, and $V_0=1$ the fixed point is found to be $\zeta_0=1.213$, $a_0=0.468$. (Continuous)
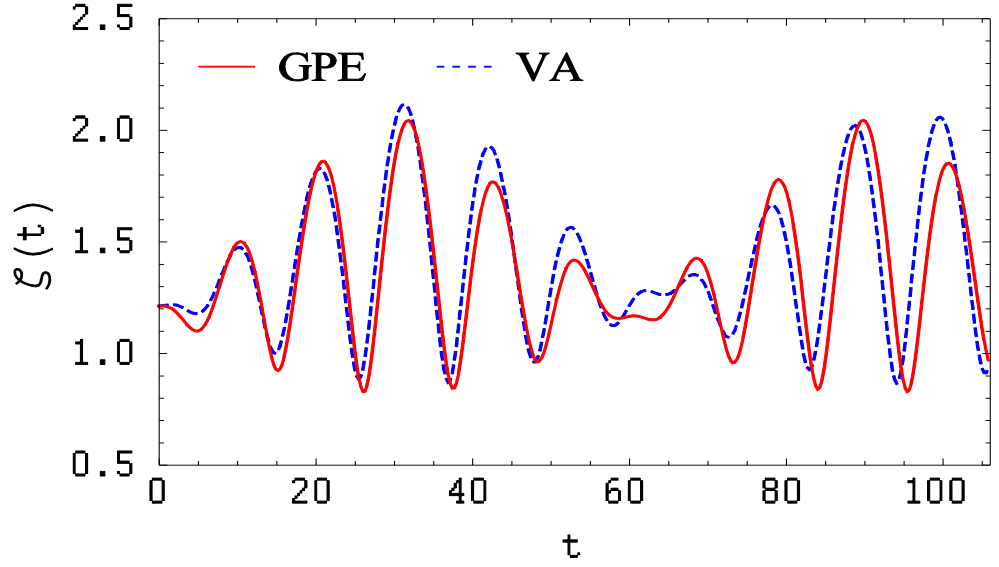
Figure 4.3: (Part III) (Continuous) nonlinear resonance in the center of mass dynamics when the coefficient of gravity is varied in time with a resonance frequency $\alpha(t) = 0.1[1 + 0.3\sin(\omega_0 t)]$. Stationary state of the soliton with parameters predicted by VA is used as initial condition. Discrepancy (phase shift) between the GPE and VA is associated with asymmetric deformation of the wave packet when reflecting from the mirror

Numerical estimate for the fixed point $\left(\zeta_0, \ a_0 \right)$, and $N = 4$, $\gamma = 1$, $V_0 = 1$ is

$$T_0 = \frac{2\pi}{\Omega_0} = 1.94,$$

which is also in good agreement with the results of GPE.

When the mathematical model has been developed, it is appropriate to mention its range of validity. As pointed out in the previous section, hard bounces of the soliton lead to its asymmetric deformation at the instant of collision with the mirror. Deviation of the waveform from the class of selected anzats equation (4.6) is the main factor compromising the accuracy of the variational approach. Therefore, the validity of the

analytical model developed in this section is limited to the domain of *soft collisions* (at small velocity) and *dense* (tall and narrow) wave packets. These conditions are satisfied when the effect of gravity is reduced $(\alpha \ll 1)$ and the soliton contains a large number of atoms, so that the nonlinearity-induced self-focusing of the wave packet is significant.

The VA is especially useful when small amplitude oscillations of the wave packet near its equilibrium position are the subject of interest. In this case the analytic formulas for the frequency of oscillations for the center-of-mass equation (4.12) and width equation (4.13) are quite accurate. If the relevant experiment shows deviation from the prediction of these formulas the results will be an indication of the presence of additional forces acting on the soliton near the surface. Actually, the experiments with BEC aimed at exploring the Casimir-Polder force near the surface use the perturbations of the frequency of center-of-mass oscillations of the condensate to detect this force (Harber et al., 2005; Obrecht et al., 2007; Sorrentino et al., 2009). Similar experiments with attractive BEC in the bouncing soliton regime would be very informative.

4.3 **Fermi type acceleration of a matter wave soliton**

The capability of the matter wave soliton to perform bouncing motion above the atomic mirror, preserving its integrity, suggests to consider the Fermi type acceleration (FA) in this system. FA is the energy gained by a particle that expose to periodic or random driving forces. It was proposed by Enrico Fermi (Fermi, 1949) to explain why cosmic rays have so high energy. For the mechanical analogue, the possibility of unbounded growth of energy by an elastic ball bouncing vertically on a single periodically oscillating plate, under the effect of gravity, was rigorously proven in Ref. (Pustylnikov, 1995). A simple derivation of the growth rate of the ball's velocity within the framework

of classical mechanics $\left(v \sim t^{1/3}\right)$ can be found in (Zaslavsky, 1984). Most studies of FA of matter waves are concerned with dynamical localization and chaotic behavior. In our model localization of the matter wave naturally arises from the nonlinearity of the condensate, and the parameter space does not contain chaotic regions.

Although the matter wave soliton does not have all necessary properties to demonstrate true FA (due to non elastic collision with the mirror, leakage of energy via tunnel effect, etc.), some features of FA can be observed, as we have revealed in numerical experiments. At first we need to prepare the initial stationary state of the matter wave packet levitating above the atomic mirror. The prediction of VA for parameters of the soliton and stationary state distance above the mirror (where the forces of gravity and repulsion of the mirror balance out) is approximated, as we have seen in the previous section. The inaccuracy leads to small amplitude oscillations of the soliton near the equilibrium state in the GPE simulations (see figure (4.3) Part II). In order to create a truly stationary initial state of the soliton above the reflecting surface we consider the first choice (a) for $V(x)$ in equation (4.4). For this ideal mirror potential, the equation (4.3) in the linear limit $\left(\gamma = 0\right)$, with boundary condition $\psi(0,t) = 0$, has analytic stationary solutions in terms of the Airy functions (Vallée & Soares, 2004),

$$\psi_n(x) = \mathcal{N} \, \mathrm{Ai}[(2\alpha)^{1/3}(x + x_n)], \tag{4.14}$$

where $\mathcal{N}$ is the normalization constant. In the following section, we shall be concerned with the ground state $(n = 0)$ of the wave packet in the gravitational cavity. The first root, given by $\mathrm{Ai}[(2\alpha)^{1/3}x] = 0$ for $\alpha = 0.1$, is found to be equal to $x_0 = -3.998$. The corresponding normalization factor is

$$\mathcal{N} = \left(\int_0^\infty \mathrm{Ai}^2[\alpha^{1/3}(x + x_0)]dx \right)^{-1/2} = 1.09. \tag{4.15}$$

In order to produce the initial state for numerical simulations of the FA, we insert the ground state wave function (4.14) with an appropriate norm into the GPE (4.3) with $\gamma = 0$ and slowly raise it to final value $\gamma = 1$ according to the law

$$\gamma(t) = \tanh\left(\frac{5t}{t_0}\right)$$

with $t_0 \sim 1000$. The obtained nonlinear waveform is shown in the abovepanel of figure (4.4).

Also in this figure we illustrate the resonant oscillations of the soliton's center of mass when the coefficient of nonlinearity (via atomic scattering length) is periodically changed in time.
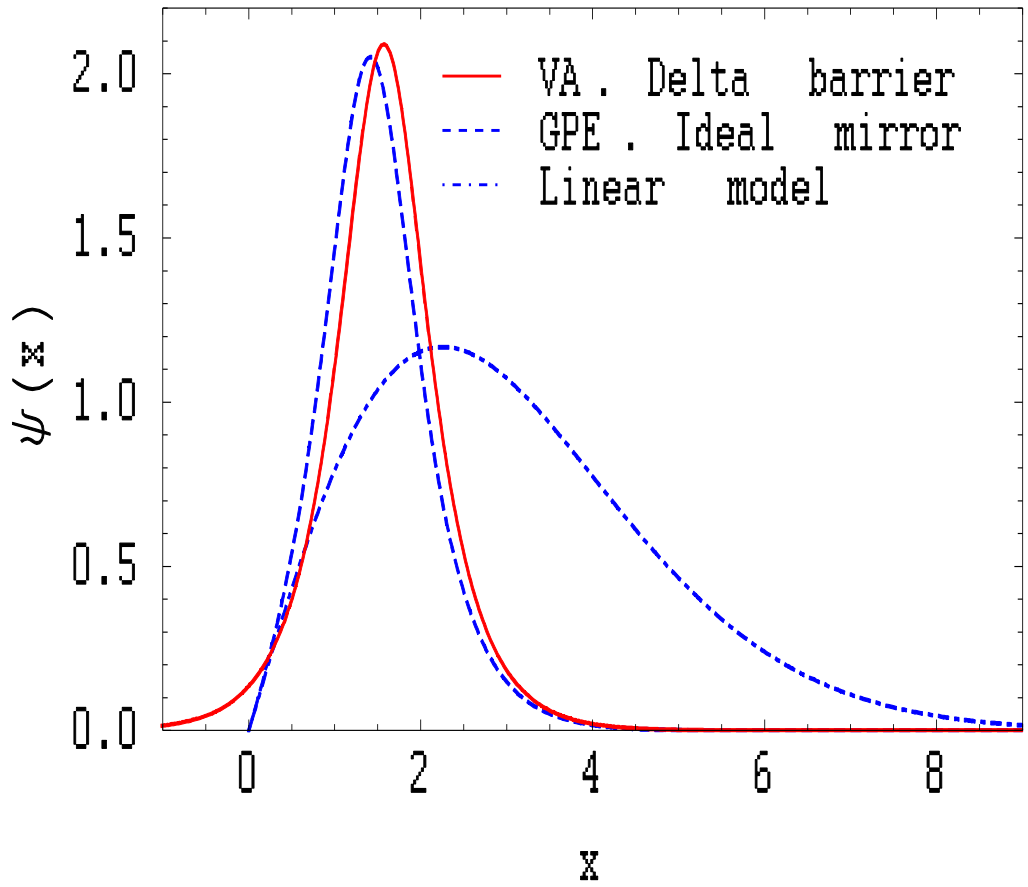
Figure 4.4: (Part I): Transformation of the ground state wave function of the linear problem (blue dot-dashed line) into solution of the nonlinear problem (blue dashed line) by slowly raising the coefficient of nonlinearity γ in equation (4.3) from zero to one. In the prediction of the VA Eqs. (4.8)-(4.9) for delta barrier potential (red solid line) the wave packet slightly penetrates into the region $x < 0$ due to the wave tunneling effect.
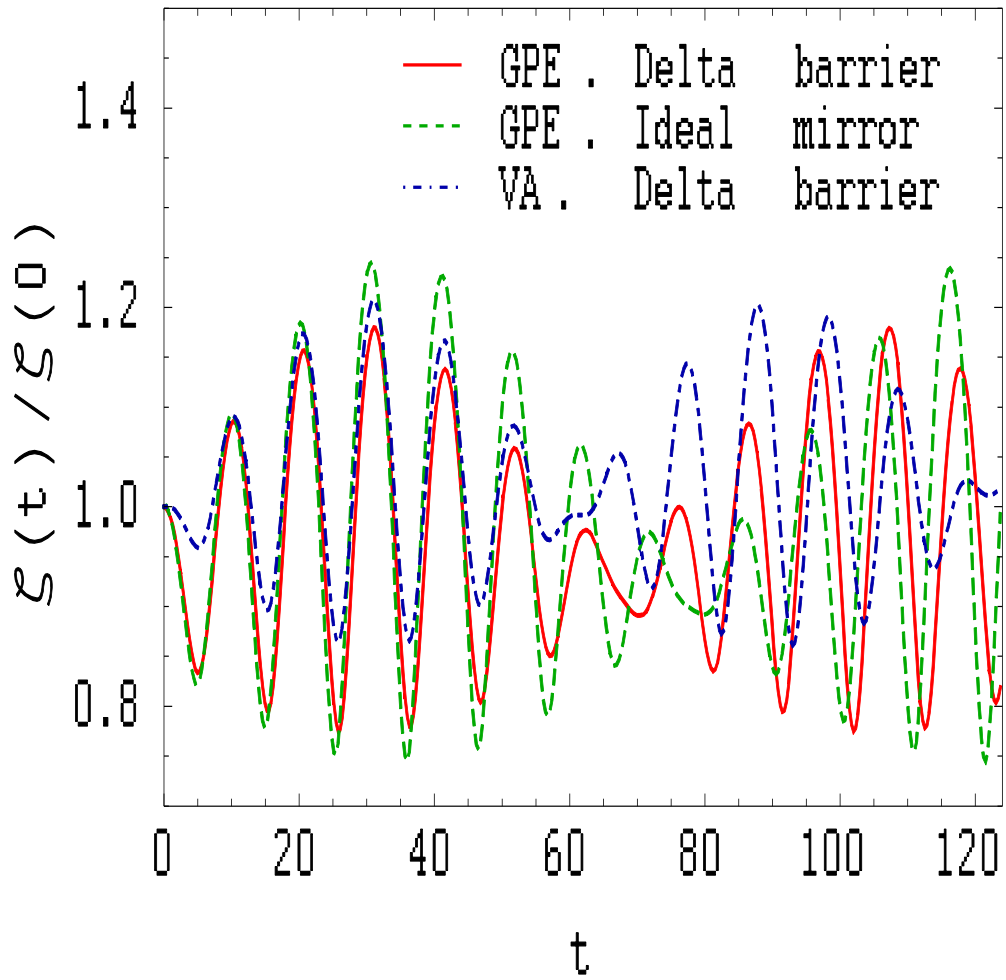
Figure 4.4: (Part II) Nonlinear resonance in the center of mass dynamics of the soliton, when the coefficient of nonlinearity is periodically varied in time $\gamma = 1 + \epsilon \sin(\omega_0 t)$
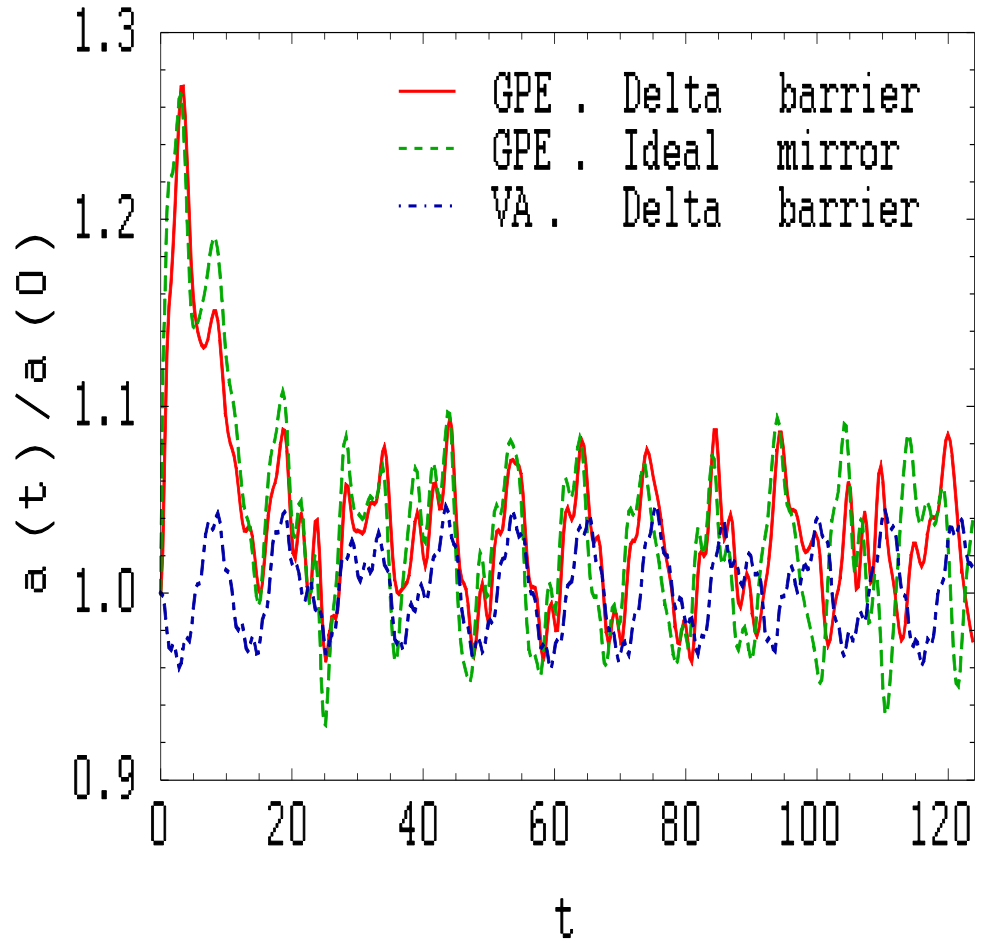
Figure 4.4: (Part III) Dynamics of the width has not resonant character due to the difference in frequencies Ω_0 and ω_0, estimated from equation (4.12)–(4.13). Parameter values $N = 4$, $\alpha = 0.1$, $V_0 = 5$, $\epsilon = 0.05$, $\omega_0 = 0.66$, $\Omega_0 = 1.7$.

It is evident that nonlinear resonance takes place at the frequency of small amplitude oscillations ω_0 estimated from the VA equation (4.12). Similar behavior was observed when the slope of the linear potential (strength of gravity) is changed with appropriate frequency (see the figure 3 Part(III)). Since the resonant frequencies are different for the center of mass $\left(\omega_0\right)$ and width $\left(\Omega_0\right)$ of the soliton, periodic modulation of the

parameter α or γ with frequency ω_0 does not induce resonant oscillations of the width, and vice versa. Characteristic feature inherent to both cases is that, oscillations show notable phase shift as compared to predictions of VA, which can be explained by asymmetric deformation of the soliton at the impact with the reflecting surface. In the VA we deal with the dynamics of a unit mass particle in the anharmonic potential. Nevertheless the VA provides qualitatively correct description of the system.

The focusing nonlinearity, inherent to BEC with negative s-wave scattering length, provides the wave packet's robustness against dispersive spreading and different kinds of perturbations. Due to this property matter wave solitons keep their integrity after reflection from the atomic mirror. In the following discussion, we consider the possibility of Fermi type of acceleration in the system. In numerical simulations we take the stationary state of the wave packet, predicted by VA as an initial condition for equation (4.3) and periodically change the vertical position of the reflecting surface or the slope of the linear potential.

Figure (4.5) illustrates the progressive gain of energy by the soliton when the position of the reflecting delta potential is periodically varied in time at a parametric resonance frequency. As the amplitude of oscillation above the mirror increases, de-tuning from the resonance occurs and further gain of energy stops. A proper synchronization would allow more increase of the kinetic energy of the soliton. Also there is a contribution of tunnel loss of the wave packet through the reflecting delta potential barrier
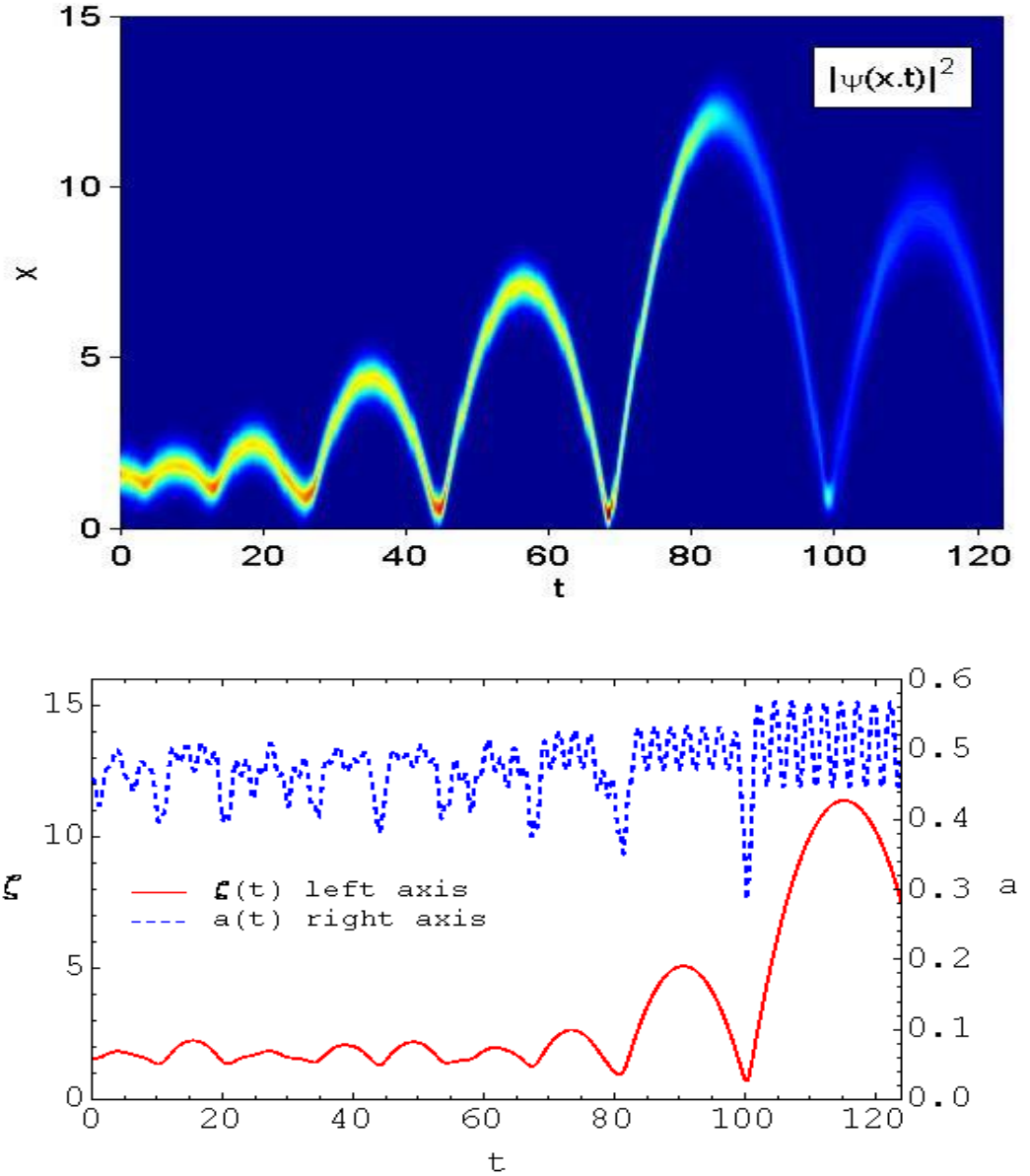
Figure 4.5: Soliton continuously increases its kinetic energy and farther departs from the stationary point $x_0 = 1.57$, when the vertical position of the delta function mirror with strength $V_0 = 5$, initially positioned at $x = 0$, is periodically changed at a parametric resonance frequency $f(t) = \varepsilon \sin(\Omega t)$, with $\varepsilon = 0.25$, $\Omega = 2\omega_0$, $\omega_0 = 0.66$, according to numerical simulations of the GPE equation (4.3). As the amplitude of oscillations increases, the de-tuning from the resonance occurs and energy gain reverses. Down panel: Corresponding prediction of the VA for the soliton's center of mass and width. A qualitative agreement with the results of the GPE is observed.

The corresponding predictions of the VA for the center of mass position ζ and width a are also shown on the down panel of figure (4.5). Note that the space coordinate in GPE and VA equations are designated by x and ζ respectively. Variation of the vertical position of the delta function mirror

$$V(x) = V_0 \delta(x + f(t)),$$

where

$$f(t) = \varepsilon \sin(\Omega t)$$

is a periodic function with amplitude ε and frequency Ω, leads to the VA equations, similar to Eqs. (4.8)-(4.9), but with replaced space variable on the right hand side

$$\zeta \to \zeta + f(t).$$

The frequency of small amplitude oscillations of the width, measured at upper turning point is $T_0 > 2.1$, $\approx$ which is close to the estimation from equation (4.13).

5 Conclusion

To conclude this thesis we summarize on main results as follow. In chapter one, we have given some background theory information about Bose-Einstein condensate and briefly described subjects studied in this thesis such as Modulation Instability, dipolar interaction and bouncing matter wave soliton reflecting on mirror, etc. In addition, we gave a brief history on the development of Bose-Einstein condensation. Furthermore, we have also given an introduction and review of the variational approximation approach.

In chapter two, we have investigated the modulational instability in a one-dimension as described by the Salerno equation. Salerno model can applied to Bose-Einstein Condensates in deep optical lattices. The analytical expression of modulation instability gain spectra is obtained, the regions and conditions of instability of plane wave solutions in the parameter space of the governing Salerno model were determined.

The existence and stability criteria for different type of strongly localized modes in discrete Salerno model have been derived. The localized solutions of Salerno model were obtained numerically using the homoclinic orbits intersection method.

In chapter three, we studied the effect of atomic dipole-dipole interactions on the dynamics of Bose-Einstein condensates by means of variational approximation and numerical simulations. Dipolar interactions give rise to an additional nonlinear term in the Gross-Pitaevskii equation which is spatially nonlocal. For qualitative analysis, we have employed a Gaussian response function in the nonlocal term. The developed model predicts the stationary shape of the soliton in dipolar BEC and its small

amplitude dynamics near the equilibrium state quite accurately. Solitons in dipolar BEC exhibit a resonant response to periodic variation of the coefficient of nonlocal nonlinearity at the main perturbation frequency and double of the main frequency, which is characteristic to the phenomenon of parametric resonance. Analytic expression for the frequency of low energy shape oscillations of the matter-wave packet has been derived, which elucidates the contribution of contact and dipolar interactions to the frequency of collective oscillations of the condensate. The obtained results can lead to a better understanding of the properties of ultra-cold dipolar quantum gases.

In chapter four the model of a quantum bouncer has been extended to a nonlinear domain of Bose-Einstein condensates. The analytical description is based on the variational approach. It has been revealed that a matter wave soliton bouncing above the reflecting surface (or atomic mirror) better preserves its integrity compared to a linear wave packet due to the focusing effect of the nonlinearity. This feature of the bright matter wave soliton allows to develop a variational approach, using an appropriate trial function, which provides a qualitatively correct description of its dynamics. A particle like behavior of the matter wave soliton bouncing above the atomic mirror is suggested to consider the Fermi type acceleration in the system. In numerical experiments, we observed the progressive energy gain by the soliton when the vertical position of the mirror is periodically varied in time. Further development of the proposed model may include the stochastic variation of the nonlinearity variation of the slope of the linear potential, and finally adjustment of the vertical position of the reflecting surface.

References

Abdullaev, F. K., & Brazhnyi, V. (2012). Solitons in dipolar Bose–Einstein condensates with a trap and barrier potential. *Journal of Physics B: Atomic, Molecular and Optical Physics, 45*(8), 085301.

Abdullaev, F. K., Gammal, A., Malomed, B. A., & Tomio, L. (2013). Bright solitons in quasi-one-dimensional dipolar condensates with spatially modulated interactions. *Physical Review A, 87*(6), 063621.

Abele, H., & Leeb, H. (2012). Gravitation and quantum interference experiments with neutrons. *New Journal of Physics, 14*(5), 055010.

Ablowitz, M. J., Prinari, B., & Trubatch, A. D. (2004). *Discrete and continuous nonlinear Schrödinger systems* (Vol. 302): Cambridge University Press.

Agrawal, G. P. (2007). *Nonlinear fiber optics*: Academic press.

Aikawa, K., Frisch, A., Mark, M., Baier, S., Rietzler, A., Grimm, R., & Ferlaino, F. (2012). Bose-Einstein condensation of erbium. *Physical review letters, 108*(21), 210401.

Alamoudi, S., Al Khawaja, U., & Baizakov, B. (2014). Averaged dynamics of soliton molecules in dispersion-managed optical fibers. *Physical Review A, 89*(5), 053817.

Anderson, D. (1983). Variational approach to nonlinear pulse propagation in optical fibers. *Physical Review A, 27*(6), 3135.

Anderson, M. H., Ensher, J. R., Matthews, M. R., Wieman, C. E., & Cornell, E. A. (1995). Observation of Bose-Einstein condensation in a dilute atomic vapor. *science, 269*(5221), 198-201.

Andreev, B. M., Magomedbekov, E. P., & Sicking, G. H. (2013). *Interaction of hydrogen isotopes with transition metals and intermetallic compounds (springer tracts in modern physics)*: Springer.

Baranov, M. (2001). Introduction to physics of ultra cold gases.

Belloni, M., Doncheski, M., & Robinett, R. (2005). Exact results for'bouncing'Gaussian wave packets. *Physica Scripta, 71*(2), 136.

Belloni, M., & Robinett, R. (2014). The infinite well and Dirac delta function potentials as pedagogical, mathematical and physical models in quantum mechanics. *Physics Reports, 540*(2), 25-122.

Benjamin, T. B., & Feir, J. (1967). The disintegration of wave trains on deep water Part 1. Theory. *Journal of Fluid Mechanics, 27*(03), 417-430.

Benseghir, A., Abdullah, W., Umarov, B., & Baizakov, B. (2013). parametric excitation of solitons in dipolar bose–einstein condensates. *Modern Physics Letters B, 27*(25).

Benseghir, A., Abdullah, W. W., Baizakov, B., & Abdullaev, F. K. (2014). Matter-wave soliton bouncing on a reflecting surface under the effect of gravity. *Physical Review A, 90*(2), 023607.

Berg, P., If, F., Christiansen, P. L., & Skovgaard, O. (1987). Soliton laser: A computational two-cavity model. *Physical Review A, 35*(10), 4167.

Bespalov, V., & Talanov, V. (1966). Filamentary structure of light beams in nonlinear liquids. *ZhETF Pisma Redaktsiiu, 3*, 471.

Bolpasi, V., Efremidis, N., Morrissey, M., Condylis, P., Sahagun, D., Baker, M., & von Klitzing, W. (2014). An ultra-bright atom laser. *New Journal of Physics, 16*(3), 033036.

Bongs, K., Burger, S., Birkl, G., Sengstock, K., Ertmer, W., Rzazewski, K., Lewenstein, M. (1999). Coherent evolution of bouncing Bose-Einstein condensates. *Physical review letters, 83*(18), 3577.

Bose, S. N. (1924). Plancks gesetz und lichtquantenhypothese. *Z. phys, 26*(3), 178.

Bradley, C., Sackett, C., & Hulet, R. (1997). Bose-Einstein condensation of lithium: Observation of limited condensate number. *Physical review letters, 78*(6), 985.

Bradley, C., Sackett, C., Tollett, J., & Hulet, R. (1995). Evidence of Bose-Einstein condensation in an atomic gas with attractive interactions. *Physical review letters, 75*(9), 1687.

Broky, J., Siviloglou, G. A., Dogariu, A., & Christodoulides, D. N. (2008). Self-healing properties of optical Airy beams. *Optics express, 16*(17), 12880-12891.

Canaguier-Durand, A., Gérardin, A., Guérout, R., Neto, P. A. M., Nesvizhevsky, V. V., Voronin, A. Y., Reynaud, S. (2011). Casimir interaction between a dielectric nanosphere and a metallic plane. *Physical Review A, 83*(3), 032508.

Carretero-González, R., Talley, J., Chong, C., & Malomed, B. (2006). Multistable solitons in the cubic–quintic discrete nonlinear Schrödinger equation. *Physica D: Nonlinear Phenomena, 216*(1), 77-89.

Chamorro-Posada, P., Sánchez-Curto, J., Aceves, A. B., & McDonald, G. S. (2014). Widely varying giant Goos–Hänchen shifts from Airy beams at nonlinear interfaces. *Optics letters, 39*(6), 1378-1381.

Chen, H.-H., & Liu, C.-S. (1976). Solitons in nonuniform media. *Physical review letters, 37*(11), 693.

Chin, C., Grimm, R., Julienne, P., & Tiesinga, E. (2010). Feshbach resonances in ultracold gases. *Reviews of Modern Physics, 82*(2), 1225.

Chiofalo, M., Succi, S., & Tosi, M. (2000). Ground state of trapped interacting Bose-Einstein condensates by an explicit imaginary-time algorithm. *Physical Review E, 62*(5), 7438.

Chremmos, I. D., & Efremidis, N. K. (2012). Reflection and refraction of an Airy beam at a dielectric interface. *JOSA A, 29*(6), 861-868.

Ciuryło, R., Tiesinga, E., & Julienne, P. (2005). Optical tuning of the scattering length of cold alkaline-earth-metal atoms. *Physical Review A, 71*(3), 030701.

Cornell, E. A., & Wieman, C. E. (2002). Nobel Lecture: Bose-Einstein condensation in a dilute gas, the first 70 years and some recent experiments. *Reviews of Modern Physics, 74*(3), 875.

Cornish, S., Parker, N., Martin, A., Judd, T., Scott, R., Fromhold, T., & Adams, C. (2009). Quantum reflection of bright matter-wave solitons. *Physica D: Nonlinear Phenomena, 238*(15), 1299-1305.

Cuevas, J., Malomed, B. A., Kevrekidis, P., & Frantzeskakis, D. (2009). Solitons in quasi-one-dimensional Bose-Einstein condensates with competing dipolar and local interactions. *Physical Review A, 79*(5), 053608.

Dalfovo, F., Giorgini, S., Pitaevskii, L. P., & Stringari, S. (1999). Theory of Bose-Einstein condensation in trapped gases. *Reviews of Modern Physics, 71*(3), 463.

Darmanyan, S., Kobyakov, A., & Lederer, F. (1998). Stability of strongly localized excitations in discrete media with cubic nonlinearity. *Journal of Experimental and Theoretical Physics, 86*(4), 682-686.

Davis, K. B., Mewes, M.-O., Andrews, M. v., Van Druten, N., Durfee, D., Kurn, D., & Ketterle, W. (1995). Bose-Einstein condensation in a gas of sodium atoms. *Physical review letters, 75*(22), 3969.

Della Valle, G., Savoini, M., Ornigotti, M., Laporta, P., Foglietti, V., Finazzi, M., Longhi, S. (2009). Experimental observation of a photon bouncing ball. *Physical review letters, 102*(18), 180402.

Desko, R., & Bord, D. (1983). The quantum bouncer revisited. *American Journal of Physics, 51*(1), 82-84.

Doncheski, M., & Robinett, R. (2001). Expectation value analysis of wave packet solutions for the quantum bouncer: Short-term classical and long-term revival behaviors. *American Journal of Physics, 69*(10), 1084-1090.

Doncheski, M. A., & Robinett, R. W. (1999). Anatomy of a quantum bounce'. *European journal of physics, 20*(1), 29.

Durfee, D., & Ketterle, W. (1998). Experimental studies of Bose-Einstein condensation. *Optics express, 2*(8), 299-313.

Eilbeck, J. C., & Johansson, M. (2003). *The discrete nonlinear Schrödinger equation-20 years on.* In Conference on Localization and Energy Transfer in Nonlinear Systems (p. 44).

Einstein, A. (1924). *Quantentheorie des einatomigen idealen Gases*: Akademie der Wissenshaften, in Kommission bei W. de Gruyter.

Fermi, E. (1949). On the origin of the cosmic radiation. *Physical Review, 75*(8), 1169.

Flach, S., & Gorbach, A. V. (2008). Discrete breathers—advances in theory and applications. *Physics Reports, 467*(1), 1-116.

Flügge, S. (1971). Practical Quantum Mechanics: Springer-Verlag, Berlin.

Gea-Banacloche, J. (1999). A quantum bouncing ball. *American Journal of Physics, 67*(9), 776-782.

Gea-Banacloche, J. (2000). A bouncing wavepacket: finite-wall and resonance effects. *Optics communications, 179*(1), 117-121.

Gibbs, R. (1975). The quantum bouncer. *American Journal of Physics, 43*(1), 25-28.

Giovanazzi, S., Görlitz, A., & Pfau, T. (2002). Tuning the dipolar interaction in quantum gases. *Physical review letters, 89*(13), 130401.

Gómez-Gardeñes, J., Malomed, B. A., Floría, L. M., & Bishop, A. (2006). Solitons in the Salerno model with competing nonlinearities. *Physical Review E, 73*(3), 036608.

Goodings, D., & Szeredi, T. (1991). The quantum bouncer by the path integral method. *American Journal of Physics, 59*(10), 924-930.

Góral, K., Rzążewski, K., & Pfau, T. (2000). Bose-Einstein condensation with magnetic dipole-dipole forces. *Physical Review A, 61*(5), 051601.

Granot, E. e., & Malomed, B. (2011). Acceleration of trapped particles and beams. *Journal of Physics B: Atomic, Molecular and Optical Physics, 44*(17), 175005.

Griesmaier, A. (2007). Generation of a dipolar Bose–Einstein condensate. *Journal of Physics B: Atomic, Molecular and Optical Physics, 40*(14), R91.

Griesmaier, A., Werner, J., Hensler, S., Stuhler, J., & Pfau, T. (2005). Bose-Einstein condensation of chromium. *Physical review letters, 94*(16), 160401.

Gross, E.P. (1961). Structure of a quantized vortex in boson systems. *Il Nuovo Cimento 20 (3)*: 454–477.

Grossmann, S., & Holthaus, M. (1995). On Bose-Einstein condensation in harmonic traps. *Physics Letters A, 208*(3), 188-192.

Harber, D., Obrecht, J., McGuirk, J., & Cornell, E. (2005). Measurement of the Casimir-Polder force through center-of-mass oscillations of a Bose-Einstein condensate. *Physical Review A, 72*(3), 033610.

Hasegawa, A. (1970). Observation of self-trapping instability of a plasma cyclotron wave in a computer experiment. *Physical review letters, 24*(21), 1165.

Ichikawa, G., Komamiya, S., & Kamiya, Y. (2014). Observation of the Gravitationally Bound Quantum States of Ultracold Neutrons with Submicron Spatial Resolution. Physical review letters, 112(7), 071101.

Jin, D., Ensher, J., Matthews, M., Wieman, C., & Cornell, E. (1996). Collective excitations of a Bose-Einstein condensate in a dilute gas. *Physical review letters, 77*(3), 420.

Karpman, V. (1967). Self-modulation of nonlinear plane waves in dispersive media. *Soviet Journal of Experimental and Theoretical Physics Letters, 6*, 277.

Kasevich, M. A., Weiss, D. S., & Chu, S. (1990). Normal-incidence reflection of slow atoms from an optical evanescent wave. *Optics letters, 15*(11), 607-609.

Keldysh, L., & Kozlov, A. (1968). Collective properties of excitons in semiconductors. *Sov. Phys. JETP, 27*, 521.

Ketterle, W., & Van Druten, N. (1996). Bose-Einstein condensation of a finite number of particles trapped in one or three dimensions. *Physical Review A, 54*(1), 656.

Kevrekidis, P. G. (2009). *The discrete nonlinear schrèodinger equation: mathematical analysis, numerical computations and physical perspectives* (Vol. 232): Springer.

Kevrekidis, P. G., Frantzeskakis, D. J., & Carretero-González, R. (2007). *Emergent nonlinear phenomena in Bose-Einstein condensates:* Theory and experiment (Vol. 45): Springer.

Köhler, T., Góral, K., & Julienne, P. S. (2006). Production of cold molecules via magnetically tunable Feshbach resonances. *Reviews of Modern Physics, 78*(4), 1311.

Kraft, S., Vogt, F., Appel, O., Riehle, F., & Sterr, U. (2009). Bose-Einstein Condensation of Alkaline Earth Atoms: Ca 40. *Physical review letters, 103*(13), 130401.

Lahaye, T., Menotti, C., Santos, L., Lewenstein, M., & Pfau, T. (2009). The physics of dipolar bosonic quantum gases. *Reports on Progress in Physics, 72*(12), 126401.

Langhoff, P. (1971). Schrödinger particle in a gravitational well. *American Journal of Physics, 39*(8), 954-957.

Lederer, F., Stegeman, G. I., Christodoulides, D. N., Assanto, G., Segev, M., & Silberberg, Y. (2008). Discrete solitons in optics. *Physics Reports, 463*(1), 1-126.

Lee, C., & Brand, J. (2006). Enhanced quantum reflection of matter-wave solitons. *EPL (Europhysics Letters), 73*(3), 321.

Lin, Y.-J., Jimenez-Garcia, K., & Spielman, I. (2011). Spin-orbit-coupled Bose-Einstein condensates. *Nature, 471*(7336), 83-86.

London, F. (1938). On the bose-einstein condensation. *Physical Review, 54*(11), 947.

Lu, M., Burdick, N. Q., Youn, S. H., & Lev, B. L. (2011). Strongly dipolar Bose-Einstein condensate of dysprosium. *Physical review letters, 107*(19), 190401.

Malomed, B. A. (2002). Variational methods in nonlinear fiber optics and related fields. *Progress in Optics, 43*, 71-193.

Marchant, A., Billam, T., Wiles, T., Yu, M., Gardiner, S., & Cornish, S. (2013). Controlled formation and reflection of a bright solitary matter-wave. *Nature communications, 4*, 1865.

Marinescu, M., & You, L. (1998). Controlling atom-atom interaction at ultralow temperatures by dc electric fields. *Physical review letters, 81*(21), 4596.

Mewes, M.-O., Andrews, M., Kurn, D., Durfee, D., Townsend, C., & Ketterle, W. (1997). Output coupler for Bose-Einstein condensed atoms. *Physical review letters, 78*(4), 582.

Naidon, P., & Julienne, P. S. (2006). Optical Feshbach resonances of alkaline-earth-metal atoms in a one-or two-dimensional optical lattice. *Physical Review A, 74*(6), 062713.

Nesvizhevsky, V. V., BoÈrner, H. G., Petukhov, A. K., Abele, H., Baeßler, S., Rueß, F. J., Petrov, G. A. (2002). Quantum states of neutrons in the Earth's gravitational field. *Nature, 415*(6869), 297-299.

Nicolin, A. I., Carretero-González, R., & Kevrekidis, P. (2007). Faraday waves in Bose-Einstein condensates. *Physical Review A, 76*(6), 063609.

Obrecht, J. M., Wild, R., Antezza, M., Pitaevskii, L., Stringari, S., & Cornell, E. (2007). Measurement of the temperature dependence of the Casimir-Polder force. *Physical review letters, 98*(6), 063201.

Ostrovskii, L. (1967). Propagation of wave packets and space-time self-focusing in a nonlinear medium. *Sov. Phys. JETP, 24*, 797.

Pasquini, T., Saba, M., Jo, G.-B., Shin, Y., Ketterle, W., Pritchard, D., Mulders, N. (2006). Low velocity quantum reflection of Bose-Einstein condensates. *Physical review letters, 97*(9), 093201.

Pasquini, T. A., Shin, Y., Sanner, C., Saba, M., Schirotzek, A., Pritchard, D. E., & Ketterle, W. (2004). Quantum reflection from a solid surface at normal incidence. *Physical review letters, 93*(22), 223201.

Pedri, P., & Santos, L. (2005). Two-dimensional bright solitons in dipolar Bose-Einstein condensates. *Physical review letters, 95*(20), 200404.

Perrin, H., Colombe, Y., Mercier, B., Lorent, V., & Henkel, C. (2006). Diffuse reflection of a Bose–Einstein condensate from a rough evanescent wave mirror. *Journal of Physics B: Atomic, Molecular and Optical Physics, 39*(22), 4649.

Pethick, C., & Smith, H. (2002). *Bose-Einstein condensation in dilute gases*: Cambridge university press.

Pitaevskii, L., (1961). Vortex Lines in an Imperfect Bose Gas. *Soviet Physics JETP-USSR* 13 (2): 451–454. 1961.

Pitaevskii, L., Stringari, S., & Leggett, A. (2004). Bose-einstein condensation. Physics Today, 57(10), 74-76.

Plumhof, J. D., Stöferle, T., Mai, L., Scherf, U., & Mahrt, R. F. (2013). Room-temperature Bose–Einstein condensation of cavity exciton–polaritons in a polymer. *Nature materials*.

Press, W. H., Flannery, B. P., Teukolsky, S. A., & Vetterling, W. T. (1990). Numerical recipes: Cambridge university press Cambridge.

Pustylnikov, L. D. (1995). On the stability of solutions and absence of Arnol'd diffusion in a nonintegrable Hamiltonian system of a general form with three degrees of freedom. *Weierstraß-Inst. f. Angewandte Analysis u. Stochastik.*

Saif, F., Naseer, K., & Ayub, M. (2014). Non-dispersive, accelerated matter-waves. *The European Physical Journal D, 68*(4), 1-4.

Saif, F., & Rehman, I. (2007). Coherent acceleration of material wave packets in modulated optical fields. *Physical Review A, 75*(4), 043610.

Sakurai, J. (1994). Modern Quantum Mechanics. *Eine der ersten Darstellungen, welche die Quantenmechanik über grundlegende Experimente aufbaut. Relativ hohes Niveau. Lehrbuchsammlung*.

Salerno, M. (1992). Quantum deformations of the discrete nonlinear Schrödinger equation. *Physical Review A, 46*(11), 6856.

Santos, L., Shlyapnikov, G., Zoller, P., & Lewenstein, M. (2000). Bose-Einstein condensation in trapped dipolar gases. *Physical review letters, 85*(9), 1791.

Savalli, V., Stevens, D., Estève, J., Featonby, P., Josse, V., Westbrook, N., Aspect, A. (2002). Specular reflection of matter waves from a rough mirror. *Physical review letters, 88*(25), 250404.

Sinha, S., & Santos, L. (2007). Cold dipolar gases in quasi-one-dimensional geometries. *Physical review letters, 99*(14), 140406.

Siviloglou, G., Broky, J., Dogariu, A., & Christodoulides, D. (2007). Observation of accelerating Airy beams. *Physical review letters, 99*(21), 213901.

Sorrentino, F., Alberti, A., Ferrari, G., Ivanov, V., Poli, N., Schioppo, M., & Tino, G. (2009). Quantum sensor for atom-surface interactions below 10 μ m. *Physical Review A, 79*(1), 013409.

Stellmer, S., Tey, M. K., Huang, B., Grimm, R., & Schreck, F. (2009). Bose-Einstein condensation of strontium. *Physical review letters, 103*(20), 200401.

Strecker, K. E., Partridge, G. B., Truscott, A. G., & Hulet, R. G. (2002). Formation and propagation of matter-wave soliton trains. *Nature, 417*(6885), 150-153.

Tabi, C., Mohamadou, A., & Kofane, T. (2010). Modulational instability in the anharmonic Peyrard-Bishop model of DNA. *The European Physical Journal B-Condensed Matter and Complex Systems, 74*(2), 151-158.

Taniuti, T., & Washimi, H. (1968). Self-trapping and instability of hydromagnetic waves along the magnetic field in a cold plasma. *Physical review letters, 21*(4), 209.

Tikhonenkov, I., Malomed, B., & Vardi, A. (2008). Anisotropic solitons in dipolar Bose-Einstein condensates. *Physical review letters, 100*(9), 090406.

Umarov, B., Benseghir, A., & Messikh, A. (2011). Modulational Instability In Salerno Model. *Australian Journal of Basic and Applied Sciences, 5*(5), 25-28.

Vallée, O., & Soares, M. (2004). *Airy functions and applications to physics*: World Scientific.

Van Zoest, T., Gaaloul, N., Singh, Y., Ahlers, H., Herr, W., Seidel, S., Kajari, E. (2010). Bose-Einstein condensation in microgravity. *science, 328*(5985), 1540-1543.

Whineray, S. (1992). An energy representation approach to the quantum bouncer. *American Journal of Physics, 60*(10), 948-950.

Yi, S., & You, L. (2000). Trapped atomic condensates with anisotropic interactions. *Physical Review A, 61*(4), 041604.

Yi, S., & You, L. (2002). Probing dipolar effects with condensate shape oscillation. *Physical Review A, 66*(1), 013607.

Zaslavsky, G. M. (1984). Stochasticity of Dynamical systems. *Nauka, Moscow*.

Publications

Part of material of this thesis has published in the following references:

A. Benseghir, W. A. T. Wan Abdullah, B. B. Baizakov, and F. Kh. Abdullaev. *Matter-wave soliton bouncing on a reflecting surface under the effect of gravity.* Physical Review A 90,023607 (2014) (ISI Cited)

A. Benseghir, W.A.T Wan Abdullah , B.A. Umarov, B. B. Baizakov. *Parametric Excitation Of Solitons In Dipolar Bose Einstein Condensates.* Modern Physics Letters B, Vol. 27, No. 25 (2013) 1350184 (12 pages) (ISI Cited)

A. Benseghir, A. Messikh, B.A. Umarov, W.A.T Wan Abdullah, A. Bouketir, C.H. Ooi. *Strongly localized modes in discrete Salerno model.* World Applied Sciences Journal 21(Mathematical Applications in Engineering) 166-171, (2013)

B.A. Umarov, **A. Benseghir,** A. Messikh. *Modulation Instability in Salerno model.* Australian Journal of Basic and Applied Sciences 5(5): 25-28, (2011) (indexed by ISI)

Appendix A:
Ordinary Differential Equations solving code

One of the most famously used method is fourth order Rang-Kutta method (RK4) to solve ordinary differential equation, the equation is given

$$\frac{\partial y(t)}{\partial t} = f(y(t), t)$$

We have

$$k_1 = dt\, f(y(t), t)$$

$$k_2 = dt\, f(y(t) + \frac{1}{2}k_1, t + \frac{1}{2}dt)$$

$$k_3 = dt\, f(y(t) + \frac{1}{2}k_2, t + \frac{1}{2}dt)$$

$$k_4 = dt\, f(y(t) + k_3, t + dt)$$

Then

$$y(t + dt) = y(t) + \frac{1}{6}k_1 + \frac{1}{3}k_2 + \frac{1}{3}k_3 + \frac{1}{6}k_4 + O\left[(dt)^6\right]$$

If we have second order ordinary differential equation such as in chapter 3 and four, we convert it to first ordinary differential by using the auxiliary function for example we have this function

$$\frac{d^2 y(t)}{dt^2} + a.\frac{dy(t)}{dt} = b$$

This second ordinary equation is transformed to the system of first ordinary equations

$$\begin{cases} \dfrac{dy(t)}{dt} = z(t) \\ \dfrac{dz(t)}{dt} = -a.z(t) + b \end{cases}$$

Fortran code, which use it to solve system of OD equation with subroutine of Runge-Kutta IV method.

ROGRAM width (or Center of mass)

IMPLICIT none

INTEGER n

PARAMETER (n=2)

REAL t, dt, tend, y(n), dydt(n), yout(n)

EXTERNAL derivs

tend=100.   ! final time

dt=tend/1000. ! time step

c---- initial conditions

t=0.

y(1)=1. ! y(0) is initial position

y(2)=0.1 ! $z(0) = y'(0)$ is initial velocity

c---- propagate the solution from 0 to tend

```fortran
      do while(t<tend)

        call rk4(a,dadt,n,t,dt,aout,derivs)

        t=t+dt

        y(1)=yout(1)

        write(7,'(1x,3f12.6)') t, yout(1)

      enddo

      close(7)

      END



      SUBROUTINE derivs(t,y,dydt)

      real pi,t,y(2),dydt(2)

       Amp= 1.0.

       alp=0.1

      pi=4.*atan(1.)

      dydt(1)=y(2)

      dydt(2)= -a*y(2)+b

      return

      END
```

```
SUBROUTINE rk4(y,dydx,n,x,h,yout,derivs)

INTEGER n,NMAX

REAL h,x,dydx(n),y(n),yout(n)

EXTERNAL derivs

PARAMETER (NMAX=50)

INTEGER i

REAL h6,hh,xh,dym(NMAX),dyt(NMAX),yt(NMAX)

hh=h*0.5

h6=h/6.

xh=x+hh

do i=1,n

  yt(i)=y(i)+hh*dydx(i)

enddo

call derivs(xh,yt,dyt)

do i=1,n

  yt(i)=y(i)+hh*dyt(i)

enddo
```

```fortran
      call derivs(xh,yt,dym)

      do i=1,n

        yt(i)=y(i)+h*dym(i)

        dym(i)=dyt(i)+dym(i)

      enddo

      call derivs(x+h,yt,dyt)

      do i=1,n

        yout(i)=y(i)+h6*(dydx(i)+dyt(i)+2.*dym(i))

      enddo

      return

      END
```

Appendix B:
Gross-Pitaevskii equation with local interaction

We used this code program to solve Gross-Pitaevskii equation, interaction, which is investigated in chapter 4.

The model equation is

$$i\frac{\partial \psi(x,t)}{\partial t}+\frac{d}{2}\frac{\partial^2 \psi(x,t)}{\partial x^2}+g\left|\psi(x,t)\right|^2 \psi(x,t)+V(x)\psi(x,t)+\alpha x\psi(x,t)=0, \quad (C.1)$$

For solving this equation, we used the split step method. The split step method is one of important method used to solve partial differential equation PDE numerically

The PDE such as GPE is written as

Which rewrite it as

$$i\frac{\partial \psi(x,t)}{\partial t}=\left(\hat{L}+\hat{N}\right)\psi(x,t) \quad (C.2)$$

The part of $\hat{L}$ represents linear part and $\hat{N}$ represents nonlinear part in equation(C.1)

The equation (C.1) can be split into linear part,

$$\frac{i\partial \psi(x,t+dt)}{\partial t}=-\frac{d}{2}\frac{\partial^2 \psi(x,t)}{\partial x^2}=\hat{L}\psi(x,t) \quad (C.2)$$

and non-linear part

$$i\frac{\partial \psi(x,t)}{\partial t}=\left(-g\left|\psi(x,t)\right|^2+V(x)+\alpha x\right)\psi(x,t)=\hat{N}\psi(x,t), \quad (C.3)$$

By using FFT (fast Fourier Transform) to get the solution

$$\psi(x,t+dt) = FFT^{-1}\left[FFT\left(e^{iD\,dt}\,e^{i\,dt\,N}\psi(x,t)\right)\right]$$
$$= FFT^{-1}\left[e^{-i\,dt\,k^2}FFT\left(e^{i\,dt\,N}\psi(x,t)\right)\right]$$

The code program is given

PROGRAM GPE_1D

IMPLICIT none

INTEGER n,i,istep,nsteps,nout

PARAMETER (n=1024)

REAL*8 L,x(n),dx,t,dt,tend,d,g,pi,x0,w0,tcl,delx

REAL*8 a,amp,xcom,wdth,norm,alp,v0,v(n),sink(n)

COMPLEX*16 u(n),smul(n)

COMMON L,dt,pi,d

open(7,file='data\Lc1.dat')

open(8,file='data\Lf1.dat')

pi=4.d0*datan(1.d0)

d=1.d0

g=0.d0

L=40.d0

x0= 10.d0

!1.2132d0 ! 3.d0 ! 1.2132d0; ! 10.d0 ! initial position of the soliton

tcl=2.d0*dsqrt(2.d0*x0) ! classical period for our scaling

dx=L/n

dt=0.001d0

tend = 4.d0*tcl

        ! 106.d0 ! 4.d0*tcl

nsteps=int(tend/dt)+1; nout=nsteps/400

alp=1.d0 ! 1.d0   ! linear potential

v0 = 1.d0 ! strength of the delta potential

amp=2.d0

a=0.8d0

c   amp=1.d0/dsqrt(dsqrt(2.d0*pi)) ! initial wave packet for linear problem

c   a=0.4679d0; amp=dsqrt(norm/(2.d0*a))

c----********* initial wave profile *****************

do i=1,n

x(i)=(i-1)*dx-L/2.d0

u(i)=dcmplx(amp/dcosh((x(i)-x0)/a),0.d0)

```
u(i)=dcmplx(amp*dexp(-(x(i)-x0)**2/a**2),0.d0)

write(8,'(1x,f12.6,f12.2,f12.6)') x(i),0.0,cdabs(u(i))**2

enddo

call center(n,x,dx,u,xcom,wdth,norm)

x0=xcom

w0=wdth

write(7,'(1x,4f12.4)') 0.d0,xcom,wdth,norm

c---- generate boundary absorption function

call absorb(n,x,L,dt,sink)

c---- evaluate spectral multiplicative

call spectr(n,smul)

c---- main cycle on time

do istep=1,nsteps

t=istep*dt

!  g=1.d0+0.3d0*dsin(0.65d0*t)         ! nonlinearity management

!      alp=0.1d0*(1.d0+0.3d0*dsin(0.65d0*t)) ! gravity strength management

!      delx=0.2d0*dsin(2.d0*0.65d0*t)          ! mirror's position varied

call pot(n,x,delx,v0,alp,v)
```

```fortran
      call nlstep(n,u,v,g,dt)

      call linstep(n,u,smul)

c---- boundary absorption

      u=u*sink

      if(istep/nout*nout.eq.istep) then

      call center(n,x,dx,u,xcom,wdth,norm)

      write(7,'(1x,4f12.4)') t,xcom,wdth,norm

c---- print the result

      do i=1,n

      write(8,'(1x,f12.6,f12.2,f12.6)') x(i),t,cdabs(u(i))**2

      enddo

      write(*,'(1x,2(a,f16.6))') 't = ',t,'   tend =',tend

      endif

      enddo

      close(7)

      close(8)

      END
```

```fortran
      SUBROUTINE pot(n,x,delx,v0,alp,v)

c---- supply the potential

      IMPLICIT none

      INTEGER i,n

      REAL*8 x(n),xd,delx,alp,v0,v(n)

      do i=1,n

c---- static ideal mirror

        if(x(i).gt.0.d0) then

          v(i)=alp*x(i)

        else

          v(i)=1000.d0

        endif

c---- static delta barrier

!       v(i)=alp*x(i)+v0*100.d0/(3.1415d0*(10000.d0*x(i)**2+1.d0))

c---- oscillating delta barrier

!       xd=x(i)+delx

!       v(i)=alp*xd+v0*100.d0/(3.1415d0*(10000.d0*xd**2+1.d0))

      enddo
```

```
            END




         SUBROUTINE spectr(n,smul)


c---- prepare spectral multiplicative 'smul' for fft


         IMPLICIT none


         INTEGER i,n


         REAL*8 om2dt,L,dt,pi,d


         COMPLEX*16 smul(n)


         COMMON L,dt,pi,d


         do i=1,n/2


           om2dt=(d/2.d0)*(2.d0*pi*dble(i-1)/L)**2*dt


           smul(i)=dcmplx(dcos(om2dt),-dsin(om2dt))


         enddo


         do i=n/2+1,n


           om2dt=(d/2.d0)*(2.d0*pi*dble(i-1-n)/L)**2*dt


           smul(i)=dcmplx(dcos(om2dt),-dsin(om2dt))


         enddo


         END
```

SUBROUTINE linstep(n,u,smul)

c---- linear step of integration

```
      IMPLICIT none

      INTEGER i,j,n,n2,isign

      REAL*8 w(2*n)

      COMPLEX*16 u(n),smul(n),tmp

      n2=2*n
```

c---- forward transform

```
      j=1

      do i=1,n2-1,2

        w(i)=dreal(u(j)); w(i+1)=dimag(u(j))

         j=j+1

      enddo

      isign=1

      call four1d(w,n,isign)
```

c---- multiply by factor 'smul'

```
      j=1

      do i=1,n2-1,2
```

```fortran
       tmp=smul(j)*dcmplx(w(i),w(i+1))

       w(i)=dreal(tmp); w(i+1)=dimag(tmp)

       j=j+1

      enddo

c---- backward transform and devide to n

      isign=-1

      call four1d(w,n,isign)

      j=1

      do i=1,n2-1,2

       u(j)=dcmplx(w(i),w(i+1))/dble(n)

       j=j+1

      enddo

      END



       SUBROUTINE nlstep(n,u,v,g,dt)

c---- nonlinear step of integration

      IMPLICIT none

      INTEGER i,n
```

```fortran
      REAL*8 dt,arg,v(n),g

      COMPLEX*16 u(n)

      do i=1,n

        arg=(g*cdabs(u(i))**2 - v(i))*dt

        u(i)=u(i)*dcmplx(dcos(arg),dsin(arg))

      enddo

      END



      SUBROUTINE absorb(n,x,L,dt,sink)

c---- a function modelling the absorbing boundaries

      IMPLICIT none

      INTEGER i,n

      REAL*8 x(n),L,dt,xleft,xright,alpha,g0,sh1,sh2,sink(n)

      PARAMETER(alpha=0.5d0, g0=20.d0)

      xleft=-L/2.d0; xright=L/2.d0

      do i=1,n

        sh1=1.d0/dcosh(alpha*(x(i)-xleft))

        sh2=1.d0/dcosh(alpha*(x(i)-xright))
```

```fortran
      sink(i)=dexp(-g0*(sh1*sh1+sh2*sh2)*dt)

      enddo

      END




      SUBROUTINE center(n,x,dx,u,xcom,wdth,norm)

c---- evaluation of energy, amplitude, width,position

      IMPLICIT none

      INTEGER i,n

      REAL*8 x(n),dx,sx,sw,sn,xcom,wdth,norm

      REAL*8 L,dt,pi,d,absu2(n)

      COMPLEX*16 u(n)

      COMMON L,dt,pi,d

      sx=0.0; sn=0.0; sw=0.0;

c---- find center-of-mass position

      do i=1,n

        absu2(i)=cdabs(u(i))**2

        sn=sn+absu2(i)

        sx=sx+x(i)*absu2(i)
```

```fortran
      enddo

      xcom=sx/sn        ! center-of-mass position

      norm=sn*dx        ! norm

c---- find the width

      do i=1,n

      sw=sw+(x(i)-xcom)**2*absu2(i)

      enddo

      wdth=dsqrt(sw/sn) ! width

      END
```

Appendix C:

Fortran codes for Gross-Pitaevskii equation non-local interaction

We used this code program to solve Gross-petavskii equation, with non-local interaction, which is investigated in chapter 3. I would like to mention that, subroutine code is taken from "Numerical recipes" [Press et al., 1996]. The code program material may used by beginner researcher and postgraduate students who are treating similar mathematical models.

The model equation is

$$i\frac{\partial \psi}{\partial t} + \frac{1}{2}\frac{\partial^2 \psi}{\partial x^2} + q\,|\,\psi\,|^2\,\psi + g(t)\psi\int_{-\infty}^{+\infty} R(|\,x-\xi\,|)|\,\psi(\xi,t)\,|^2\,d\xi = 0,$$

We can rewrite in this form

$$iu_t + \frac{1}{2}u_{xx} + q\,|\,u\,|^2\,u + g(t)uw(x) = 0$$

Where nonlocal term w(x) is evaluated via convolution theorem

PROGRAM GPE

IMPLICIT none

INTEGER n, i, istep, nsteps, nout

PARAMETER (n=1024)

REAL*8 L, x(n), dx, t, dt, dtt, tend, pi, v0, v(n), sink(n), q, g

```fortran
      REAL*8 a, amp, norm, mu, krnl(2*n), absu2(n), w(n), n0, dmy

      COMPLEX*16 u(n), smul(n)

      COMMON L, dt, dx, pi

      COMMON /nonl/ q, g

      pi=4.d0*datan(1.d0)

      L=12.d0*pi; dx=L/n

      dt=0.001d0; tend=100.d0

      nsteps=int(tend/dt);  nout=nsteps/500

      q  = -1.d0      ! local term

      g  = 100.d0! nonlocal term = 2*d^2

      v0 = 0.d0       ! strength of optical lattice

      n0 = 1.d0       ! norm variable

      a=1.55375d0; amp=dsqrt(n0/(a*dsqrt(pi)))  ! Gaussian's norm = n0

c---- initial wave profile

      do i=1,n

       x(i)=(i-1)*dx-L/2.d0

       read(6,*) dmy,u(i)

!  u(i)=dcmplx(amp*dexp(-x(i)**2/(2.d0*a**2)), 0.0)
```

```
      v(i)=v0*dsin(dsqrt(pi)*x(i))**2

      write(8,'(1x,3f14.6)') x(i),0.0,cdabs(u(i))**2

      enddo

      close(6)

c---- generate boundary absorption function

      call absorb(n,sink)

c---- evaluate spectral multiplicative

      call spectr(n,smul)

c---- prepare FT of the kernel function

      call kernel(n,x,krnl)

c---- main cycle on time

      t=0.d0

      dtt=0.5d0*dt

      do istep=1,nsteps

      t=istep*dt

      g=100.d0*(1.d0 + 0.01d0*dsin(0.965d0*t))

      absu2=cdabs(u)**2

      call nlstep(n,u,absu2,v,krnl,dx,dt)
```

```fortran
      call linstep(n,u,smul)

c---- boundary absorption

      u=sink*u

      if(istep/nout*nout.eq.istep) then

      norm=sum(cdabs(u)**2)*dx

c---- renormalize the wave function to = n0

      call energy(n,x,u,v,w,a,amp,mu)

      write(9,'(1x,5f12.6)') t,a,amp,norm,mu

      write(*,'(1x,5(a,f10.4))') ' time =',t,'   norm =', norm, ' mu =', mu,'

                        Amp=',amp,'   width=',a

      do i=1,n

      write(8,'(1x,3f14.6)') x(i),t,cdabs(u(i))**2

      enddo

      endif

      enddo

      close(8)

      close(9)

      END
```

```fortran
SUBROUTINE spectr(n,smul)

c---- prepare spectral multiplicative 'smul' for fft

IMPLICIT none

INTEGER i,n

REAL*8 om2dt,L,dt,dx,pi

COMPLEX*16 smul(n)

COMMON L,dt,dx,pi

do i=1,n/2

  om2dt=0.5d0*(2.d0*pi*dble(i-1)/L)**2*dt

  smul(i)=dcmplx(dcos(om2dt),-dsin(om2dt))

enddo

do i=n/2+1,n

  om2dt=0.5d0*(2.d0*pi*dble(i-1-n)/L)**2*dt

  smul(i)=dcmplx(dcos(om2dt),-dsin(om2dt))

enddo

END
```

SUBROUTINE linstep(n,u,smul)

```
c---- linear step of integration

      IMPLICIT none

      INTEGER i,j,n,n2,isign

      REAL*8 w(2*n)

      COMPLEX*16 u(n),smul(n),tmp

      n2=2*n

c---- forward transform

      j=1

      do i=1,n2-1,2

        w(i)=dreal(u(j)); w(i+1)=dimag(u(j))

         j=j+1

      enddo

      isign=1

      call four1d(w,n,isign)

c---- multiply by factor 'smul'

      j=1
```

```
do i=1,n2-1,2

  tmp=smul(j)*dcmplx(w(i),w(i+1))

  w(i)=dreal(tmp); w(i+1)=dimag(tmp)

  j=j+1

enddo

c---- backward transform and devide to n

isign=-1

call four1d(w,n,isign)

j=1

do i=1,n2-1,2

  u(j)=dcmplx(w(i),w(i+1))/dble(n)

  j=j+1

enddo

END
```

SUBROUTINE nlstep(n,u,absu2,v,krnl,dx,dt)

```
c---- nonlinear step of integration

      IMPLICIT none

      INTEGER n,i,isign

      REAL*8 dx,dt,arg,v(n),q,g,krnl(2*n),u2(2*n),conv(2*n),absu2(n)

      COMPLEX*16 u(n)

      COMMON /nonl/ q,g

      do i=1,n

        u2(2*i-1)=absu2(i)

        u2(2*i)=0.d0

      enddo

c---- forward transform and multiply by krnl

      isign=1

      call four1d(u2,n,isign)

      do i=1,n

        conv(2*i-1)=u2(2*i-1)*krnl(2*i-1)

        conv(2*i)=0.d0
```

```
      enddo

c---- backward transform

      isign=-1

      call four1d(conv,n,isign)

      conv=conv/dble(n)


      do i=1,n

        arg=(q*absu2(i) + g*conv(2*i-1)*dx + v(i))*dt

        u(i)=u(i)*dcmplx(dcos(arg),dsin(arg))

      enddo

      END
```

```fortran
SUBROUTINE kernel(n,x,krnl)

IMPLICIT none

INTEGER i,n,isign

REAL*8 pi,x(n),w,w2,tmp,krnl(2*n)

pi=4.d0*datan(1.d0)

w=5.d0

w2=2.d0*w*w

tmp=1.d0/(dsqrt(2.d0*pi)*w)

c---- response function (arranged as prescribed in Num. Recipes)

do i=1,n/2

  krnl(2*i-1)=tmp*dexp(-x(i+n/2)**2/w2)

  krnl(2*i)  =0.d0

enddo

do i=n/2+1,n

  krnl(2*i-1)=tmp*dexp(-x(i-n/2)**2/w2)

  krnl(2*i)  =0.d0

enddo
```

```fortran
      isign=1

      call four1d(krnl,n,isign)

      return

      END




      SUBROUTINE energy(n,x,u,v,w,a,amp,mu)

      IMPLICIT none

      INTEGER i,n

      REAL*8 L,dt,dx,sa,sn,sk,sq,sp,si,absu2(n)

      REAL*8 x(n),v(n),a,amp,mu,q,g,pi,w(n)

      COMPLEX*16 u(n)

      COMMON L,dt,dx,pi

      COMMON /nonl/ q,g

      sa=0.d0; sk=0.d0; sq=0.d0; sp=0.d0; si=0.d0; amp=0.d0

c---- evaluate the norm, kinetic, potential and interaction energies

      absu2=cdabs(u)**2

      sn=sum(absu2)

      do i=2,n-1
```

```
      sk=sk+cdabs((u(i+1)-u(i-1))/(2.d0*dx))**2

c---- local cubic nonlinearity

  sq=sq+absu2(i)**2

  sp=sp+v(i)*absu2(i)

  si=si+absu2(i)*w(i)

  if (cdabs(u(i)).gt.amp) amp=cdabs(u(i))

enddo

a=sn*dx/(amp**2*sqrt(pi))

mu=(0.5d0*sk - sp - q*sq - g*si)/sn

END



SUBROUTINE absorb(n,sink)

c---- a function modelling the absorbing boundaries

IMPLICIT none

INTEGER i,n

REAL*8 x,dx,xleft,xright,alpha,g0,sh1,sh2,sink(n)

REAL*8 L,dt,pi,d

PARAMETER(alpha=1.d0, g0=20.d0)
```

```fortran
COMMON L,dt,pi,d

dx=L/n; xleft=-L/2.d0; xright=L/2.d0

do i=1,n

  x=(i-1)*dx-L/2.d0

  sh1=1.d0/dcosh(alpha*(x-xleft))

  sh2=1.d0/dcosh(alpha*(x-xright))

  sink(i)=dexp(-g0*(sh1*sh1+sh2*sh2)*dt)

enddo

END




SUBROUTINE four1d(data,nn,isign)

IMPLICIT none

INTEGER isign,nn

REAL*8 data(2*nn)

INTEGER i,istep,j,m,mmax,n

REAL*8 tempi,tempr

REAL*8 theta,wi,wpi,wpr,wr,wtemp

n=2*nn
```

```
      j=1

      do 11 i=1,n,2

      if(j.gt.i)then

      tempr=data(j)

      tempi=data(j+1)

      data(j)=data(i)

      data(j+1)=data(i+1)

      data(i)=tempr

      data(i+1)=tempi

      endif

      m=n/2

1     if ((m.ge.2).and.(j.gt.m)) then

        j=j-m

        m=m/2

      goto 1

      endif

      j=j+m

11    continue
```

```fortran
      mmax=2

2     if (n.gt.mmax) then

       istep=2*mmax

       theta=6.28318530717959d0/dble(isign*mmax)

       wpr=-2.d0*dsin(0.5d0*theta)**2

       wpi=dsin(theta)

       wr=1.d0

       wi=0.d0

       do 13 m=1,mmax,2

        do 12 i=m,n,istep

      j=i+mmax

      tempr=wr*data(j)-wi*data(j+1)

      tempi=wr*data(j+1)+wi*data(j)

      data(j)=data(i)-tempr

      data(j+1)=data(i+1)-tempi

      data(i)=data(i)+tempr

      data(i+1)=data(i+1)+tempi

12    continue
```

```
        wtemp=wr

        wr=wr*wpr-wi*wpi+wr

        wi=wi*wpr+wtemp*wpi+wi

13continue

     mmax=istep

goto 2

endif

return

END.
```